THE EFFECTS OF β-ADRENERGIC STIMULATION ON POST-TETANIC POTENTIATION OF CONCENTRIC FORCE IN FAST SKELETAL MUSCLE FROM WILDTYPE AND skMLCK DEVOID MICE.

Stephen Roy Morris, B.Sc. (Honors Kinesiology)

Submitted in partial fulfillment of the requirements for the degree of
Master of Science in Applied Health Sciences (Kinesiology)

Faculty of Applied Health Sciences,
Brock University
1812 Sir Isaac Brock Way
St. Catharines, Ontario
L2S 3A1

© May, 2016

Abstract

Stimulation induced myosin RLC phosphorylation, catalyzed by the skeletal myosin light chain kinase (skMLCK) is known as the primary mechanism for twitch force potentiation (PTP). We assessed concentric PTP in the absence and presence of epinephrine (1 μM). To this end, extensor digitorum longus (EDL) muscles from wildtype (WT) and skMLCK$^{-/-}$ (KO) mice were incubated for 30-minutes in normal (CON) or epinephrine containing (EPI) Tyrode's solution (*in vitro, 25°C)*; undergoing a series of twitches before and after a standard conditioning stimulus (CS; 4x100 Hz) to determine PTP (post-CS/pre-CS). Epinephrine initially enhanced PTP compared to the WT and KO control values, respectively; peaking at 19.3 ± 1.6% and 15.7 ± 10.2% by the 8-minute mark ($P < 0.0001$) without altering myosin phosphorylation ($P = 0.503$). WT muscles were significantly elevated above KO values at all time points ($P < 0.05$); with the exception of the final 8-minute value ($P = 0.172$). However, both genotypes showed similar responses to epinephrine ($r^2 = 0.895$), demonstrating that epinephrine may primarily act on a pathway independent of myosin phosphorylation.

Acknowledgements

Dr. Vandenboom

I have you to thank for my growth as an academic, as well as an individual. Thank you for always pushing me to be my best and for believing in my abilities. I will carry these lessons with me into whatever the future holds.

My Supervisory Committee

Thank you to Dr. LeBlanc and Dr. O'Leary for your tremendous input on this project. You have both worked to challenge me and encourage me to be more focused and driven; you have significantly improved the quality of work present.

Fellow Lab Members and Classmates

To those who have been there from the start, or have gone on to bigger things; I have all of you to thank for creating one of the most truly creative, open-minded, and inviting environments to spend the last two years. I have never been a part of such a cohesive group of driven individuals – there is no doubt you will all achieve greatness.

Bill

To say that all of this wouldn't be possible without you would be an understatement. Thank you for being such an incredible mentor and friend. I hope nothing but the best for you and your family, and I know you will make a great father.

Josh

For as long as I've known you, I have always admired your drive and tenacity for hard work. I think that "3'rd year you" would be amazed with what you've been able to accomplish thus far, and that you will continue to do so. Don't lose the things that have made you what you are, never stop moving forward.

Jordan

Thank you for always being someone that pushes me academically. As we move forward from this experience, I know that you'll find nothing but success. You have the ability to do what you love, just don't give up, it will come.

To Those Reading

If you are reading this document, then you are observing a defining point of my life. As such, I want to share with you something I have learned thus far. As far as I can tell, your own success is dependent on one person, as are your failures, and your will to move forward; that person is you. You are the key to achieving your dreams, and sometimes that will be a hard notion to maintain invested in. However, I promise you that if you do – you will end up where you want to be.

Never be afraid to ask the tough questions, never be afraid to try something new, and never be afraid to fail; with that, you are ready for anything.

Table of Contents

List of Abbreviations

Ca^{2+} = Calcium
CaM = Calcium-Calmodulin
CON = Control Group
CREB = cAMP response element-binding protein
EDL = Extensor digitorum longus
EPAC = Exchange protein activated by cAMP
EPI = Epinephrine
FoxO = forkhead transcription factor
G_B = B subunit of G protein
G_{ai} = inhibitory subunit of G protein
G_{as} = Stimulatory subunit of G protein
G_Y = Y subunit of G protein
GSK = glycogen synthase kinase
L_o = Optimal Muscle Length
P_o, P_t = Peak Tetanic Force, Peak Twitch Force
PKA = cAMP dependent protein kinase A
PTP = Post-Tetanic Twitch Potentiation
RLC = Regulatory Light Chain
skMLCK = Skeletal Muscle Myosin Light Chain Kinase
skMLCP = Myosin Light Chain Phosphatase
SR = Sarcoplasmic Reticulum
V_{max}, V_o = Maximal Shortening Velocity, Unloaded Shortening Velocity
WT, KO = Wildtype, Knockout

List of Tables

List of Equations

List of Figures

Introduction

Mammalian skeletal muscle has unique roles in metabolism, thermogenesis, and most notably, locomotion. To help fulfill these roles, skeletal muscle is highly heterogeneous in nature, varying greatly in regard to muscle/fiber type (fast-type II vs. slow-type I) as well as neuronal innervation. The ability of muscle to perform mechanical work, i.e. while shortening against an external load, begins at the level of the sarcomere. The sarcomere is recognized as the functional unit of muscle, and as such is host to myriad actomyosin complexes responsible for muscle force, shortening, and work production. The actomyosin complex is composed of the two major contractile proteins, actin, and myosin. Variations in muscle motor performance and fiber type are intrinsically related to variations in myosin heavy chain (MyHC) isoform. For example, MyHC isoform differences in cross-bridge cycling probability, duty cycle and/or rate may account for differences in locomotion seen at the functional/animal level. One difference in this regard may be the posttranslational modification of myosin by phosphorylation of the regulatory light chain (RLC), a change that may modulate myosin motor function (Szczesna-Cordary, 2003; Sweeney et al., 1993) within the sarcomere and account for the phenomenon of potentiation. First observed over 100 years ago (Lee, 1907), potentiation may be defined as the transient increase in isometric twitch force observed during or after muscle activity, and is now regarded as a fundamental property of fast twitch skeletal muscle function.

Work performed on intact rodent and cat skeletal muscles showed that the application of a brief tetanic stimulation increased isometric twitch force independent of

change to peak tetanic force; thus potentiation increased the twitch to tetanus ratio (Bagust et al., 1974). The fact that similar observations have been made in frog skeletal muscle fibers (Ramsey & Street, 1941) demonstrates that the molecular origin for this so-called "post-tetanic potentiation" was intrinsic to the muscle cell, and perhaps the sarcomere, itself. Indeed, subsequent biochemical work performed on mouse and rat skeletal muscle has shown that post-tetanic potentiation (PTP) is temporally correlated with the phosphorylation of the myosin regulatory light chain (RLC). For example, as identified by Vandenboom et al. (2013) robust correlations have been obtained between the extent of RLC phosphorylation and the magnitude of PTP in both rat and mouse fast twitch skeletal muscle within the temperature range 15 - 35° C (Klug et al. 1982; Manning and Stull, 1979; 1982; Moore and Stull, 1984; Moore et al., 1990; Palmer and Moore, 1989; Vandenboom et al 1995; 1997). Zhi et al. (2005) was the first to provide evidence that these correlations may also represent causality through fast twitch muscles from mice devoid of the ability to phosphorylate the RLC; they also did not exhibit PTP. This finding was later confirmed by Gittings et al. (2011). Thus, although this does not exclude other mechanisms, it appears that the RLC phosphorylation mechanism is responsible for some or most of for the PTP displayed by mammalian fast twitch skeletal muscle.

The catalytic activity of myosin light chain kinase (skMLCK) is opposed by the myosin RLC phosphatase (skMLCP) and thus it is the balance between the activities of skMLCK and skMLCP which will determine net phosphorylation of the myosin RLC. Although a considerable amount has been learned regarding the advantage of isometric twitch force potentiation, there is still much that remains to be learned regarding how

potentiation influences overall organismal function (Vandenboom, 2013), for example the influence of β-agonists in dynamic models of potentiation. One major consideration is the influence of intact extra-cellular signaling and it's affect on potentiation. Recent work by Decostre et al. (2000) shows that β-adrenergic stimulation prolongs the potentiated state and alters twitch kinetics and characteristics in isolated mouse fast muscle. These outcomes implicate a role for potentiation during the sympathetic fight-or-flight response of mammals. To date, no conclusions have been reached regarding how adrenaline causes this prolongation of twitch potentiation, however it has been hypothesized that adrenaline inhibits skMLCP through the phosphorylation of inhibitor-1 (I-1). Decostre et al. (2000) indicated that after 300 seconds (normal time course for potentiation dissipation) myosin phosphorylation was maintained (0.51 mol P/mol LC2) in the EPI condition, a value that was significantly higher than the controls (0.31 mol P/mol LC2), however there was no significant effect on the RLC phosphorylation or isometric twitch force in resting muscle. In addition, the prolongation of twitch potentiation was observed as long as RLC phosphorylation was elevated. The evidence presented primarily by Decostre et al. (2000) suggest a prolongation of myosin phosphorylation in the presence of adrenaline, however this effect may not be mediated via skMLCK as myosin phosphorylation was not increased with adrenaline incubation (Manning & Stull, 1982; Decostre et al., 2000). In addition, although these researchers observed increases in resting [Ca^{2+}] and peak [Ca^{2+}] transient both with and without adrenaline, these values returned to normal after 300 seconds, giving even more support for MLCP as adrenalines mechanistic pathway. Thus, adrenergic stimulation may not increase phosphorylation of RLC per se but may slow the reduction in RLC phosphorylation via inhibition of skMLCP.

Review of Literature

2.0.0 Skeletal Muscle: The Contractile Apparatus

From an idea as big as that of locomotion, to that of a much more isolated nature, all skeletal muscle relies on the same contractile anatomy to carry out it's function. This function, at its core, is to convert stored chemical energy (ATP) into mechanical energy. This generation of muscular force is reliant on the constituent parts of its system, in this case, specialized proteins of actin and myosin. It is the interaction between these two proteins, which gives life to the sliding filament theory (Hanson & Huxley, 1953; Huxley & Hanson, 1954; Huxley, 1957). This concept stipulates that chemically driven power strokes of the myosin protein result in mechanical work, producing force. Each unit of the contractile apparatus in a muscle fiber is composed of the actin (thin) and myosin (thick) myofilaments. The actin filament is helical in structure, and is composed of 7 actin molecules as well as troponin (Tn) and tropomyosin (Tm). (Gordon, Homsher, & Regnier, 2000). The myosin filament (**Figure 1**) on the other hand consists of two heavy chains, and two pairs of light chains (ELC, essential light chain; RLC, regulatory light chain). Actin is anchored to each end of the functional unit (sarcomere) while myosin is in the center of each unit, held in position by the structural protein of titin. Stimulation of this functional unit results in the myosin head 'pulling' the actin filament towards its center (Huxley, 1957; 1969).

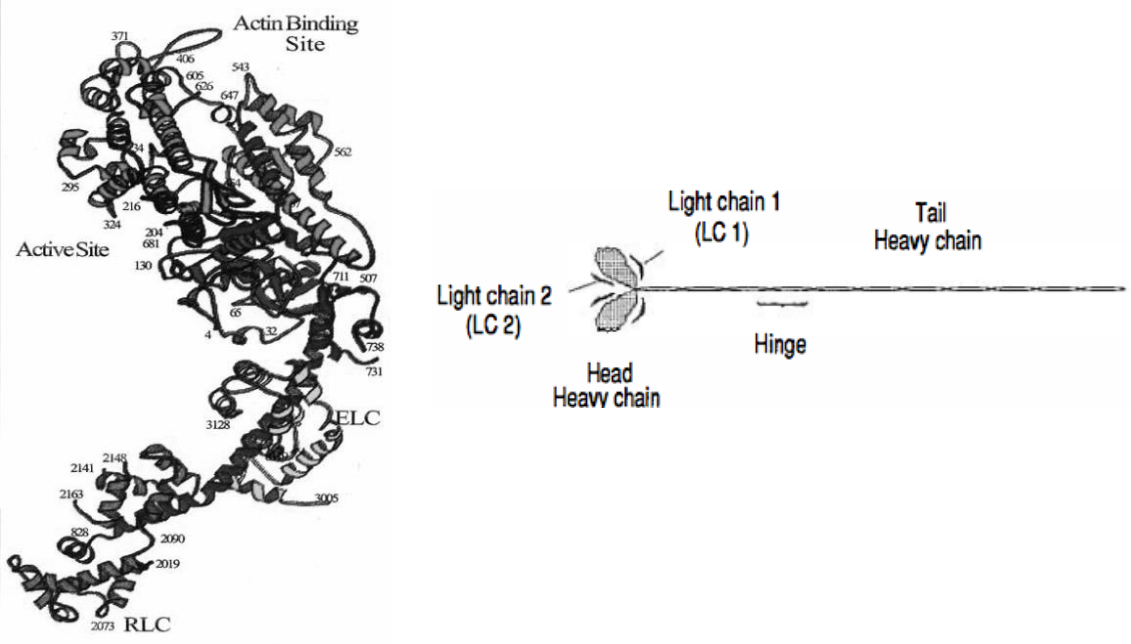

Figure 1. Myosin filament, and myosin head microanatomy (Rayment et al., 1993; Warrick & Spaudich, 1987).

2.1.0 Excitation Contraction Coupling (ECC)

In vertebrate skeletal muscle, force development is not only reliant on the contractile apparatus, and in fact this machinery is contingent upon a much larger control of [Ca^{2+}] regulation in the cytoplasm. This regulation is a feature of the excitation-contraction coupling (ECC) mechanism native to skeletal muscle. ECC begins with an action potential passing along the surface membrane and into a network of t-tubules (Lamb, 2000). This action potential results in depolarization, which is detected by dihydropyridine receptor (DHPR) molecules, also known as voltage-sensors (Schneider, 1994; Melzer, Herrmann-Frank, & Luttgau, 1995) allowing for a way to directly activate the Ca^{2+} -release channels (RyR1) in the adjacent sarcoplasmic reticulum (SR) seen in **Figure 2**.

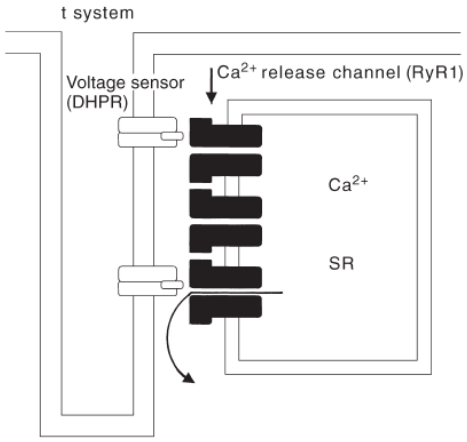

Figure 2. Voltage sensor-controlled Ca^{2+} release in skeletal muscle (Lamb, 2000)

Upon activation, the SR will release Ca^{2+} via these RyR1 channels, and flood the cytoplasm with calcium, so much so that the resting level of ~50nM (Berchtold, Brinkmeier, & Muntener, 2000) will be elevated ~100 fold. Upon release, this cytosolic calcium will rapidly bind to TnC and activate contraction by allowing myosin to bind to the active sites of actin, before being completely pumped back into the SR via SERCA protein pumps (Ca^{2+} ATPase), this cycle can be seen in **Figure 3**.

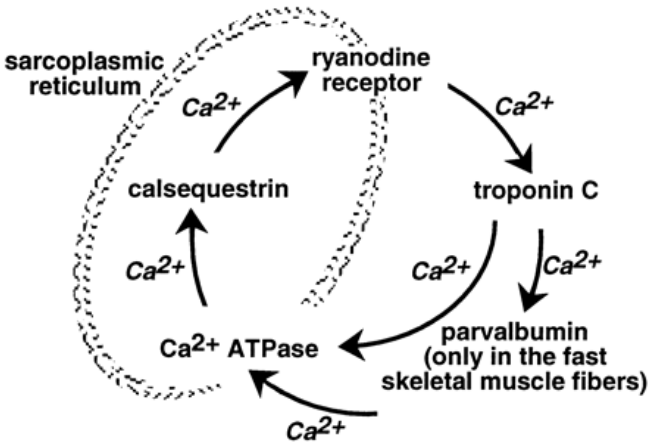

Figure 3. Cycling of calcium between SR and cytoplasm (Berchtold, Brinkmeier, & Muntener, 2000)

2.2.0 Physiological Consequences: Myosin Regulatory Light Chain Phosphorylation

The RLC is important for both the structure and function of the myosin head during muscle contraction, it's region of the myosin heavy chain (**Figure 1**) can undergo conformational changes, important for working muscle (Rayment et al, 1993; Uyeda, & Spudich, 1993). The RLCs role in contraction has been studied using *in vitro* motility assays, which show that the removal of RLC will result in reduced velocity of actin movement (Lowey, Waller, & Trybus, 1993), an observation that was reversible with the reconstitution of the myosin RLC.

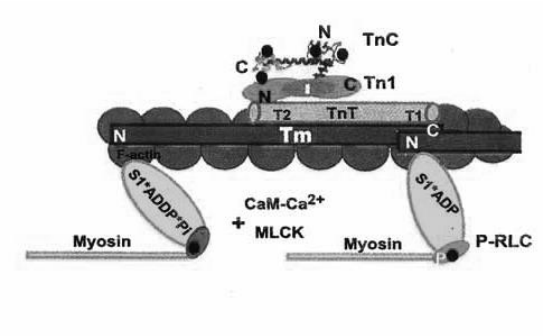

Figure 4. Change of myosin head position from weakly bound to strongly bound state with RLC phosphorylation (Szczesna-Cordary, 2003).

Section 2.1.0 outlines the effects of calcium regulation on contraction via TnC, however another destination for calcium after release from the SR is Ca^{2+}/CaM. When calcium binds with the CaM (Calmodulin) the result is an activation of skMLCK, which causes phosphorylation of the RLC. The effects of RLC phosphorylation in intact rabbit skeletal muscle have been studied *in vivo*, showing that tetanic stimulation significantly elevates RLC phosphorylation (Moore et al. 1985). The major physiological outcomes of RLC phosphorylation have been demonstrated to be a change of Ca^{2+} sensitivity of force development (Metzger, Greaser, & Moss, 1989; Sweeney, Bowman, & Stull, 1993; Szczensa et al, 2002) as well as a raise in maximal steady state force (Szczensa et al,

2002). The structural connection between the phosphorylation of the RLC and the outcome of potentiated force is most likely a result of the recruitment of more strongly bound cross-bridges (Sweeney, Bowman, & Stull, 1993) because RLC phosphorylation causes the myosin head to move away from it's thick filament backbone and become more accessible to actin. This was demonstrated using electron micrographs of skinned rabbit fibers, which lost their periodic arrangement of the relaxed state with the phosphorylation of RLC (Yang et al, 1998), a change that most likely reflects a change in charge due to phosphorylation, increasing myosin head mobility and accessibility to actin. In terms of outcome, this means that a phosphorylation induced change in position of the myosin head may be responsible for increasing the number of cross-bridges involved in cycling, through up regulation of actin-induced phosphate release (Davis, Satorius, & Epstein, 2002) i.e. transitioning from the weakly bound to the strongly bound state.

2.2.1 Potentiation in Skeletal Muscle

Force potentiation has been documented as a fundamental characteristic of fast skeletal muscle first seen in literature over 100 years ago (Lee, 1907). Potentiation is usually observed as a transient increase in isometric twitch force, which has been observed independent of alteration to peak tetanic force (Bagust et al, 1974). The earliest work to show this phenomenon was performed on intact rodent and cat skeletal muscle (Brown & von Euler, 1938; Standaert, 1964), however similar findings in frog skeletal muscle fibers (Ramsey & Street, 1941) demonstrated that this isometric force potentiation is not species dependent, and is intrinsic to the muscle cell itself. More recent work showed that which potentiation in rodent muscle is strongly associated with myosin

regulatory light chain (RLC) phosphorylation. In fact, as Vandenboom et al. (2013) demonstrated, isometric twitch potentiation is temporally correlated with RLC phosphorylation after different types of conditioning stimuli. Although, studies which have multiple measurements of isometric twitch potentiation and RLC phosphorylation produced both non-linear (Klug et al., 1982) and linear relationships (Manning and Stull 1979; Moore et al., 1990; Palmer and Moore 1989; Vandenboom et al., 1995, 1997; Xeni et al., 2011), these show a consistent relationship between RLC phosphorylation and potentiation. Thus, there is a direct and predictable influence of RLC phosphorylation on the isometric twitch force of fast twitch skeletal muscle; although this effect increases as temperature approaches the physiological range, temperature is just one of many factors that will affect the magnitude and duration of potentiation with other notable influences being muscle length (short > long), fiber type (IIb > Ia), contraction type (concentric > isometric), and stimulation paradigm. In addition, Gittings et al, (2012) demonstrated potentiation is shortening speed dependent, such that faster muscle speeds of shortening, produced increased potentiation.

2.2.2 Manifestation of Twitch Force Potentiation

There are two main types of potentiation: staircase potentiation and post-tetanic potentiation. Staircase potentiation refers to a progressive increase in isometric twitch force during low frequency stimulation (e.g., 10 Hz over 30 seconds), while the second type, post-tetanic potentiation (PTP) refers to a step-like increase in isometric twitch force, seen after a brief bout of high frequency stimulation (e.g., 150 Hz over 1 second). An example paradigm for both of these manifestations can be found in **Figure 5**. When staircase potentiation is elicited, one may see a decreased isometric twitch force before

seeing an eventual rise to a new peak. Under this condition, the peak amplitude depends on both stimulus rate and number. Potentiated twitch force will deteriorate when stimulation is stopped, slowly at first before deteriorating more rapidly (Krarup, 1981a). Alternatively, PTP yields an acute increase in isometric twitch force in response to a high (Close and Hoh, 1968b) or low-frequency stimulus. Just like staircase potentiation, PTP is reliant on both stimulus frequency, as well as duration. During PTP paradigm, twitch force displays an initial increase to a peak shortly after stimulation before rapidly, then slowly, dissipating over the course of several minutes (Krarup, 1981a). An example of stair case potentiation over a 60 second time course, and PTP over a 600 second time course can be found in **Figure 5**.

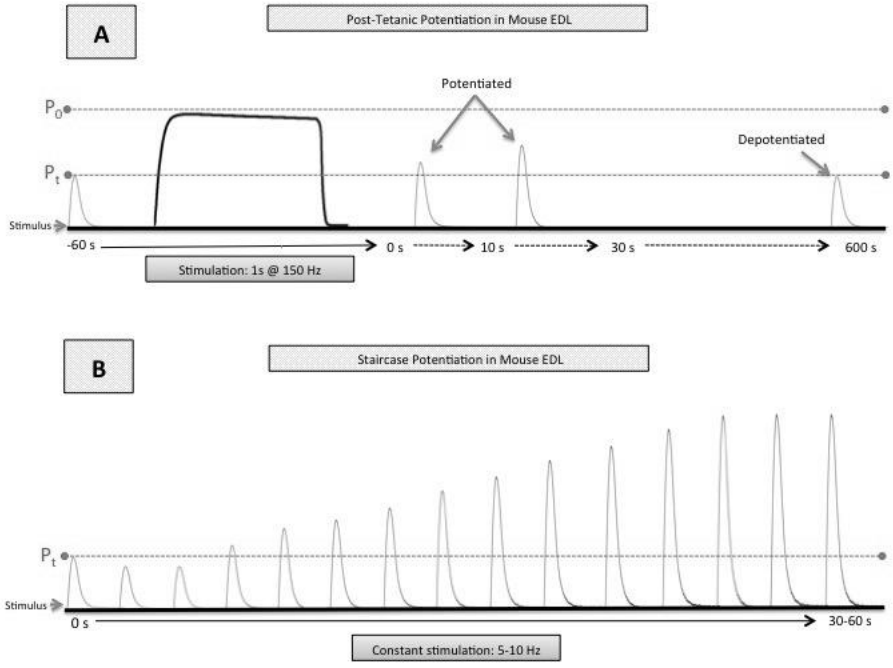

Figure 5. An example of both post-tetanic potentiation (**a**) and staircase potentiation (**b**) in fast twitch skeletal muscle under typical experimental paradigms. Modified from (Vandenboom et al. 2013).

Evidence from skinned (or permeabilized) fibers was the first model to provide mechanistic evidence that RLC phosphorylation increased force. For example, Persechini et al. (1985) showed that the addition of skMLCK both increased phosphorylation of the RLC (0.10 mol P/ mol LC to 0.80 mol P/mol LC) and increased steady-state tension at submaximal Ca^{2+} activation of rabbit psoas fibers, however maximal force was not increased. Later work described how RLC phosphorylation-induced potentiation of steady state force was inversely associated to actin activation levels (Davis et al., 2002; Metzger et al., 1989; Patel et al., 1996, 1998; Szczesna et al., 2002). This finding provided an important mechanistic link between the skMLCK-catalyzed phosphorylation of RLC and twitch force potentiation. While it wasn't until the 1970's that skMLCK was recognized for it's action on the RLC (**Figure 4**) as well as a role in Ca^{2+} activation, the first identification of the kinase was by Pires et al. (1974) who determined that phosphorylation of myosin was reliant on calcium concentration in all muscle types (Blumenthal & Stull, 1980). The importance of these findings serves as the cornerstone for most recent studies in the field of skeletal muscle potentiation, as it helps characterize and identify twitch potentiation.

2.2.3 Evidence From Knock-Out (skMLCK$^{-/-}$) Models

Results from skMLCK knock-out models have helped confirm the suggested role and relationship of RLC phosphorylation mediated force potentiation. For example, Zhi et al. (2005) showed that brief tetanic stimulation of wildtype muscle increased RLC phosphorylation by ~ four fold and twitch force by 1.8 fold. However, when the same conditioning stimulus was applied to knock out muscle (skMLCK$^{-/-}$) neither RLC phosphorylation or twitch force was elevated. This crucial research by Zhi et al. (2005)

confirmed that RLC phosphorylation by Ca^{2+}/calmodulin dependent skMLCK is the primary mechanism of PTP in fast-twitch mouse muscle. Moreover, skMLCK over-expression showed to enhance the rate of RLC phosphorylation and staircase potentiation in mouse EDL (Ryder et al., 2007). Although these results of the $skMLCK^{-/-}$ models do give support to the role of skMLCK, however, they also showed that low frequency repetitive stimulation registered an attenuated stair case potentiation of roughly 50% when compared to the wild type muscle. These data suggest that although skMLCK-catalyzed phosphorylation of RLC is the primary mechanism for PTP, an additional mechanism may contribute to staircase potentiation (Zhi et al., 2005; Gittings et al., 2011).

2.2.4 Contraction Type Dependence

One of the most vital mechanical factors that modulates the ability of RLC phosphorylation to potentiate muscle is that of contraction type (Vandenboom et al., 2013). The relationship between RLC phosphorylation and the potentiation of skeletal muscle has been characterized, in large part using isometric contractions. However, to date it has been seen that both rat and mouse skeletal muscle can be potentiated by the same conditioning stimulus for both isometric as well as concentric (dynamic force, work, and power) functions: 1 s at 160 Hz (Abbate et al., 2000), 3 of 500 ms at 100 Hz in 10 seconds (Caterini et al., 2011). The analysis of PTP under dynamic conditions gives a more realistic mechanical model for assessing locomotor muscle function than does isometric contractions (James et al., 1996; Stevens and Syme, 1993a). While it had been suggested that an increased effect of Ca^{2+} on cross-bridge formation was a mechanism of PTP (Palmer & Moore, 1989), it has since been hypothesized that PTP is induced by

RLC phosphorylation, which is thought to increase the number of cross-bridges in the force generating state (Sweeney & Stull, 1990). To this end, a case can be made for the shortening speed dependence of concentric PTP (Abbate et al., 2000; Gittings et al., 2012; Caterini et al., 2011) where at high shortening velocities, it is not possible for cross-bridges to remain in a force-generating state for a long time. Thus, it is at high velocities the effects of PTP on force generation are much more pronounced as the cross-bridge distribution generally favors a non-force generating state which accounts for the noticeable effect of PTP, where as at slower speeds, phosphorylation mediated alterations to myosin structure favor a force-generating state (Caterini et al., 2011) therefore exerting less of an effect on force.

2.2.5 β-Agonists and Force Potentiation

The effects of β-adrenergic stimulation on muscle potentiation first appeared in the literature over 100 years ago. Since then, studies often examined the use of, but weren't limited to, adrenaline and potassium chloride (Brown et al. 1949; Brown & Euler, 1938) and generally focused on twitch tension. Most recently, work on isolated mouse fast twitch skeletal muscle shows that β-adrenergic stimulation extends the potentiated state, demonstrating a possible function during the fight or flight response in mammals (Decostre et al., 2000). Furthermore, Grange et al. (1995) determined that even small force potentiation of the twitch can yield a significant increase in muscle force, work and power in the living animal. In this instance, the twitch is a fundamental mechanical output of an activated motor unit, where adrenergic stimulation will maintain this improvement for a longer time, thus allowing an animal to better cope with stressful situations.

Examination of the effects of adrenaline in the fatigued state date back to about the 1950's, slowly giving rise to research involving PTP and the use of adrenaline, among other sympathetic amines. Contrary to literature at the time, evidence showed that a fatigued state of muscle was not necessary for demonstrating the potentiation effect of adrenaline (Goffart & Brown 1947). By 1948 it had been hypothesized that the main site of action of adrenaline on fatigued muscle was the fiber it's self, and that adrenaline could augment twitch tension under circumstances in which no failure of transmission could be shown (Brown, Bulbring, & Burns, 1948). Research also gave evidence to the effects of ionic balance in the fluid surrounding the muscle (Goffart & Brown, 1947; Goffart, 1949) and the muscle itself (Goffart, 1947). Adrenaline had been seen to increase demarcation potential (Brown, Goffart, & Vianna Dias, 1950) as well as decrease K^+ loss from muscles (Goffart & Perry, 1951). These results lead to conclusions that adrenaline prolonged the active state (Hill, 1949 b) of skeletal muscle, accounting for the observed increase in tension of twitches.

Direct observation of the effects of β-adrenoceptor activation on contraction in both isolated fast and slow twitch skeletal muscle was being examined by the 1990's (Cairns & Dulhunty, 1993). In rat soleus, β_2-adrenoceptor agonists were used and induced an average of 15% potentiation of peak twitch and peak tetanic force. Interestingly, adrenaline had shown the ability to increase peak tetanic force by ~7% in both normal and denervated soleus fibers (Cairns & Dulhunty, 1993). This research displayed a contradictory result of potentiation in slow rodent fibers using terbutatline and adrenaline; this was attributed to greater β_2-adrenoceptor density in the slow twitch muscles, as well as greater enhancement of adenylate cyclase activity. The most recent

work regarding β_2-adrenoceptor agonists and post-tetanic potentiation has been conducted by Decostre et al. (2000) whose work will serve as a backbone for this section of the review. This paper identifies the effects of adrenaline on the PTP effect in the EDL of C57BL mouse skeletal muscle at (20°C).

2.2.6 β-Agonists and Mechanical Characteristics

Adrenaline has been cited in literature for having a very small (Cairns & Dulhunty, 1993), or absent (Manning and Stull, 1982) effect on the isometric force of pre-tetanic twitches, although it has also been reported to increase by 15% (Goffart & Ritchie, 1952). More recently, this characteristic was supported in mouse EDL by both Decostre et al. (2000), as well as Andersson (2012) who observed increased isometric twitch force with 1 uM isoproterenol incubations. Decostre et al. (2000) found that adrenaline had small positive (+4%) effect on isometric force of pre-tetanic twitches. The intracellular effect of adrenaline has been mimicked using 8-bromo-cAMP and analogous compound, to help characterize whether adrenaline has specific action, or if these effects can be characterized across other β-adrenergic stimulants. The use of 8-bromo-cAMP in mouse EDL showed significant (+7%) increases in twitch force (Decostre et al., 2000).

2.2.7 Temporal Twitch Parameters

The effects of adrenaline stem beyond altering twitch force in fast muscle. Evidence as far back as the 1950s shows adrenaline has an impact on the temporal parameters or kinetics of an isomeric twitch (Brown et al., 1948; Bowman & Ziamis, 1958; Goffart & Ritchie, 1952) with relation to time to peak force (TPT; time required to reach max active force in ms), rate of force development (instantaneous rate of force development in mN/ms), and half relaxation time (time required for force to diminish

50% in ms). Decostre et al., (2000) saw that adrenaline slightly increased the time to peak force (20, and 300 s after tetanus), however this effect was small, a finding that corroborates some of the earliest findings (Goffart & Ritchie, 1952) suggesting adrenaline increased TPT more as time elapsed. Furthermore, adrenaline increased the rate of force development (CON 7.8 ms ± 0.9; EPI 8.8 ms ± 1.1) as well as the half relaxation time (CON 24.4 ± 1.2; EPI 29.9 ± 2.2). Thus, adrenaline may be responsible for an increased average twitch force as well as altered twitch kinetics, especially in combination with the enhancement of dF/dt that is a general characteristic of potentiated rodent muscle (Grange et al. 1995).

2.2.8 Proposed Mechanisms of Epinephrine

In 1979, myosin light chain phosphorylation and phosphorylase A activity in rat EDL was observed by Manning and Stull. Results showed prolonged tetanic stimulation lead to increased phosphorylation of LC2 (0.92 mol P/mol LC2) – helping confirm the role of LC2 phosphorylation in a twitch. Furthermore, phosphorylase A activity was low at rest, but after tetanic stimulation, activity of the enzyme increased in a time-dependent manner which attained maximum values after 2-3 seconds of relaxation. After achieving maximum activity, the phosphorylase activity diminished rapidly. Interestingly, post-tetanic potentiation followed the same pattern that LC2 phosphorylation did, with a rapid rising phase followed by a slower descending phase. These researchers determined that these activities also required calcium concentrations greater than those at rest, implicating not only the role of myosin phosphorylation but transient calcium levels. Several years later, Manning and Stull (1982) examined the specific dephosphorylation of LC2 and the role of skMLCP. It was noted that slow rates of kinase inactivation coupled with low

activity of phosphatase could account for the persistence of LC2 phosphorylation well after tetanic stimulation, giving support to the possibility for prolongation of potentiation.

The maintenance of LC2 phosphorylation in the presence of adrenaline is not yet fully understood, and thus its mechanisms are yet to be completely defined. On its own, adrenaline does not seem to activate the skMLCK at rest as LC2 phosphorylation does not increase in its presence (Manning & Stull, 1982; Decostre et al., 2000). Furthermore, the addition of adrenaline does not significantly increase phosphorylation level after a conditioning tetanus nor does the phosphorylation of skMLCK have any effect on skeletal muscle skMLCK (Edelman & Krebs, 1982). This cAMP-dependent protein kinase is also known to partially inhibit smooth muscle MLCK (Adelstein et al., 1978; Conti & Adelstein, 1981). The fact that adrenergic stimulation does not increase phosphorylation of RLC per se, but still maintains the high level following stimulation suggests an inhibition of the skMLCP (see **Figure 4**). The skMLCP (or PP1-M) is a class 1-protein phosphatase, responsible for the dephosphorylation of LC2, countering the action of skMLCK. The most recent evidence suggests that PP1-M shares a common catalytic subunit with glycogen-bound protein phosphatase (PP1-G), another class 1 PP (Cohen, 1989; Gailly et al., 1996; Johnson et al., 1996; Egloff et al., 1997; Moorhead et al., 1998). In this case, it is well known that adrenergic stimulation leads to phosphorylation of the PP1-G, causing it's catalytic sub-unit to dissociate (Hubbard and Cohen, 1989; Dent et al., 1990; Walker et al., 2000) and is subsequently inhibited by the phosphorylated form of inhibitor-1 (I-1, an endogenous PP inhibitor). I-1 is known to bind to the catalytic sub-unit of the type 1 phosphatases, although when unphosphorylated, I-1 is inactive and does not bind (Cohen, 1989; Bollen & Stalmans,

1992). The phosphorylation of the I-1 is catalyzed by a cAMP – activated protein kinase (Huang & Glinsmann, 1976) and in skeletal muscle, studies show that an increase of the phosphorylated (active) form of I-1 was present as a result of adrenergic stimulation (Foulkes & Cohen, 1979; Khatra et al., 1980). Thus, the current proposition by Decostre et al. (2000) is that PP1-M may follow the same mechanism of inhibition as PP-1G when subject to adrenergic stimulation, such that phosphorylation of the regulatory sub-unit, detachment and inhibition of the catalytic sub-unit happens via the binding of activated inhibitor-1.

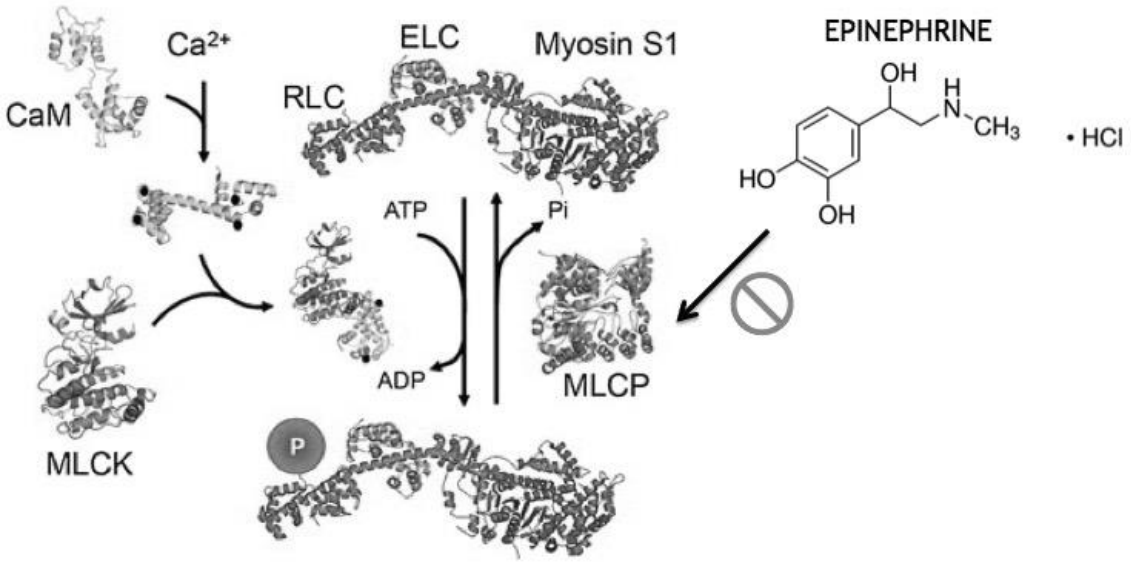

Figure 6. Potential mechanism of adrenaline during post-tetanic activation; inhibition of skMLCK. Modified from Stull et al., (2011).

2.3.0 Sympathetic Nervous System & Adrenoceptors

The purpose of this literature review is to identify the role of β-adrenergic stimulation on mammalian skeletal muscle with special focus on β-agonist stimulation and post-tetanic muscle potentiation in mouse muscle. However, data from cats, rabbits, and human will be included. To do this, relevant literature regarding the structure, biochemistry, function, location, signaling mechanics, and history of β-adrenoceptors will be presented. These opening sections will not act as a complete and comprehensive review of each given topic, but merely fill in the gaps necessary to understanding the β-adrenergic action on skeletal muscle. The review is comprised of five sections, including: a description of the sympathetic nervous system and adrenoceptor subgroups, identifying the role of β-adrenergic agonists, signaling mechanics of β-adrenoceptors within skeletal muscle, effects of β_2-agonists in skeletal muscle, and the relationship between sympathomimetics and post-tetanic twitch potentiation in rodent muscle models. Section 2.0 describes the sympathetic nervous system and adrenoceptors, including their sub groups. This section takes an overarching approach to elucidating the key components to sympathetic response, including: G-proteins and G-protein coupling receptors (GPCRs), β-adrenoceptor structure and sub-types, as well as α-adrenoceptor structure and sub-type. This section will approach each segment with consideration of location, biochemical properties, structure, function, and role within the system.

Among many functions, the role of the sympathetic nervous system (SNS) is defined by catecholamines, which elicit the responses governed by individual adrenoceptor within the system. In this case, the major signaling compounds under examination are adrenaline (epinephrine) or noradrenaline (norepinephrine)- each of

which can cause their own specific action on a given receptor. It is this ability that enables adrenoceptors to be targeted not only by physiologically present catecholamines such as adrenaline, but also as the target of synthetically altered agents as well. For example, in the case of therapeutic drug treatment, this synthetic tailoring is usually reserved for treatment of cardiovascular disease. β-adrenoceptors have been the main focus, specifically β_2-adrenoceptors in the clinical setting.

As previously stated, the SNS relies on two major signaling compounds: epinephrine and norepinephrine. Epinephrine is a product of the adrenal gland, while norepinephrine stems from nerve axons following stimulation from acetylcholine (Lynch & Ryall, 2008). The binding of either of these compounds will prompt a physiological response depending on the receptor subtype targeted. Since 1948, these receptors have been referred to as adrenoceptors (Ahlquist, 1948). Within the classification of adrenoceptors, there are two major subgroups that have been the focus of academic attention. These two subgroups are known as the beta (β-adrenoceptor) and the alpha (α-adrenoceptor). In 1948, Raymond Ahlquist published a paper about the effects of six different sympathetic stimulators, primarily on cardiac muscle. In this study he designed two groups: the alpha (excitatory responses) and the beta (inhibitory responses). Although, today we know that these concepts are considerably more complex than proposed by Ahlquist, this delineation between the two types of adrenoceptor sub-types still exists. In fact, presently we can see nine different adrenoceptors: six alpha, and three beta. In the case of skeletal muscle, it is important to note that β-adrenoceptors dominate. Furthermore, over the last 20 years, β-adrenoceptor stimulation has shown to be useful in growth promotion in skeletal muscle (Agbenyega & Wareham, 1990; Carter et al., 1991).

2.3.1 G-Protein Coupled Receptor Family (GPCRs)

The guanine nucleotide G-protein-coupled receptor family is the largest group of cell surface receptors in mammals, comprising greater than 1% of the human genome (Fredriksson et al., 2003). All adrenoceptors then, can be classified as belonging to the GPCR family. Of the GPCRs, the rhodopsin receptor is the most well known and characterized, this includes: dopaminergic, adenosine, histamine, α- and β-adrenoceptors (Fredriksson et al., 2003). All GPCR receptors, such as rhodopsin, couple with heterotrimeric guanine nucleotide-binding regulatory proteins (G Proteins). Under physiological conditions, adrenaline and noradrenaline take effect by acting on a group of 9 GPCRs- the adrenoceptors (Bylund et al., 1994; Davis et al., 2008). Adrenoceptors are broken into subtypes, which are coded by specific genes, all of which have selective agonists and antagonists for each receptor type (Alexander et al., 2007). When activated, all sub-types of the β-adrenoceptor can cause increases in intracellular levels of cAMP– however it is confirmed that this isn't the only signaling pathway (Lefkowitz et al., 2002; Galandrin & Bouvier, 2006). A list of adrenoceptor subtypes and their respective G proteins and effectors can be found in this section of the review (see **Table 1**). G-Proteins are found in the cytoplasm, and conduct intracellularly to interact with an intracellular loop of the GPCR. In its active state, the Gβγ subunits bind tightly to the intracellular plasma membrane, where as G_a is in the inactive state, and remains attached to the Gβγ subunit.

When binding occurs with a ligand to the GPCR, the result is a conformational change leading to guanine diphosphate (GDP) being displaced from the G_a subunit by guanine triphosphate (GTP), in turn activating the G_a subunit and exposing the effector

site on the Gβγ dimer (Bockaert & Pin, 1999; Gilman, 1995). The G_a subunit alone can be divided into four major families: G a_s, $Ga_{i/o}$, $Ga_{q/11}$, and Ga_{12}, which regulate activity of different second messenger systems. These delineations are based on primary sequence. With regards to β-adrenoceptors, current literature shows a strong coupling with G_{as} and G_{ai} to initiate effectors for downstream pathways, of these include: adenylyl cyclase (AC), protein kinase A (PKA) and phospholipases (Dascal, 2001; Wenzel & Seifert, 2000).

2.3.2 The β-Adrenoceptor

Under physiological conditions, epinephrine found in the blood is as a response to stress, fright or exercise, and undeniably affects performance. Desired effects stem from drugs, which act directly, or indirectly on β-adrenoceptor in both the brain and peripheral tissue (such as skeletal muscle). Since the mid 1980's, three subtypes of on β-adrenoceptors have been identified: β_1-, β_2-, β_3- (Dixon et al., 1986; Emorine et al., 1989) and has been recognized as the most dominant adrenoceptor found in skeletal muscle, belonging to the GPCR family (Jossard, Durieux, & Freyssenet, 2013). In fact, the soleus of the rat contains 80-85% β_2-adrenoceptors and 15-20% β_1, while the plantaris of the rat is almost completely β_2 (Kim et al., 1991). Experiments conducted on mice lacking β_1-, β_2-, or both, have shown that β_2-adrenoceptors are responsible for the hypertrophy and anti-atrophy effects in muscle (Hinkle et al., 2002). With regards to specific subtype, the β_2–subtype is most prevalent, with only roughly 7–10% of β_1 present (Kim et al., 1991; Williams et al., 1984). Furthermore, when comparing β-adrenoceptor density and fiber type composition, it has been observed that slow twitch muscles have a greater density than their fast twitch counter parts (Martin et al., 1989; Ryall et al., 2002; Ryall et al.,

2004). In some cases, this has been shown by radioligand binding assay (Kim et al., 1991; Ryall et al., 2002, 2006; Williams et al., 1984). However, the work of McCormick et al. (2010) has challenged this using western blotting. Although it is unclear what this difference means with regard to function, the β-agonist response seems to be higher in fast muscle than slow (Ryall et al., 2002; Ryall et al., 2006; Kline et al., 2007). Interestingly, these results may seem counterintuitive considering that greater β-adrenoceptor density would seemingly lead to greater response to stimulation, but it is hypothesized that this difference could come from rapid dampening of receptor function by phosphorylation in slow muscle (McCormick et al., 2010).

On the other hand, β_2-adrenoceptor subtypes have wider distribution than the β_1, and control a large portion of functions in the body, as well as mediate inotropic and chronotropic effect in the heart (Brodde, 2008). With regard to skeletal muscle, β_2-adrenoceptor stimulation has observed effects including increased growth, contraction force, and speed, as well as glycogenolysis (Bowman & Anden, 1981).

The signaling transduction pathway of β-adrenoceptors will be covered fully in the following sections of the review, although at this point it is important to touch briefly on signal transduction in general. Classically, it is believed that the majority of β-adrenoceptor signaling happens through G_s coupling, which activates adenylate cyclase and thus, increases intracellular levels of cAMP (Rang et al., 2003; Alexander et al., 2007). This classical assumption has recently been developed into a new outlook on β-adrenoceptor signaling, with many layers of complexity where each receptor/G-protein couple show a wide variety of signaling mechanisms (Lefkowitz et al., 2002). Two factors that are important determinants of the pathway, which will be utilized are: 1)

protein-binding motifs of adrenoceptors, and 2) the agonist used to stimulated the adrenoceptor. When comparing β_1-adrenoceptors and β_2-adrenoceptors we see that the β_1 subtype couples with G_s and does not internalize well, however, the β_2 subtype shows a much greater capacity for internalization. Furthermore, β_2 subtypes can couple with both the G_s and the G_i for signal transduction, a term newly referred to in skeletal muscle as 'dual coupling' (Gosmanov, Wong, & Thomason, 2002; Xiao, 2001).

Table 1. *Adrenoceptor subtypes and G proteins; AKAP, A kinase anchoring protein; AC, adenylyl cyclase; PKA, protein kinase A. Modified from (Jossard, Durieux, & Freyssenet, 2013).*

Adrenoceptor Subtypes and Respective G Proteins and Effectors

Adrenoceptor	**Beta**	
Isoform	β_1	β_2
Predominant Gα isoform coupled	$G\alpha_s$	$G\alpha_s$ $G\alpha_i$ family ($\alpha_{i1,i2,i3}$)
Effector	Activation of AC ↑ cAMP Activation of PKA Activation of L-type Ca^{2+} channels	**$G\alpha_s$ mediated** activation of AC ↑ cAMP Activation of PKA Activation of L-type Ca^{2+} channels **$G\alpha_i$ mediated** Inhibition of AC ↓ cAMP Inhibition of PKA
Common secondary interacting proteins	β-Arrestins AKAPs β_1/β_2-AR β_1/α_2-AR	β-Arrestins AKAPs β_2/α_{1D}-AR β_2/β_1-AR
Primary location	Heart Skeletal muscle	Heart Lungs Vessels Kidney Skeletal muscle
Major effect on skeletal muscle	N/A	Hypertrophy

2.4.0 The β-adrenoceptor Agonist

β-adrenoceptor agonists such as adrenaline are responsible for the stimulatory action of β-adrenoceptors. Common agonists include: salbutamol, bamuterol, terbutaline, fenoterol, mapenterol, formeterol, tulobuterol, carbuterol, bromobuterol, crimbuterol, salmeterol, and clenbuterol [1-(4-amino-3,5-dichlorophenyl)-2-ter-bu-tylaminoethanol]. Clenbuterol is a sympathomimetic amine, which mimics adrenalines action on receptors. Furthermore, like most agonists, clenbuterol is used for asthma and related bronchospasm (Maltin et al., 1993). Although used therapeutically for asthma, there is a clear ability to increase muscle mass and decrease body fat (Emery et al., 1984), known as the repartitioning effects. Due to these repartitioning effects, β-agonist administration has been examined in both animal and human models – hoping to fight muscle wasting (Carter el al., 1991; Kissel et al., 1998; Lynch et al., 2001; Maltin et al., 1993). Furthermore, those in bodybuilding, as well as strength and power sports for these same reasons have quickly adopted the use of β-agonists. (Lynch, 2002; Prather et al., 1995). Adrenaline accounts for 5-10% of the total catecholamines in the central nervous system, although its function is not fully understood, it is thought to control blood pressure and respiration.

As previously mentioned, while there are a multitude of β-agonists to describe, the main focus of this paper is on epinephrine. This is, in part, due to its substantial physiological significance- considering it's role in mammalian responses like the flight-or-flight response. Furthermore, epinephrine's extensively researched background as a therapeutic aid renders it a prime candidate for further discussion on its benefits for skeletal muscle tissue. Considering the dominance of β_2 receptors in skeletal muscle, a

primary focus will be β_2 receptor agonists, such as adrenaline. Epinephrine belongs to a group of compounds known as catecholamines, which have an integral role in regulation and modulation of physiological responses in living organisms (Gulcin, 2009). Epinephrine acts as a neurotransmitter as well as a hormone. Release of the neurotransmitter is usually in response to stresses as an attempt to regulate physiological functions such as blood pressure, respiratory rate, vasoconstriction, cardiac stimulation, relaxation of smooth muscle, as well as several metabolic processes (Gulcin, 2009; Hoffman, 1996). Within the adrenal medulla, it is in the chromaffin cells and adrenaline-containing cells that adrenaline is located (Gulcin, 2009; Verhofstad et al., 1985). Adrenaline is responsible for influencing the constriction of blood vessels, controlling tissue metabolism, as well as raising the blood glucose levels (Gulcin, 2009; Vollmer et al., 1997) and lactic acid levels (Gulcin, 2009; Cui et al., 2001). Although a crucial regulator of metabolic processes, adrenaline may be most well known for its role in acute stress reaction. This catecholamine is important in the physiological response to conditions that pose a threat to the physical integrity of the body– commonly known as the fight-or-flight response system. Physiological concentration of epinephrine have been determined to be anywhere from 0.1–10nM in rats (Peters et al., 1998). Furthermore, a review of literature reveals that resting epinephrine varies from 4–140 nM in mice, however, more recent research using retro orbital bleeding observes a much smaller basal concentration of 1.1 nM (Grouzmann et al., 2003) thus showing great variability in this value, dependent on methods. In addition to findings by Grouzmann et al. (2003), the stress of a decapitation method elicited blood plasma levels of epinephrine to jump to 27.3 nM, showing a methodological dependence of results. Regardless, the effects of β_2

agonists on skeletal fibers are well documented. Responses range from showing decreased proportion of slow fibers and increased number of fast fibers in rat soleus muscle (Bricout et al., 2004; Dodd et al., 1996; Oishi et al., 2002; Ryall et al., 2002; Soic-Vranic et al., 2005; Zeman et al., 1988) to increasing mass and isometric force production by roughly 15-20% (Beitzel et al., 2004; Harcourt et al., 2007; Lynch et al., 1999).

2.5.0 β-adrenoceptor signaling in skeletal muscle

2.5.1 β_2-Adrenoceptor Signaling of cAMP

The signaling of AC and cAMP by G_{as} is the most well defined signaling pathway of β_2-adrenoceptors (Hinkle et al., 2002; Navegantes et al., 2000). The second messenger function of cAMP in skeletal muscle is both spatially and temporally regulated in muscle by numerous mechanisms (Tasken & Aandahl, 2004). These two mechanisms are *1)* AC and *2)* phosphodiesterases. It is well founded that AC is responsible for the conversion of ATP to cAMP, a process that plays host to a number of downstream affects in skeletal muscle. Thus, AC plays a major role in β_2 agonist mediated signaling. The activity of each AC isoform generally increases after binding with a stimulatory G_a protein or decreases after binding with an inhibitory G_i protein (Hanoune & Defer, 2001).

The second mechanism for regulation of the effects of cAMP is phosphodiesterase (PDE). With 50 different PDE proteins stemming from 21 genes, the PDE family is vast (Venter et al., 2001). In mammals, there is a very similar structural framework to PDEs (Essayan, 1999; Francis et al., 2001), important in ensuring that these enzymes (PDEs) are used in hydrolyzing and inactivating cyclic nucleotides into 5-AMP (Bloom, 2002; Sham et al., 1991; Tasken, 2004). Therefore, intracellular cAMP levels are a product of the equilibrium between cAMP production via AC converting ATP, and degradation of

cAMP via PDEs. In other words, PDE is phosphorylated by PKA, leading to the hydrolysis of cAMP (Dodge-Kafka & Kapiloff, 2006), thus PKA has a negative feedback mechanism, which limits the temporal expression of cAMP. In skeletal muscle, there are multiple isoforms of PDEs expressed, and the activity of one specific PDE can strongly impact processes regulated by cyclic nucleotides (Bloom, 2002; Hetman et al., 2000; Sham et al., 1991). Work by Bloom (2002) was the first report on the expression profile of skeletal muscle PDEs since their discovery. Bloom defines three isoforms of PDE responsible for hydrolyzing cAMP: PDE4, PDE7, and PDE8. Interestingly, using cAMP assays, this researcher determined that PDE4 is the biggest contributing isoform of the three, for the degradation of cAMP. With regard to regulation of PKA, the MAPK family is found to decrease PDE activity (Dodge-Kafka et al., 2005; Hoffmann et al., 1999). Adrenaline has affects on PKA, and as such, the phosphorylation of PDEs as well.

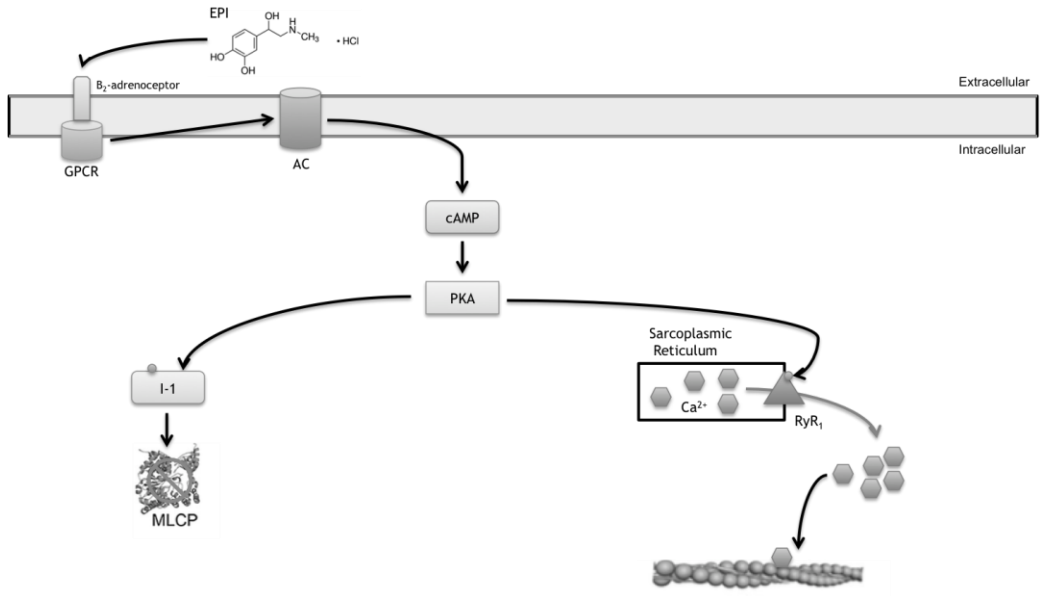

Figure 7. Gαs -, Gαi -, and Gβγ signaling pathways in skeletal muscle, all activated by a β_2-agonist stimulation via the β2-adrenoceptor.

2.6.0 The effects of β-adrenoceptor on skeletal muscle function

2.6.1 β_2-Agonist on Skeletal Muscle Fiber Type, Force, and Force Development

The effects that β_2-agonists have on skeletal muscle are vast. Current literature defines a role of β_2-receptors, which includes: positive outcomes on fiber type, size, and force, among other things. β_2-agonist administration has shown decreases of slow fiber proportions and increases of fast fibers in skeletal muscle, specifically in the soleus of rats (Bricout et al., 2004; Dodd et al., 1996; Oishi et al., 2002; Ryall et al., 2002; Soic-Vranic et al., 2005; Zeman et al., 1988). In addition to the effects resulting in fiber type changes, there is increases in muscle mass as well as increased max isometric force production of skeletal muscle by 15-20% (Beitzel et al., 2004; Harcourt et al., 2007; Lynch et al., 1999). In an acute setting, major differences exist between fiber types when comparing the affects of epinephrine on force production (fast ↑, slow ↓), adrenoceptor density (fast ↓, slow ↑). Work by Andersson (2012) supports these conclusions, as these researchers reported increased isometric twitch force of the mouse EDL, with 1 uM isoproterenol *in vitro*. On the other hand, a number of studies on chronic exposure to β2-agonist in animals have showed that when used in high doses (greater than human tolerance), β-agonists can elicit significant increases in muscle mass by 10-25% over 10–20 days (Agbenyega & Wareham, 1990; Baker et al., 1984; Bardsley et al., 1992; Beermann et al., 1987; Carter et al., 1991). This capability of increased force vanishes several weeks after stopping treatment (Ryall et al., 2007), although, normalized force of muscle remains unchanged – this suggests that the increased ability to produce force is likely an effect of muscle mass (Beitzel et al., 2004; Harcourt et al., 2007; Lynch et al., 1999). Furthermore, collagen deposits have been detected with treatment in skeletal

muscle, which may alter contractile properties of the muscle (Kumar and Sharma, 2006; Patiyal and Katoch, 2006). Literature also suggests a decrease in capillary density (Suzuki et al., 1997) and skeletal muscle blood flow (Beitzel et al., 2004; Rothwell et al., 1987). Together, these changes could increase the distance for oxygen to diffuse, reduce oxygen supply to skeletal muscle, and increase muscle fatigability during extended contractile activity. So it would seem that there is equilibrium to be found between increasing max isometric force of the muscle, and the adverse effects on exercise capacity, which may limit the usefulness of β_2-agonist on skeletal muscle.

The first examples of epinephrine directly influencing skeletal muscle contractions came from Oliver and Schaefer (1895) who used extracts of the adrenal medulla to increase muscular contractions. This work has been supported dating back to before the 1900's, and since then adrenaline has been known for it's ability to increase max twitch tension in unfatigued muscle (Oliver & Schaefer, 1895; Gruber, 1922a, b; Goffart & Brown, 1947; West & Zaimis, 1949; Brown, Goffart & Dias, 1950; Goffart & Ritchie, 1952; Huidobro, Cubillos & Eyzaguirre, 1952; Goffart, 1952, 1954; Montagu, 1955). By the 1950's it had already been concluded that epinephrine and norepinephrine increased postural tone, improved respiration and increased contraction of other muscles. Furthermore, it was demonstrated that this increase in max tension was not in fact characteristic of all skeletal muscles. Although earlier work by Goffart and Ritchie (1952) concluded epinephrine depressed max tetanic tension, these results were considered flawed due to their methods resulting in vasoconstriction. Bownman and Ziamis (1958) showed that cat soleus muscle responded in the opposite fashion. Using three different amines (epinephrine, norepinephrine, and isoprenaline) these researchers showed that cat

tibialis anterior muscle consistently increased in sub-max and max twitch tension, while the soleus decreased in all cases. Along with increases in max twitch tension, these amines showed altered twitch time courses, where rate of development of tension decreased, while time to peak tension increased in the tibialis anterior, boosting the overall twitch duration by 17% (Bowman and Ziamis, 1958). This increase in time to peak had been observed earlier (Goffart & Ritche, 1951), who suggested that because in some cases time to peak increased, but not tension – these two factors or not closely interdependent. This lead to the idea that in skeletal muscle, adrenalines effects during the rising phase didn't act through increased recruitment, because time to peak tension slowed as opposed to sped up.

In the soleus muscle, similar characteristics were affected, where max twitch tension was diminished by 18% and overall duration of the twitch reduced by 33%. Interestingly, relaxation time of soleus muscle increased. One of the most profound results of this study was the delineation between muscle type and sensitivity to sympathetic amines, which had been noted by Goffart and Ritchie (1952), who believed that amine effect was relative to proportion of red to white fibers. The soleus was found to be much more sensitive to epinephrine and isoprenaline compared to the tibialis anterior, and ~ 50 fold less sensitive to norepinephrine than epinephrine or isoprenaline (see Table 2). This difference in sensitivity was hypothesized to be the cause for feeling weakness in the limbs during states of emergency or fright by decreasing tension in postural muscles by circulating adrenaline. These experiments began to show early signs of differences in fiber type sensitivity to β_2 agonist/antagonists, as well as confirm

adrenaline's action on muscle contractility, and show changes in rate of development of tension as well as time to peak tension.

Table 2. *The required intravenous dose (μg/kg) for minimal effect of epinephrine, norepinephrine and isoprenaline in the tibialis anterior and soleus. (Bowman and Zaimis, 1958).*

	Minimal Effect Intravenous Dose (μg/kg)		
Muscle	*Epinephrine*	*Norepinephrine*	*Isoprenaline*
Tibialis anterior	3-10	5-15	2-8
Soleus	0.06–05	5-20	0.06-0.4

2.6.2 β_2-Agonist Molecular Signaling for Increased Force and The Role of Ca^{2+}: Proof From Genetic Knock-Out Mice

Currently, it is well established that skeletal muscle displays increased peak force upon adrenergic stimulation (Brown et al. 1948; Cairns & Dulhunty, 1993b). However, despite its recognized role of this response, its molecular mechanism is still not fully defined. Up to this point, this review establishes that β_2-agonists stimulate G_s protein receptors, which in turn activates AC, causing cAMP generation to activate PKA (Rockman et al. 2002). Furthermore, it is well documented that fast muscle fibers evoke a strong inotropic response to β_2-agonists, as a result of a potentiated increase in $[Ca^{2+}]$ (Cairns & Dulhunty 1993a). This missing link between PKA mediated phosphorylation, and changes in $[Ca^{2+}]$ were recently addressed by Andersson et al (2012). These researchers used genetically altered mice, whom express a mutated RyR1 (ryanodine receptor type 1, on the sarcoplasmic reticulum) which cannot be phosphorylated by PKA, to show that mammalian fast muscle β_2-agonists dependent increases in $[Ca^{2+}]$ and force are reliant on phosphorylation of the RyR1. Thus, implementing the sarcoplasmic reticulum as the connection between β-receptor stimulation and altered force.

To support their work, Andersson and colleagues (2012) observed changes in twitch force of the EDL in both wildtype mice, as well as the RyR1 mutated mouse. Results indicated that, before the addition of β-agonists, both strains were similar in force development and force generation. However, after the β-agonist (isoproterenol) was added, wildtype muscles had significantly increased twitch force (control 140 kPa; isoproterenol 159 kPa) as seen in **Figure 2**, while the mutated mice exhibited no change in force (control 145 kPa; isoproterenol 142 kPa). Furthermore, rate of force development increased in wildtype mice, while there was no change in the mutated mice. These results suggest the importance of RyR1 phosphorylation as a mechanism for β-agonist action on the SR, and that this phosphorylation is critical in promoting enhanced Ca^{2+} release during contraction.

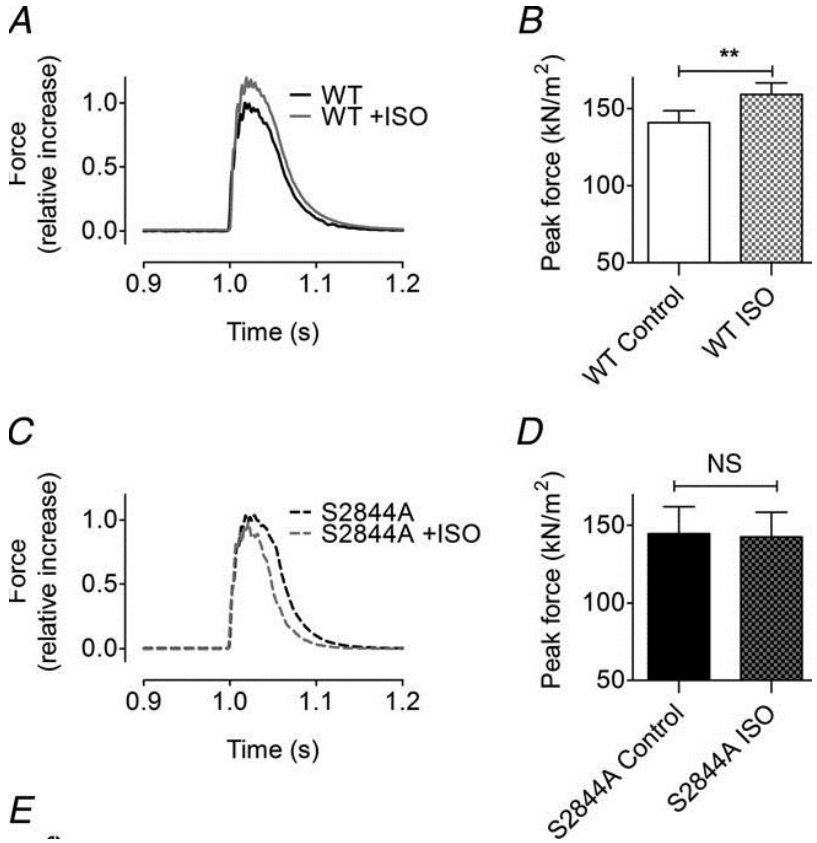

Figure 8. A. Effect of isoproterenol on force generation in wildtype EDL; **B.** Effect of isoprterenol on peak force in wildtype EDL; **C.** Effect of isoproternol on force generation in RyR1 mutated EDL; **D.** Effect of isoproternol on peak force in RyR1 mutated EDL. (Anderson et al. 2012)

Statement of The Problem

3.1.0 Central Research Question

The primary objective of the proposed research was to test whether β-adrenergic stimulation augments the time-course and characteristics of concentric twitch potentiation, and if these changes could be correlated to altered myosin phosphorylation. To this end, we assessed concentric twitch potentiation as well as myosin phosphorylation in wildtype as well as skMLCK$^{-/-}$ knockout mice, in both the presence and the absence of epinephrine.

3.2.0 Hypothesis

We hypothesized that a prolongation of the potentiated state in response to epinephrine incubation would be observed in wildtype muscles. In contrast, we expected that no prolongation of PTP would be observed in skMLCK$^{-/-}$ knockout muscles. We expected this difference to be due to the fact that epinephrine prolongs myosin phosphorylation (Decostre et al. 2000), a mechanism that will affect wildtype but not skMLCK$^{-/-}$ knockout muscles. On the other hand, a contrary result would be grounds to reject the null hypothesis, confirming that epinephrine incubation alters concentric twitch potentiation via some other mechanism.

3.3.0 Assumptions

We assumed that there are no phenotypical differences between the wildtype and skMLCK$^{/-}$ mouse, other than the skMLCK gene ablation and coat color (aguti coat). For example, the work of Gittings et al. (2011) genotyped both wildtype and skMLCK$^{-/-}$ EDL function and structure; showing there was no significant difference between fiber compositions of the EDL between genotypes (**Figure 9**), and that the ablation of the skMLCK gene has little effect on unloaded shortening velocity. In addition, we assumed that there is no presence of other intracellular kinases that are capable of phosphorylating the myosin RLC.

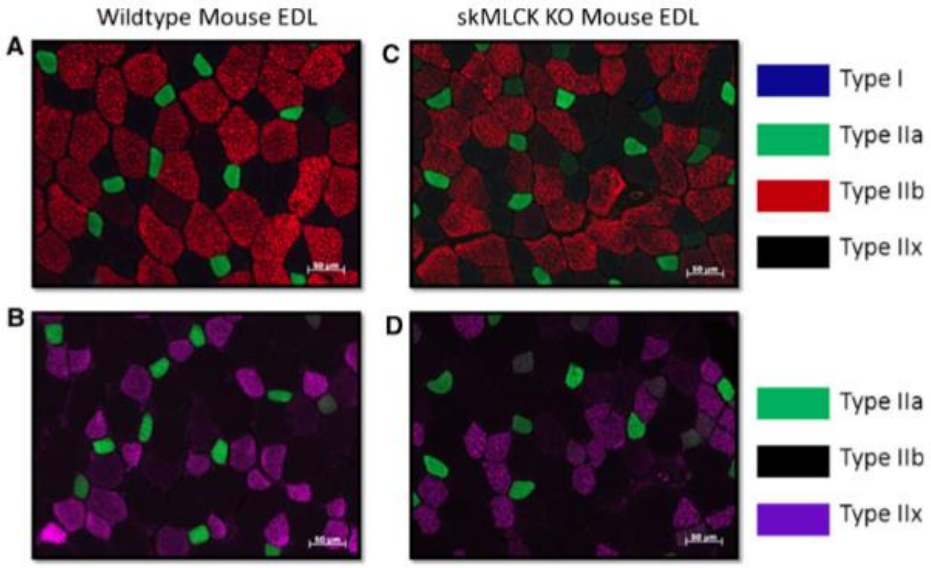

Figure 9. MHC expression in mouse EDL muscle (Gittings et al., 2011); (**A, B)** Representative EDL cross- sections from wildtype (a) and skMLCK knockout (c) mice incubated with antibodies to identify type I (blue), type IIa (green), type IIb (red), and type IIx (unstained) fibers. (**C, D)** Representative EDL serial cross-sections of (a) and (b) from aildtype (b) and skMLCK knockout (d) mice stained with antibodies to identify type IIA (green) and type IIx (purple) fibers. Fibers with positive staining for two MHC isoforms were identified as Hybrid fibers. Bars represent 50 uM.

Methods

4.1.0 Wild-Type (WT) & skMLCK Knockout (KO) Mice

Two independent strains of C57BL/6 adult mice (2-5 months) were used through the experiment. The first strain, wildtype mice acquired were ordered from Charles River, Drummondville QC Canada, and housed at Brock for ~1 week before experiments began. The second strain, the skMLCK$^{-/-}$ mice (C57Bl/6 background) were obtained from our own breeding colony at Brock University. The non-dominant coat color allele is spatially associated with the targeted gene for myosin light chain kinase knockout, allowing convenient manipulation of coat phenotype as a marker for each genetic strain. As such, all wildtype (WT) mice were black (homozygous for the recessive non-agouti allele) and all skMLCK knockout (KO) mice were agouti (light brown). Mice were housed in small groups (1-5) and given free access to standard chow and water until required for experimental procedures. All experiments are approved by the Brock University Animal Care and Use Committee (AUP # 14-06-01).

4.2.0 Experimental Apparatus

All contractile experiments were completed using a custom-designed apparatus (from Aurora Scientific, Inc.) capable of accurately controlling muscle length and a variety of environmental factors. The mouse extensor digitorum longus (EDL) muscle was suspended in an oxygenated organ bath (Radnoti Glass Technology, Inc) containing a physiological salt solution maintained at constant temperature using an Isotemp 3013S circulator (Fisher Scientific). Muscle stimulation was applied using flanking platinum electrodes driven by a Model 701B biphase stimulator (Aurora Scientific, Inc.). Muscle length was monitored using a horizontal stereo zoom microscope (Bausch & Lomb),

which could be manually controlled at increments of 0.01mm using a sliding micrometer (Velmex, Inc). Contractile data was collected at 1000Hz using a 305B servomotor acquired through a 604C analog to digital interface, and controlled by a dual-mode lever system (ASI). Data acquisition and basic analysis was performed using ASI 600a software (Version 1.60) run on a LINUX based operating system, and further examined using Prism 6 Graphpad.

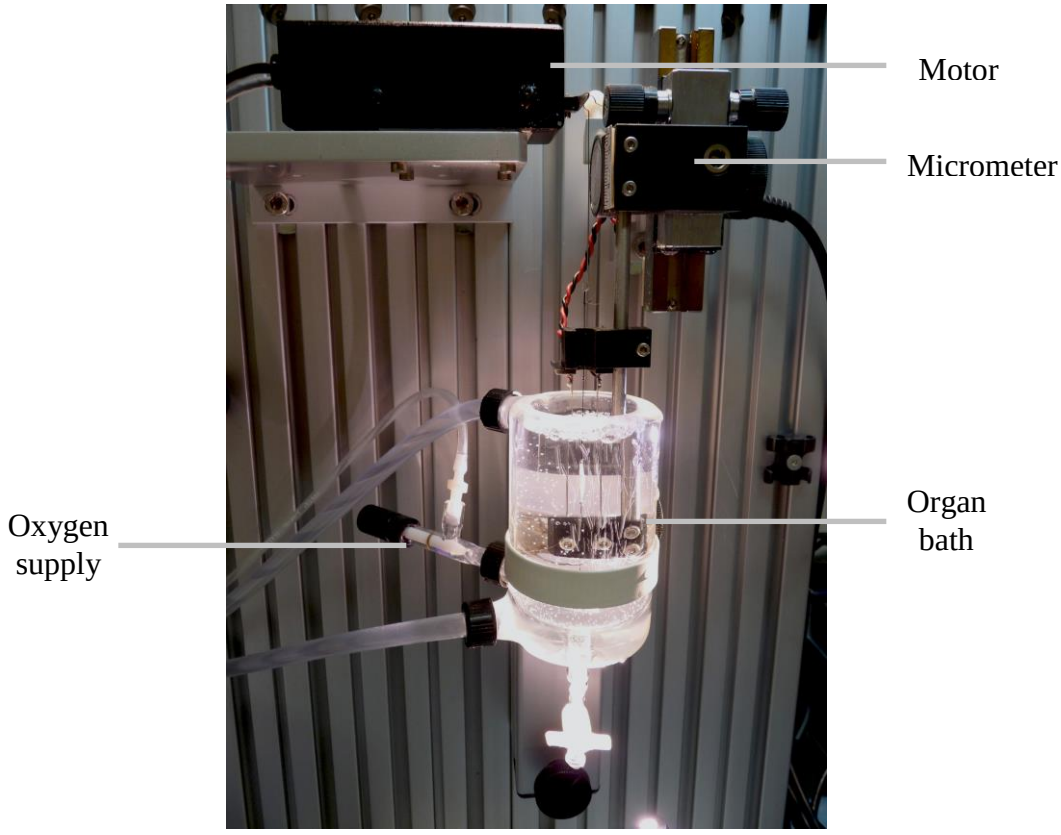

Figure 10. ASI organ bath containing Tyrode's solution for *in vitro* intact muscle experiment.

4.3.0 Surgical Removal of EDL & Muscle Preparation

Surgical removal procedure has been standardized in the lab of Dr. Rene Vandenboom (Vandenboom et al., 2013; Gittings et al., 2014). Animals were initially sedated with an intraperitoneal injection of Somnitol (Soldium-Pentobarbitol, see **Appendix A, Table A.1**) diluted 1:10 with saline (0.025ml/g body weight). The EDL was carefully excised from each hind limb after a non-absorbable braided silk (4-0) suture is fastened to the proximal and distal tendons. One EDL was mounted into the experimental apparatus immediately while the other was maintained in an oxygenated Tyrode's solution on ice (see **Appendix A**, **Table A.2**). Following EDL removal (See **Appendix B**), the animals were euthanized by lethal injection into the heart (0.05ml/g body weight) and disposed of according to Brock University Animal Facility protocol.

The Tyrode solution proposed for use in all experiments served as a favorable environment for muscle contraction and was intended to provide muscle tissue with the essential substrates and ions present in vivo. Final ionic concentrations are (in mM): 121 NaCl, 5 KCl, 24 $NaHCO_3$, 0.4 NaH_2P0_4, 0.5 MgCl, 1.8 CaCl, 5.5 D-Glucose, and 0.1 EDTA. The solution was continuously gassed (95% O_2, 5% CO_2) using a scintillated glass dispersion valve (Radnoti) and maintained at 25° C (+/- 0.5 ° C).

4.4.0 Experimental Design

The isolated *EDL in vitro* model was used for all experiments to elucidate the role of epinephrine administration on post-tetanic twitch potentiation. Two identical sets of experiments were conducted on EDL muscles from wildtype and $skMLCK^{-/-}$ mice for analysis of: 1) contractile function, and 2) biochemical quantification of RLC phosphorylation. Each set of contractile experiments involved the quantification of post-

tetanic potentiation and contractile performance, as well as phosphorylation of the myosin RLC. Contractile data was collected from a total of 8 muscles from each group (wildtype and skMLCK$^{-/-}$) using matching experimental procedures. An example of experimental design and protocol can be found in **Figures 11** and **12**, below.

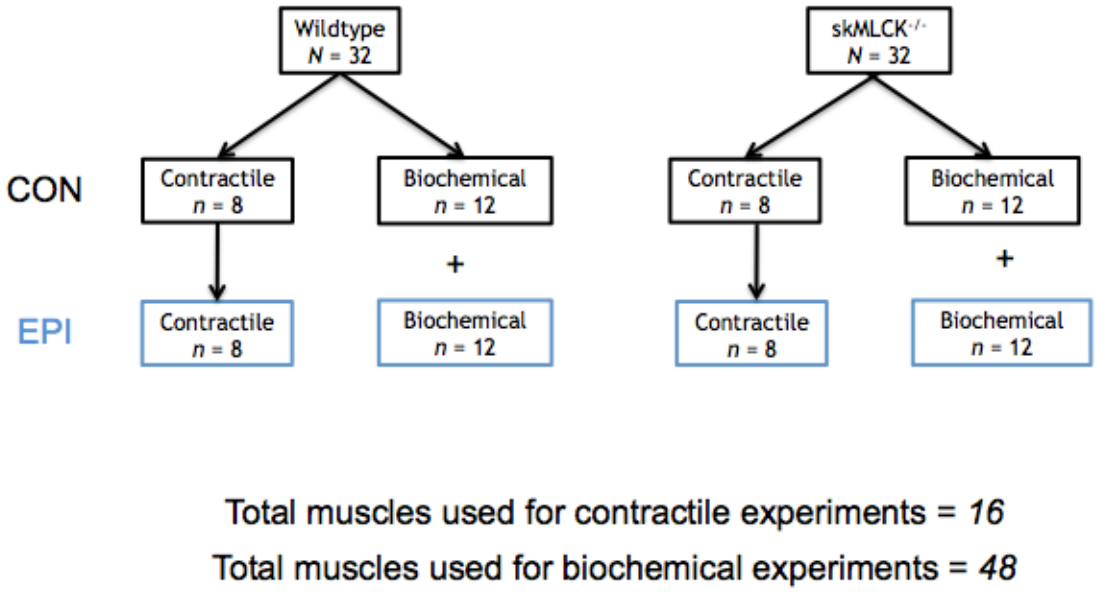

Figure 11. Experimental Group Design (CON, Control; EPI, Epinephrine)

The second set of experiments was conducted to observe the EDL in the potentiated state, under the influence of varying amounts of epinephrine, after which the EDL was rapidly removed from the *in vitro* environment (<15 seconds) and freeze clamped for biochemical analysis. The collective data proposed in this project therefore represents an analysis of twitch force modulation by post-tetanic potentiation during resting conditions and a more comprehensive account of contractile function and physiological/biochemical status under the influence of epinephrine.

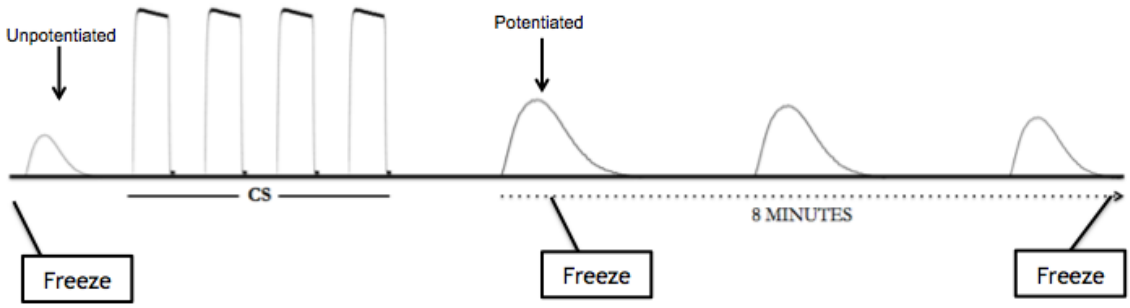

Figure 12. Experimental Protocol (CS, Conditioning stimulus)

4.4.1 Epinephrine Preparation

On the day of an experiment, fresh epinephrine [(±)-Epinephrine hydrochloride, E4642 SIGMA] was prepared into a 1mM stock solution. Next, each Tyrode bath was prepared separately depending on the epinephrine concentration for that experiment (1 μM). Experimental concentrations of epinephrine were determined based on previous *in vitro* experiments (Decostre et al. 2000; Andersson 2012) as well as pilot experiments of epinephrine titrations to determine optimal concentration of 1 μM (that which caused maximum effect on PTP) seen in **Figure 13**.

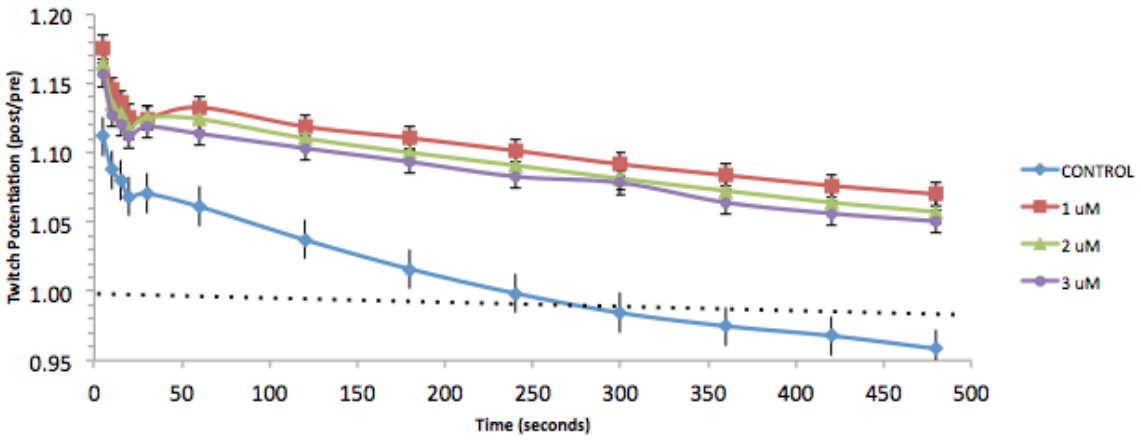

Figure 13. Titration of three different epinephrine concentrations (1, 2, 3 uM) on concentric PTP time course of wildtype EDL 25°C

4.4.2 Optimal Length

To normalize all force data fiber diameter, resting muscle length and optimal muscle length (L_o) was measured during initial force-length measurements. Optimal length (L_o) is defined as the length at which peak active twitch force (P_t) was elicited and will be used as the reference length for all shortening amplitudes. Considerable attention was given to the control of muscle length, as twitch force potentiation is highly length-dependent.

4.4.3 EDL Stimulation

Two pre-programmed stimuli were used to excite the EDL preparations during all contractile experiments. All were applied at supramaximal voltage to ensure that all motor units were fully activated. For tetanic contractions, 150Hz stimulation represents a supramaximal motor-unit firing rate producing completely fused tetani. The conditioning stimulus (CS) for the potentiation protocol is standard for our lab, and was intended to maximize RLC phosphorylation and PTP, while simultaneously minimizing fatigue.

4.4.4 Stimulation Profiles

- S1. Single Muscle Twitch ➔ 1Hz
- S2. Conditioning Stimulus (CS) ➔ 4, 100Hz, 400ms, 10s

4.5.0 Calculation of Pre-Tetanic and Post-Tetanic Twitch Force

Central to the calculation of relative measures such as force potentiation was the determination of a representative control contraction to serve as a reference. For each experiment, twitch force was measured prior to the conditioning stimulus as an average force of three twitches at 20 second intervals. After the conditioning stimulus, twitch force was measured several times as the value of post-tetanic twitch force. The ratio of post-tetanic to pre-tetanic twitch force (post / pre) at any given time represents a normalized value of potentiation.

The PTP protocol was designed to produce long lasting PTP in wildtype muscles as well as a lesser potentiation in skMLCK$^{-/-}$ muscles. After applying the standard conditioning stimulus (100Hz, 400ms, 10s), concentric twitches were measured at 5, 10, 15, 30, 60, 120, 180, 240, 300, 360, 420, and 480-seconds (following cessation of the CS). The concentric twitches were shortened from 1.05 to 0.95 L_o at a speed of 30% V_{max}. Therefore, the time to shorten will be 77 milliseconds.

4.6.0 Peak Force Production

Peak force is defined as the highest or maximal tension produced in response to twitch (P_t), measured in mN. To obtain the peak active force for each individual twitch, we used the measured total force and subtract the passive force. The resulting traces are shown below in **Figure 14**.

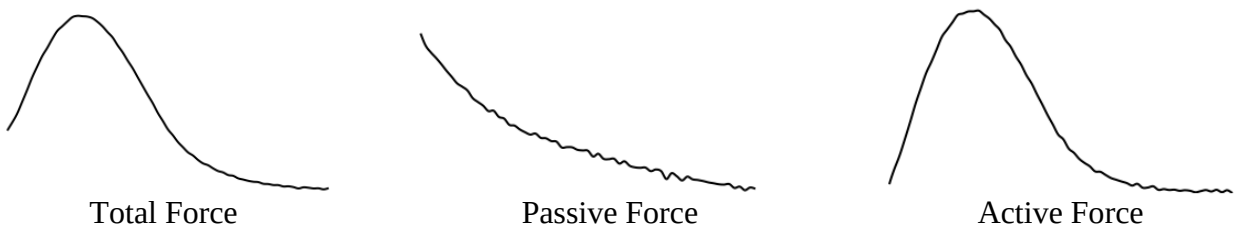

Figure 14. Total, Passive, and Active Force Traces of a Concentric Twitch (EDL). Active force during shortening is calculated by subtracting passive force from total force.

4.7.0 Rate of Force Development (dF/dt)

The peak values for rates of force development (mN/ms) were determined using the ASI 600a software package, which plots a rate function of instantaneous values of dF/dt following smoothing using a Savitsky-Golay Filter.

4.8.0 Biochemical Analysis of Muscle Tissue

4.8.1 Quantitative Determination of Proteins: Bradford Assay

Materials and methods for performing Bradford assay using BSA standard were provided by the lab of Dr. Sandra Peters (Bradford, 1976; from J. R. Choptiany). These experiments used a BSA standard and fresh (day of) whole muscle homogenate of wildtype EDL muscle prepared in lysis buffer. Muscle samples were removed from the -80C freezer and immediately placed in liquid nitrogen. After removing the silk sutures from each end of the muscle, samples underwent buffer treatment with both acetone and water-based protein percipitation solutions (**Appendix D**) and homogenization in a glass homogenizer. Upon removing frozen muscles from the -80C freezer, protein content of each sample was determined using Gen5 2.09 analysis software by running homogenate samples against a dilution spectrum of BSA standard (1, 0.5, 0.25, 0.125, 0.05, 0) and measuring relative absorbance (BIO-TEK *Synergy HT*). A full list of materials, reagents, procedure, apparatus and results used during this protocol can be found in **Appendix C**.

4.8.2 Gel Electrophoresis and Western Blotting

Materials and methods for performing gel electrophoresis and immunoblotting for myosin RLC phosphorylation were provided by the lab of Dr. James Stull (Zhi et al., 2005; Ryder et al., 2007; Gittings et al., 2014). A detailed list of solutions and methods used in this process can be found in **Appendix D**. Myosin regulatory light chains are small (18-20 *kDa*) acidic (net charge of -18) proteins that migrate easily in polyacrylamide gels containing glycerol for density. RLCs are denatured with tricholoroacetic acid (TCA) and solubilized in urea to dissociate RLC from myosin heavy chain. The addition of single phosphate introduces two additional negative charges at pH 8.6 (that of the running buffer) so the phosphorylated protein migrates faster than the non-phosphorylated RLC. The first day of procedures involves solution preparation, sample preparations, electrophoretic separation, transferring the protein to a nitrocellulose membrane, followed by blocking and overnight incubation with the primary antibody. The second day of procedures involves immunoblotting and imaging. Determination of percentage (%) phosphorylation is measurement of the band density for the mono-phosphorylated band divided by the band density of the total protein (**Equation 1**).

***% Phosphorylation* = (Density Mono-P band) / (Density Total protein)**

$$\therefore$$

***% Phosphorylation* = (Density Mono-P band) / (Density Mono-P + Density Non-P)**

Equation 1. Calculation for determining the % phosphorylation of RLC protein bands. Mono-P, *mono-phosphorylated RLC band;* Non-P, *non-phosphorylated RLC band.*

Myosin RLC phosphorylation was measured in isolated mouse extensor digitorum longus muscles after being snap-frozen in in clamps pre-cooled in liquid nitrogen. Samples were then placed in an acetone-based protein precipitation solution (0.5 g TCA; 7.71mg DTT; 5 mL Acetone) slurry and brought to room temperature. Following this,

silk sutures were removed and muscle samples were placed into a glass homogenizer containing water-based protein precipitation solution (0.5 g TCA; 7.71mg DTT; 5 mL dH_2O). Once homogenized, resuspension takes place by washing protein pellets in ether and adding urea sample buffer. Prepped samples then underwent electrophoretic separation, where the nonphosphorylated RLC is separated from the mono-phosphorylated RLC (Zhi et al., 2005; Ryder et al., 2007). Antibodies raised in rabbits to purified skeletal RLCs (proided by the lab of James Stull) were used for the appropriate analyses. Goat Anti-Rabbit IgG horseradish peroxidase (Santa Cruz Biotechnology) secondary antibodies were used with ECL prime luminol and oxidizing reagents (GE Healthcare), and quantitative measurements were processed on a Li-COR C-DiGit Blot Scanner and analyzed in Image Studio.

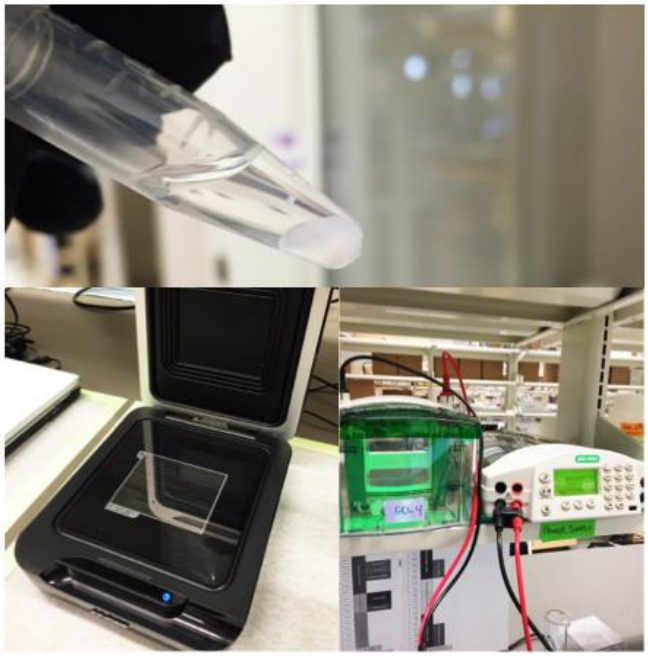

Figure 15. Images of each step of the urea/glycerol-PAGE method used in this project. *Top Middle*, an example of whole EDL muscle homogenate during ether washing to remove residual TCA; *Bottom Left*, C-DiGit Blot Scanner used in the quantification of myosin RLC phosphorylation; *Bottom Right*, Electrophoresis and transfer tank (Bio-Rad Technologies) along with power supply.

4.9.0 Laboratory Procedures

Prior to a standard 30-minute equilibration period, the EDL was stimulated (150Hz, 1000ms) to produce a contraction forceful enough to remove any compliance and possible slippage in the tendon-suture unions. Subsequently, a single twitch was applied at 0.05Hz while sequentially increasing current intensity until a maximum twitch force was reached. The stimulus intensity was then be increased ~25% and remained at this magnitude for the duration of each experiment to ensure maximal excitation of all motor units.

The resting EDL was then manipulated to determine optimal length, L_o. Starting at ~0.7L_o the muscle will be lengthened at 0.02 L_o increments while receiving a twitch stimulus at each length. The muscle length at which active twitch force reached a maximum was documented as L_o and used as the reference length for all subsequent length steps. The accuracy of all length changes and positions was corroborated manually using a stereo zoom microscope (Bausch & Lomb) to provide measurements of actual muscle length (mm).

Following these standard preliminary procedures, a contractile experiment was conducted. Each experiment was officially terminated when the EDL is rapidly freeze-clamped and stored at -80° C for future analysis. Prior to the mounting of each fresh EDL muscle, the Tyrode solution was replaced with a fresh aliquot and given sufficient time to equilibrate.

4.10.0 Data Analysis & Statistics

The primary investigation of this research was the effect of epinephrine on concentric twitch force potentiation in mouse EDL muscle. Data was initially screened for outliers, and checked for statistical assumptions of normal distribution and equality of variances. Following this screening, appropriate analysis was selected for each set of data. For each measure, significant difference between groups will be determined using ($p < 0.05$). All data will be presented as the sampled mean +/- SEM and was analyzed in Prism 6 Graphpad.

To analyze *within genotype* factors such as absolute concentric twitch force, relative concentric twitch force (i.e., wildtype vs. wildtype) a two-way repeated measures ANOVA for each condition was used, followed by a Holm-Sidak's correction. To analyze *within genotype* factors affected by epinephrine (i.e., wildtype control vs. wildtype epinephrine) a two-way repeated measures ANOVA was used, followed by a Sidak's multiple comparisons test.

To analyze *between genotype* factors such as absolute concentric twitch force, relative concentric twitch force (i.e., wildtype vs. skMLCK$^{-/-}$) a two-way repeated measures ANOVA for each condition was used, followed by a Sidak's correction. To analyze peak tetanic force values *between genotypes,* multiple t-tests were conducted using by Sidak's correction ($P < 0.05$).

To determine the effect of the CS on myosin phosphorylation in wildtype muscles, a two-way ANOVA was conducted, followed by a dunnet's test for significance over time. Multiple t-tests were used for each time-point to determine the effect of epinephrine on myosin phosphorylation (wildtype control vs. wildtype epinephrine).

In order to fully characterize the results of this study, the contractile data before treatment with epinephrine (i.e., *mean* twitch force, *peak* twitch force, and tetanic force) and was analyzed in two ways; *absolute force* and *relative*, which will be denoted using subheadings. Within each measure of force, a *between* genotype (wildtype vs. skMLCK$^{-/-}$) as well as *within* genotype (effect of time) analysis was conducted. Following this, the epinephrine data was analyzed in the same fashion. After illustrating the effect of epinephrine treatment on contractile function, the twitch kinetics data was examined (rate of force development, rate of relaxation, time to peak tension) both with and without epinephrine treatment. Lastly, analysis of the biochemical data (myosin phosphorylation) collected in this study was conducted.

Statistical test specifics i.e., main effect, F-score and statistical significance will be located in the text, while details regarding statistical testing, levels of significance and post-hoc analysis can be found in figure and table captions. Any data or statistical information not presented directly in the **Results** section can be found throughout the **Appendix D, E, F, and G** as referenced**.**

Results

5.1.0 Mouse Characteristics

In these experiments, adult mice (3-5 months) from two different genotypes (wildtype and skMLCK$^{-/-}$) were split into two experimental categories: contractile and biochemical. No significant difference was found for mass (g) between wildtype and skMLCK$^{-/-}$ mice used in the biochemical experiments; however the mean mass of wildtype mice in the contractile experiments was found to be significantly higher than mean skMLCK$^{-/-}$ mass ($P < 0.05$). The exact age of mice (days) in the wildtype genotype could not be determined as it was not presented from the breeder (Charles River), however this group is confirmed to be adult mice aged ~91-152 days. On the other hand, mice from the skMLCK$^{-/-}$ mice had a mean age of 97.5 days, a result that may account for the difference in weight between genotypes. For the present discussion, it is noted that animals in both genotypes have reached sexual maturity (Fox et al., 2006); thus differences in both age and mass probably did not significantly influence the structure or function of the EDL muscles enough to influence the main results. Means ± SEM for mice involved in either contractile or biochemical experiments are presented in **Table 3.**

Table 3. *Mean mass for mice used in both contractile and biochemical experiments.*

	Mean Mouse Mass (grams)		
Genotype	**Contractile Experiments**		**Biochemical Experiments**
Wildtype	25.8 ± 0.6 g	> *	28.3 ± 0.9 g
skMLCK$^{-/-}$	19.4 ± 0.1 g		22.3 ± 2.9 g

Values are presented as mean ± SEM**;** mass in grams (g) for mice in contractile experiments ($n = 5$) and biochemical experiments ($n = 6$ - 12);***** Value is significantly greater than skMLCK$^{-/-}$ genotype (Tukey's HSD, $P < 0.05$).

5.2.0 Contractile Measures

5.2.1 Absolute Concentric Twitch Force

5.2.1.1 Within Genotype Analysis

Absolute *mean* concentric twitch force was enhanced in both genotypes above unpotentiated values following the conditioning stimulus. Results of a two-way repeated measures ANOVA indicated that both genotypes displayed enhanced mean force over time (**Table 4;** Wildtype, P <0.0001; skMLCK$^{-/-}$, P <0.0001). A second two-way repeated measures ANOVA was then conducted to analyze the effect of the conditioning stimulus and time on absolute *peak* concentric force. Results of the ANOVA indicated that absolute peak force followed a similar trend to mean force in both wildtype (P < 0.0001) and skMLCK$^{-/-}$ muscles (P < 0.0001); displaying significantly elevated levels after the conditioning stimulus (**Table 4**). One difference, however, is that skMLCK$^{-/-}$ control muscles did not exhibit elevated peak twitch force by the 8-minute mark (P = 0.907).

5.2.1.2 Between Genotype Analysis

A between genotype analysis showed wildtype muscles displayed a larger increase in absolute twitch force than skMLCK$^{-/-}$ muscles after the conditioning stimulus (**Table 4;** P < 0.0001); in contrast there was no significant difference between the unpotentiated mean twitch force (P = 0.078). In addition to twitch force measurements, an analysis of peak tetanic force during the CS was conducted (**Table 4**). Indeed, **Figure 16** shows that peak tetanic forces (control condition) were not significantly different between genotypes. Full results of the post-hoc multiple comparison tests of mean force, peak force, and peak tetanic values are presented as means ± SEM in **Table 4.**

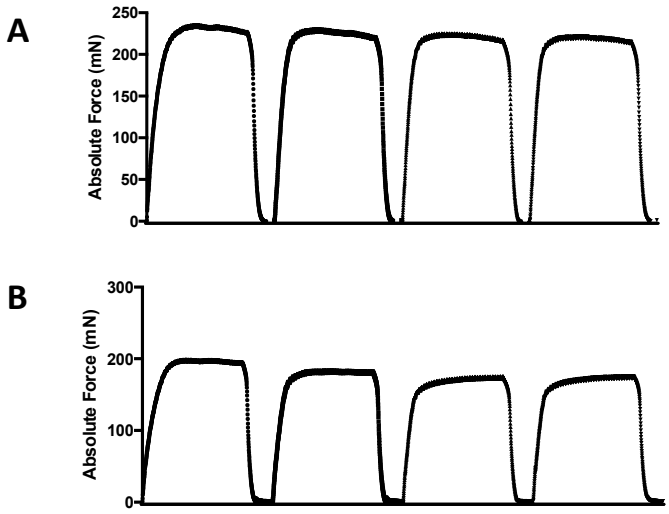

Figure 16. Representative trace of tetanic force (mN) in wildtype **(A)** and skMLCK$^{-/-}$ **(B)** control muscles during the conditioning stimulus (100Hz).

5.2.2 Relative Concentric Twitch Force: PTP

It was initially hypothesized that wildtype muscles would show greater concentric force potentiation (post-CS/pre-CS) than skMLCK$^{-/-}$ muscles over the 8-minute time course. To this end, a two-way repeated measures ANOVA was conducted for *mean* concentric force potentiation between wildtype and skMLCK$^{-/-}$ muscles which indicated that there was a main effect for genotype in the control condition (**Table G.1**; $P < 0.01$). Furthermore, a two-way ANOVA was conducted to determine the effect of time in combination with a condition stimulus on relative force production. This analysis established a significant main effect for time in both wildtype ($P < 0.01$) and skMLCK$^{-/-}$ ($P < 0.0001$); the results of which are presented as means ± SEM in **Table 4.**

A new two-way repeated measures ANOVA was then conducted to determine the effect of the CS on relative *peak* concentric force. Results of the ANOVA revealed that peak concentric force potentiation showed similar trends to that of mean force; displaying significantly increased PTP after the CS (**Table 4**). Moreover, while skMLCK$^{-/-}$ muscles

($P < 0.0001$) exhibited a slight decrease in PTP by the 8-minute mark, wildtype muscles ($P < 0.0001$) exhibited a maintenance of ~4.00 ± 0.02% PTP by 8-minutes; in contrast to mean force PTP, which returned completely to unpotentiated values. The full 8-minute time course of PTP for peak twitch force and mean twitch force are depicted in **Figure 17** and **Figure 19,** respectively.

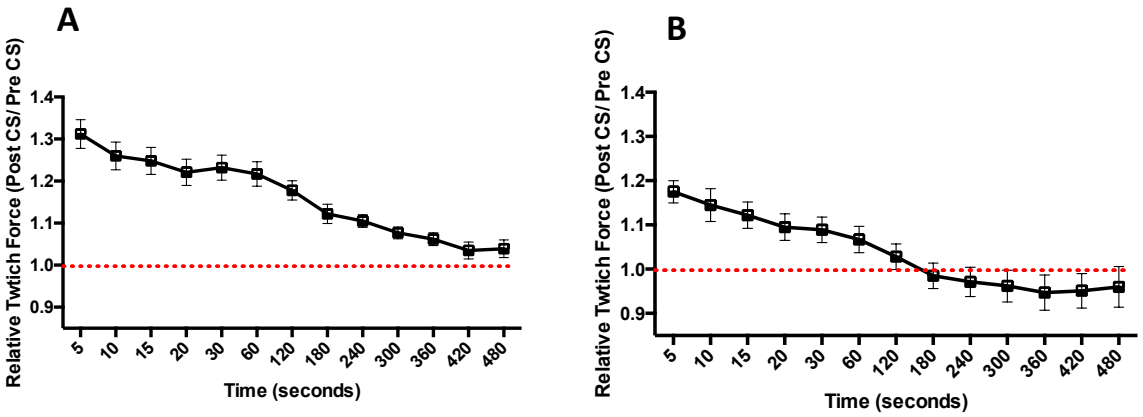

Figure 17. Relative peak concentric twitch potentiation (post-CS/pre-CS) of Wildtype **(A)** and skMLCK$^{-/-}$ **(B)** control muscles during 8-minute experimental time course following high-frequency conditioning stimulus ($n = 8$).

5.3.0 Effect of Epinephrine Treatment on Force Production and Post-tetanic Potentiation

5.3.1 Absolute Concentric Twitch Force

5.3.1.1 Within Genotype Analysis

Following control condition experimental protocol, EDL muscles from both genotypes underwent a 30-minute incubation periods in a 1 μM epinephrine-Tyrode's solution. A two-way repeated measures ANOVA for mean concentric twitch force indicated a main effect for condition in both the wildtype ($P < 0.0001$) and skMLCK$^{-/-}$ muscles ($P < 0.0001$). Follow up multiple comparisons tests reveled that epinephrine

treatments enhanced mean concentric twitch force by 11.8 ± 3.0% and 11.1 ± 2.4% [5 seconds post-CS] compared to the wildtype and skMLCK$^{-/-}$ control values, respectively (**Table 4**: $P < 0.0001$). Moreover, epinephrine incubation was able to maintain elevated levels of concentric twitch force in wildtype (24. 3 ± 5.0%, $P < 0.0001$) and skMLCK$^{-/-}$ muscles (20.1 ± 5.3%, $P < 0.0001$) by the 8-minute mark. In addition, epinephrine incubation had no effect on the unpotentiated mean concentric twitch force of skMLCK$^{-/-}$ muscles ($P = 0.99$); however, wildtype muscles displayed a small change following treatment (**Table 4**; $P < 0.05$).

As expected, epinephrine treatment also affected absolute peak twitch force of wildtype ($P = 0.0002$) and skMLCK$^{-/-}$ muscles ($P = 0.0042$). Values of peak twitch force showed nearly identical trends with response to epinephrine in contrast to mean force; exhibiting elevated values at all time points after the CS in wildtype and skMLCK$^{-/-}$ muscles (**Table 4**; $P < 0.0001$). Furthermore, epinephrine treatment was unable to elevate the unpotentiated peak twitch force of skMLCK$^{-/-}$ muscles ($P = 0.45$); while wildtype muscles displayed a 6.2% increase. In addition to twitch force measurements, an analysis of peak tetanic force during the CS was conducted to determine the impact of epinephrine treatment, as well as to ensure muscles would redevelop tetanic force after the 30-minute incubation period. Indeed, tetanic force was redeveloped, and no variation was detected between wildtype and skMLCK$^{-/-}$ muscles (**Figure 18**).

5.3.1.2 Between Genotype Analysis

A second two-way ANOVA was conduced to compare the impact of epinephrine treatment and peak twitch forces between genotypes. Results of the two-way ANOVA revealed an interaction between genotype and epinephrine treatment ($P = 0.0041$);

indicating that epinephrine treated wildtype muscles exhibited greater peak concentric forces than skMLCK$^{-/-}$ muscles. Results of follow-up tests from each two-way ANOVA conducted for the affect of epinephrine on force are provided as means ± SEM in **Table 4.**

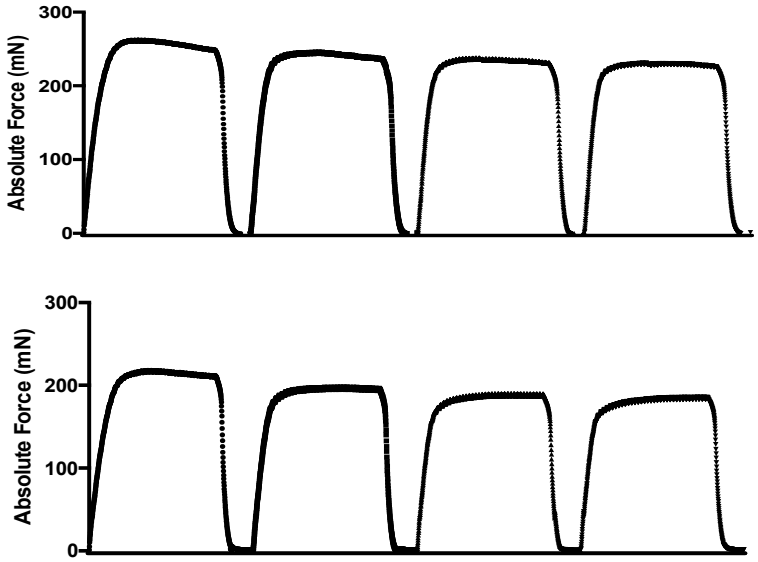

Figure 18. Representative trace of tetanic force (mN) in wildtype **(A)** and skMLCK$^{-/-}$ **(B)** epinephrine treated muscles during the conditioning stimulus (100Hz).

5.3.2 Relative Concentric Twitch Force: PTP

5.3.2.1 Within Genotype Analysis

An analysis of post-CS concentric force responses following epinephrine incubation was conducted using a two-way repeated measures ANOVA. Results indicated a significant interaction between mean concentric PTP and treatment with epinephrine in wildtype ($P < 0.0001$) and skMLCK$^{-/-}$ muscles ($P < 0.0001$). A follow up multiple comparisons test exhibited that epinephrine incubation enhanced *mean* concentric PTP by 9.6 ± 2.6% and 10.2 ± 4.2% compared to the wildtype and skMLCK$^{-/-}$ control values, respectively (**Table 4**; $P < 0.0001$). Furthermore, at the 8-minute mark; epinephrine treated muscles from both wildtype and skMLCK$^{-/-}$ mice displayed a 19.3 ±

1.6% and 15.7 ± 10.2% increase to PTP compared with their control values, respectively ($P < 0.001$). Data plotted in **Figure 19** shows how concentric PTP of both epinephrine treated and control muscles peaked immediately after the CS in wildtype and skMLCK$^{-/-}$ muscles; slowly dissipating over the course of the 8-minute time window studied.

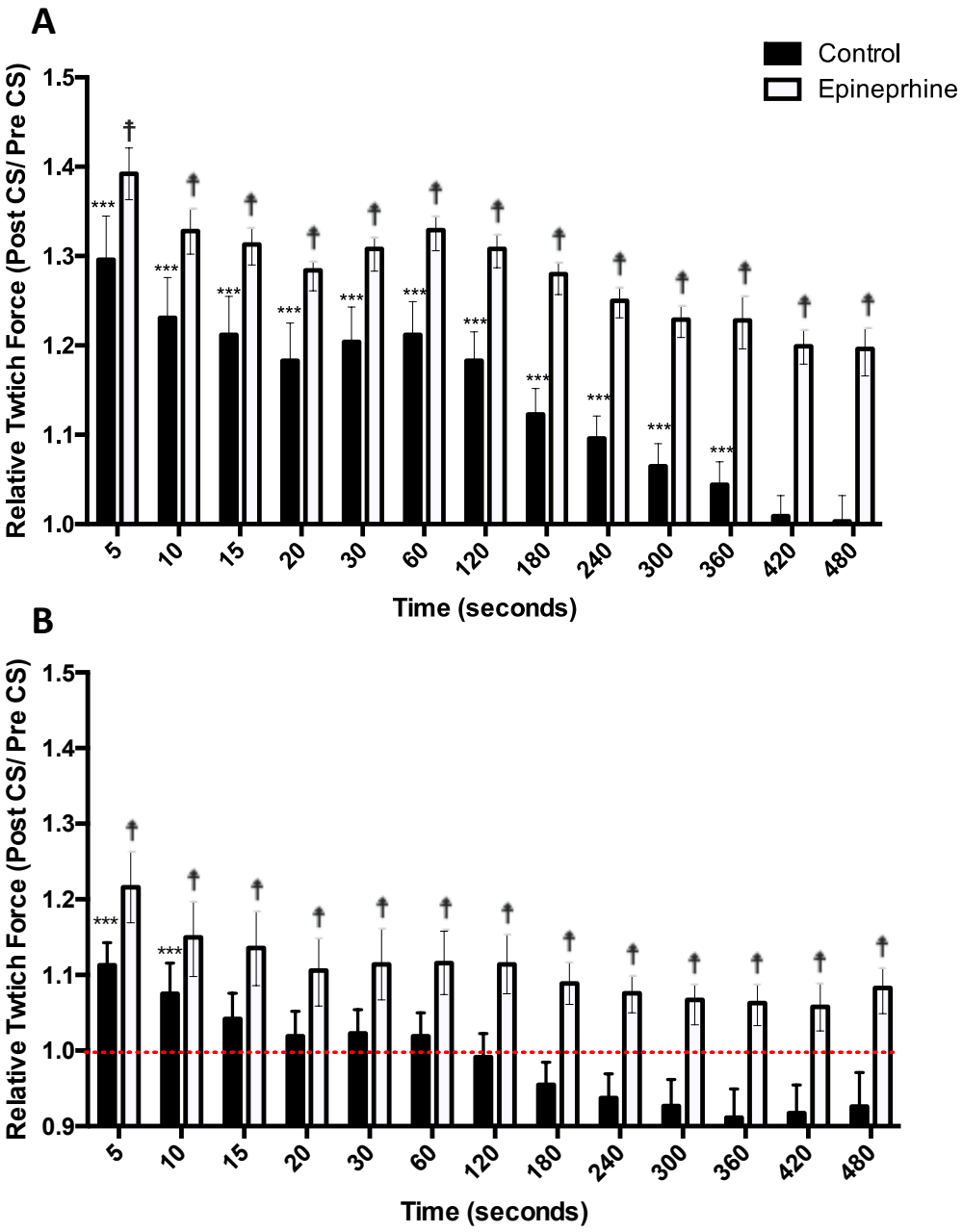

Figure 19. Effect of epinephrine on concentric twitch force potentiation after a CS in Wildtype (**A**) and skMLCK$^{-/-}$ (**B**) mouse EDL at 25°C (n = 8). Relative twitch force, determined by normalizing experimental twitch force to unpotentiated twitch force (Post-CS / Pre-CS); Closed bars, *Control*; Open bars, *Epinephrine Treated*; *** indicates that value is significantly greater than unpotentiated control value (*Within Genotype*, Holm-Sidak's correction, $P < 0.0001$); † Indicates that value is above unpotentiated value as well as CON (*Within Genotype*, Sidak's correction, $P < 0.001$)

Table 4. *The effect of 1 μM epinephrine incubation on force production and PTP in wildtype and skMLCK$^{-/-}$ mouse EDL (25°C)*

	Time Point					
			Potentiated			
	Un-potentiated	%Δ	**5 Seconds**	%Δ	**8 Minutes**	%Δ
Mean Concentric Force (mN)						
Wildtype	10.0 ± 0.9	4.0%	13.0 ± 1.3	12.3%‡	10.0 ± 0.9	24.0%‡
Wildtype +	10.4 ± 0.8		14.6 ± 1.0***†		12.4 ± 1.0***†	
skMLCK$^{-/-}$	6.7 ± 0.5	1.4%	7.4 ± 0.5	12.2%‡	6.1 ± 0.4	21.3%‡
skMLCK$^{-/-}$ +	6.8 ± 0.4		8.3 ± 0.5***		7.4 ± 0.5***	
Mean Concentric PTP (post-CS/pre-CS)						
Wildtype	1.0	-	1.30 ± 0.03***†	10.0%‡	1.00 ± 0.30†	20.0%‡
Wildtype +	1.0		1.40 ± 0.03***†		1.20 ± 0.03***†	
skMLCK$^{-/-}$	1.0	-	1.11 ± 0.03***	10.0%‡	0.93 ± 0.04	17.0%‡
skMLCK$^{-/-}$ +	1.0		1.21 ± 0.02***		1.10 ± 0.03***	
Peak Concentric Force (mN)						
Wildtype	24.1 ± 2.4	6.2%‡	31.7 ± 3.2***†	9.1%‡	24.9 ± 2.4***	16.8%‡
Wildtype +	25.6 ± 2.2		34.6 ± 3.1***†		29.1 ± 2.6***†	
skMLCK$^{-/-}$	17.6 ± 1.7	4.5%	20.7 ± 2.1***	8.2%‡	16.7 ± 1.5	17.9%‡
skMLCK$^{-/-}$ +	18.4 ± 1.4		22.4 ± 1.7***		19.7 ± 1.4**	
Peak Concentric PTP (post-CS/pre-CS)						
Wildtype	1.0	-	1.31 ± 0.03***†	4.0%‡	1.04 ± 0.02*	10.0%‡
Wildtype +	1.0		1.35 ± 0.03***†		1.14 ± 0.02**†	
skMLCK$^{-/-}$	1.0	-	1.18 ± 0.02***	5.0%‡	0.96 ± 0.05	14.0%‡
skMLCK$^{-/-}$ +	1.0		1.23 ± 0.04***		1.10 ± 0.03**	
Peak Tetanic Force (mN)						
Wildtype	226.3 ± 19.3	9.9%‡		-		-
Wildtype +	248.6 ± 21.5					
skMLCK$^{-/-}$	177.0 ± 14.0	12.5%‡		-		-
skMLCK$^{-/-}$ +	199.1 ± 15.1					

Value are means ± SEM (n = 6 for tetanic data; n = 8 muscles for twitch force data); Mean force and peak force, *twitch force determined by subtracting passive force from total twitch force at a given time point*; *** indicates that value is significantly greater than unpotentiated value (*Within Genotype*, Holm-Sidak's correction, $P < 0.001$), ** indicates that value is significantly greater than unpotentiated value (*Within Genotype*, Holm-Sidak's correction, $P < 0.01$), † Indicates that skMLCK$^{-/-}$ is significantly different than Wildtype at that time point (*Between Genotype*, Sidaks correction, $P < 0.05$), ‡ Indicates that epinephrine significantly enhanced value at that time point (*Within Genotype*, Sidak's correction, $P < 0.05$).

5.3.2.2 Between Genotype Analysis

A two-way ANOVA was used to determine the influence of epinephrine on *mean* concentric PTP between genotypes (wildtype vs. skMLCK$^{-/-}$). This analysis determined a significant interaction between epinephrine treatment and genotype ($P < 0.01$). To this end, a follow-up test was then used to confirm where differences existed between genotypes (**Table 4**). This analysis revealed that following epinephrine incubation, wildtype muscles were significantly elevated above skMLCK$^{-/-}$ values at all time points ($P < 0.05$); with the exception of the final 8-minute value ($P = 0.172$).

To determine if the ability to phosphorylate myosin RLC significantly affected the *in vitro* response to epinephrine incubation; the disparity between wildtype and skMLCK$^{-/-}$ mean PTP values (Wildtype PTP value – skMLCK$^{-/-}$ PTP value) was analyzed in both conditions. Multiple un-paired t-tests were used to compare average disparity of PTP between genotypes from the control condition against the epinephrine condition. Full results for the average disparity of concentric PTP values are presented in **Table 5** as means ± SEM. These data indicated that there was no point after the CS where the disparity between genotypes in the epinephrine condition was greater than that of the control condition. Moreover, to investigate how similar the responses of wildtype and skMLCK$^{-/-}$ muscles were to epinephrine - a linear regression (**Figure 20**) of the 13 post-CS time points was conducted. Interestingly, results of the regression analysis demonstrated a very strong correlation between the responses of control to epinephrine treated muscle ($r^2 = 0.89$).

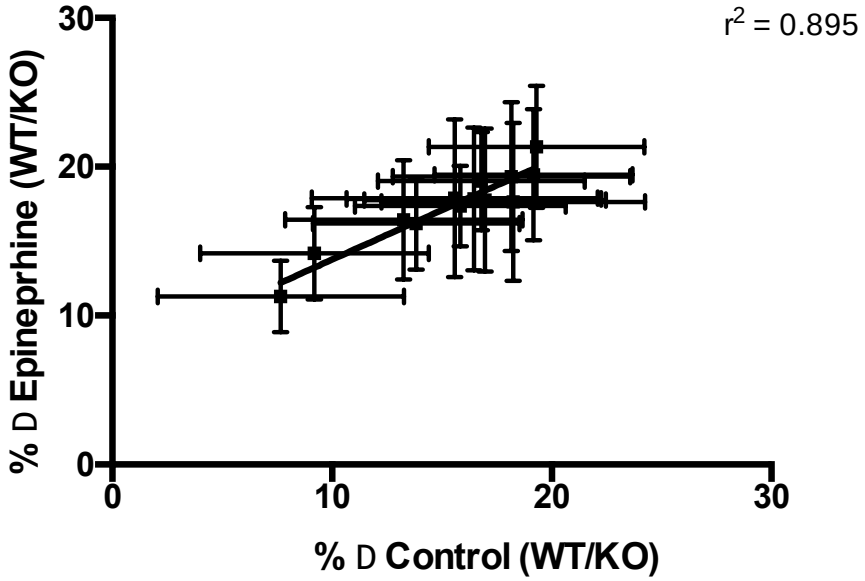

Figure 20. *Relative difference in twitch force between Wildtype and skMLCK$^{-/-}$ muscles with and without epinephrine incubation;* values are means ± SEM (n = 13). Each point was calculated from the difference in PTP between Wildtype and skMLCK$^{-/-}$ muscles at that time; *%Δ Control*, derived from dividing Wildtype control PTP value from skMLCK$^{-/-}$ control PTP value at a given time point; *%Δ Epinephrine*, derived from dividing Wildtype epinephrine PTP value from skMLCK$^{-/-}$ epinephrine PTP value at a given time point.

$$(\text{PTP Difference EPI condition})_{T1} - (\text{PTP Difference CON condition})_{T1} = \Delta \textit{ relative effect of epinephrine}$$

Equation 2. The difference between PTP in the epinephrine condition and the control condition. This value indicates the effect of epinephrine between genotypes at a given time point (*T*), a value of 0 represents epinephrine affects both genotypes equally i.e. both wildtype and skMLCK$^{-/-}$ muscles improved by 10%.

Table 5. *The difference in concentric force potentiation between Wildtype and skMLCK$^{-/-}$ for both control and epinephrine treated EDL at 25°C*

Time Point (sec)	Condition		%Δ (using Equation 1)
	Control	Epinephrine	
5	18.2 ± 6.1%	17.6 ± 5.4%	-0.6
10	15.6 ± 6.5%	17.9 ± 5.4%	2.3
15	17.0 ± 5.5%	17.8 ± 5.0%	-0.8
20	16.5 ± 5.8%	17.8 ± 5.0%	1.4
30	18.2 ± 5.4%	19.3 ± 5.1%	1.2
60	19.3 ± 4.9%	21.4 ± 4.1%	2.0
120	19.2 ± 4.5%	19.5 ± 4.4%	0.2
180	16.8 ± 4.5%	19.1 ± 3.3%	2.3
240	15.8 ± 4.7%	17.4 ± 2.7%	1.5
300	13.8 ± 4.8%	16.2 ± 3.1%	2.4
360	13.3 ± 5.4%	16.5 ± 4.0%	3.2
420	9.2 ± 5.2%	14.2 ± 3.1%	5.0
480	7.7 ± 5.6%	11.3 ± 2.4%	3.6

Value are means ± SEM where applicable (n = 8 muscles); Control, *Derived from dividing Wildtype control PTP value from skMLCK$^{-/-}$ control PTP value at a given time point*; Epinephrine, *Derived from dividing Wildtype epinephrine PTP value from skMLCK$^{-/-}$ epinephrine PTP value at a given time point*; %Δ, The difference of disparity between conditions determined using Equation 1; Analysis determined no statistically significant change after epinephrine treatment (un-paired t-test, Sidak-Bonferroni correction, $P < 0.05$).

5.4.3 Concentric Twitch Kinetics

Concentric twitch kinetics was analyzed at three representative time points before (unpotentiated) and after (peak and final) the potentiating stimulus. Measurements include time to peak tension (TPT), half-relaxation time ($RT_{1/2}$), rate of force development (+dP/dt) and rate of relaxation (-dP/dt). Within group differences as a result of epinephrine administration were analyzed using a repeated measure ANOVA, while a series of unpaired *t*-tests were used to determine significant differences between genotypes at each time point. The results of this analysis as well as representative twitch traces for each major time point can be found below in **Figure 21** and **Table 6.**

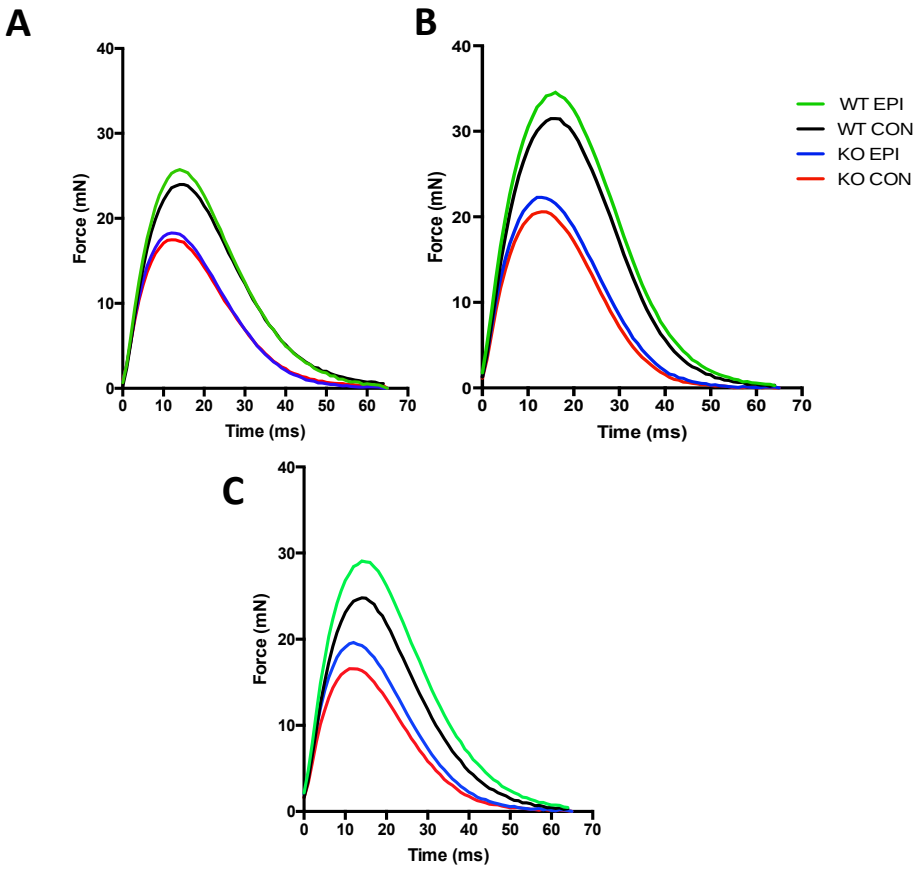

Figure 21. Absolute peak concentric twitch force traces (mN) from Wildtype from skMLCK$^{-/-}$ muscles before (**A**), 5 seconds after (**B**) and 8 minutes after (**C)** a conditioning stimulus (n = 8); Peak force, *twitch force determined by subtracting passive force from total twitch force at a given time point*; Green line, *Denotes Wildtype epinephrine treated muscles;* Blue line, *Denotes skMLCK$^{-/-}$ epinephrine treated muscles;* Black line, *Denotes Wildtype control muscles;* Red line, *Denotes skMLCK$^{-/-}$ control muscles.*

Table 6. *The effect of 1 μM epinephrine incubation on concentric twitch kinetics in Wildtype and skMLCK$^{-/-}$ mouse EDL at 25°C*

	Un-potentiated	Potentiated 5 Seconds	Potentiated 8 Minutes
TPT (ms)			
Wildtype	13.8 ± 0.8	15.5 ± 0.9	14.6 ± 1.2
Wildtype +	13.7 ± 0.6 †	15.4 ± 1.0 †	14.0 ± 0.8 †
skMLCK$^{-/-}$	12.8 ± 0.7	13.4 ± 0.7 †	11.4 ± 0.6
skMLCK$^{-/-}$+	12.2 ± 0.7	12.7 ± 0.6	12.0 ± 0.5
RT$_{1/2}$ (ms)			
Wildtype	26.1 ± 2.2	25.4 ± 2.1	26.4 ± 2.2
Wildtype +	26.1 ± 2.1	25.3 ± 2.1	26.0 ± 2.1
skMLCK$^{-/-}$	26.1 ± 2.1	25.8 ± 2.1	26.8 ± 2.2
skMLCK$^{-/-}$+	26.4 ± 2.2	26.1 ± 2.1	26.5 ± 2.2
+dP/dt (mN•ms^{-1})			
Wildtype	2.3 ± 0.3	3.1 ± 0.3	2.4 ± 0.3
Wildtype +	2.6 ± 0.3*	3.4 ± 0.6*	3.0 ± 0.3*
skMLCK$^{-/-}$	2.2 ± 0.2	2.6 ± 0.2	2.0 ± 0.3
skMLCK$^{-/-}$+	2.4 ± 0.2*	2.8 ± 0.3*	2.5 ± 0.3*
-dP/dt (mN•ms^{-1})			
Wildtype	1.4 ± 0.2	1.7 ± 0.2	1.3 ± 0.2
Wildtype +	1.4 ± 0.1	1.8 ± 0.2	1.4 ± 0.1*
skMLCK$^{-/-}$	1.0 ± 0.1	1.2 ± 0.2	1.0 ± 0.1
skMLCK$^{-/-}$+	1.1 ± 0.1	1.3 ± 0.1	1.1 ± 0.1*

Values are means ± SEM (*n = 7)*. TPT, *Time to peak tension*; RT$_{1/2}$, *Half-relaxation time*; +dP/dt, *Rate of force development*; -dP/dt, *Rate of relaxation*; *+, Denotes the presence of epinephrine*. * Indicates that epinephrine condition is significantly different than control at that time point (*Within Genotype*, Sidak's correction, $P < 0.05$); † Indicates that skMLCK$^{-/-}$ is significantly different than Wildtype at that time point (*Between Genotype*, un-paired t-test, two tailed, $P < 0.05$).

5.5.0 Myosin RLC Phosphorylation

It was initially hypothesized that wildtype muscles would exhibit greater myosin phosphorylation than skMLCK$^{-/-}$ muscles, and that epinephrine would significantly alter myosin RLC phosphorylation in wildtype muscles but not skMLCK$^{-/-}$. A 2-way ANOVA was used to determine the difference in the effect of epinephrine on myosin RLC phosphorylation between genotypes (**Table G.1**). This analysis determined a main effect for time ($P < 0.0001$) but not for condition ($P = 0.503$). At no point was the level of myosin RLC phosphorylated significantly different between wildtype control and epinephrine conditions; however, a dunnet's test revealed that myosin RLC phosphorylation was higher in the first 5 seconds after the CS, ($P < 0.001$) a value that remained elevated in epinephrine treated muscles ($P < 0.05$) but dissipated by 8-minutes in the control condition (**Figure 22**). Furthermore, muscles from skMLCK$^{-/-}$ mice had no detectable amounts of phosphorylated myosin; example western blots from all genotypes and conditions can be found in **Figure 23**.

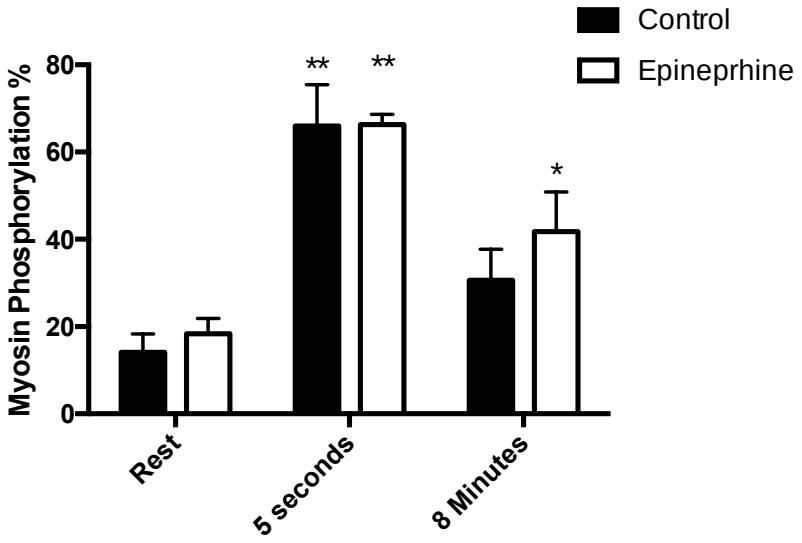

Figure 22. The effect of time (x-axis) and epinephrine treatment on myosin RLC phosphorylation in Wildtype EDL at rest, 5 seconds, and 8 minutes (n = 4-5); * Indicates significant increase from rest value (*Within Genotype*, dunnet's test, $P < 0.05$), ** Indicates significant increase from rest value (*Within Genotype*, dunnet's test, $P < 0.001$).

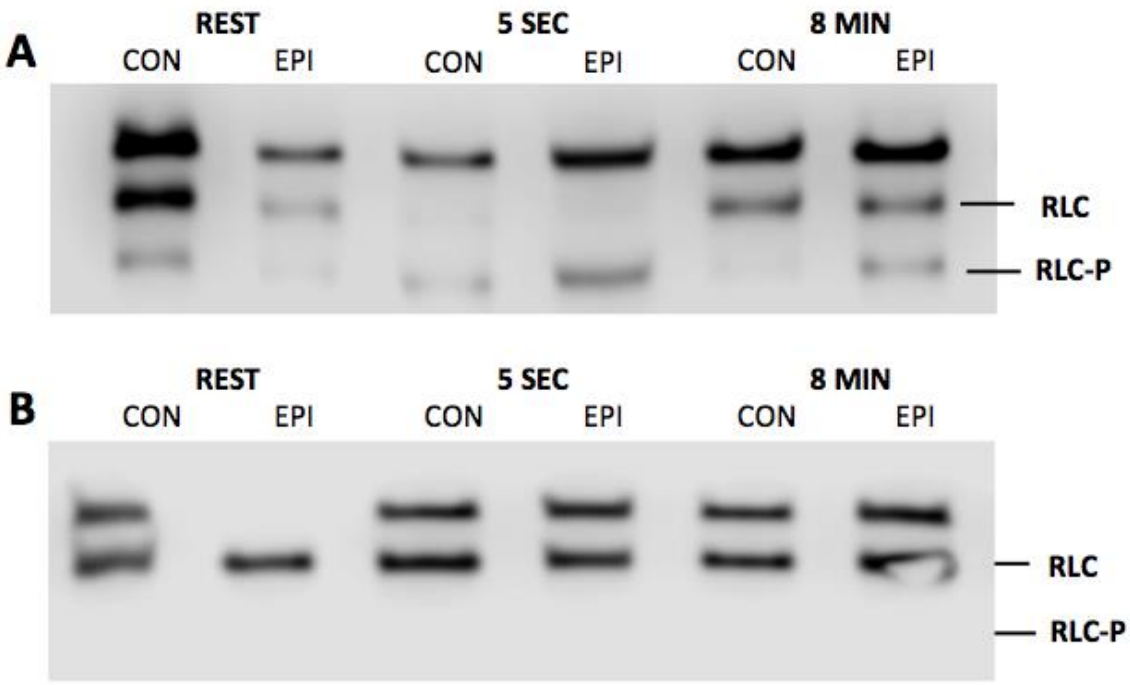

Figure 23. Cropped images from **Appendix F**, Urea/glycerol PAGE blots of myosin light chain phosphorylation in Wildtype (**A**) and (**B**) skMLCK$^{-/-}$ muscles from both control (CON) and epinephrine (EPI) conditions. Resting muscles from each group were frozen after a 30 minute equilibration period in either Tyrode's solution or epinephrine bath, while stimulated muscles (5 sec and 8 min) were frozen within ~15 seconds of twitch. Negatively charged mono-phosphorylated (RLC-P) bands are identified based on specific increase in protein migration (Zhi et al., 2005) relative to non-phosphorylated (RLC). RLC-P content was manually determined using LI-COR software to analyze band densities; RLC, *Denotes non-phosphorylated myosin RLC band*; RLC-P, *Denotes mono-phosphorylated myosin RLC band*.

Discussion

6.1.0 General Summary of Results and Findings

This study is the first to directly examine the effects of epinephrine on concentric PTP and myosin phosphorylation over an 8-minute time course by utilizing skMLCK$^{-/-}$ mice as a negative control to parse out the effect of myosin phosphorylation. The purpose of this study was to test whether β-adrenergic stimulation augments the time-course and characteristics of concentric twitch potentiation, and if this is observed with alterations to myosin phosphorylation. To this end, we assessed concentric PTP, twitch kinetics, and myosin phosphorylation in both control and epinephrine (1 μM) treated muscles from wildtype and skMLCK$^{-/-}$ mice. The main findings of this project illustrated that the elimination of myosin RLC phosphorylation via gene ablation (skMLCK$^{-/-}$) only has a small influence, and does not significantly alter the affect of epinephrine on concentric force potentiation (PTP), concentric force production (mN), or twitch kinetics (TPT, $RT_{1/2}$, +dP/dt, -dP/dt). Furthermore, we predicted that epinephrine incubation would significantly alter myosin phosphorylation in wildtype mice. While, there is no evidence supporting the idea that epinephrine incubation significantly alters myosin RLC phosphorylation within 8 minutes of a conditioning stimulus in either wildtype or skMLCK$^{-/-}$ mice; epinephrine treatment did maintain phosphorylation values significantly above rest in wildtype muscles. Thus, it is likely that myosin RLC phosphorylation plays only a small secondary role in epinephrine-induced changes in muscle function and twitch characteristics over time.

The following discussion explores these observations, and aims to justify the central finding that epinephrine incubation amplifies and maintains contractile

performance over time, in both the presence and absence of myosin phosphorylation. The observation that muscle twitch force and PTP are enhanced by epinephrine without significant alteration to myosin phosphorylation disagrees with the present hypothesis that epinephrine influences PTP by maintaining high levels of myosin phosphorylation (Decostre et al. 2000).

6.2.0 Relation to Previous Studies

The work of Decostre et al. (2000) served as the background for this project. These researchers examined the effect of 1μM epinephrine on PTP and myosin RLC phosphorylation over 300 seconds. Interestingly, these researchers found that epinephrine enhanced isometric PTP ~15% and could maintain force production (8% PTP by 300 s) relative to control muscles. Our data confirms these findings from Decostre et al. (2000) and also suggests that the effects of epinephrine may be sensitive to factors such as contraction type (concentric > isometric) and time. In addition to contractile properties, Decostre et al. (2000) showed that myosin phosphorylation was maintained over 300 seconds in the presence of epinephrine; our data also confirmed this finding. A comparison of their data juxtaposed our results (**Figure 22**) shows a strong similarity in the phosphorylation response to epinephrine over time, however not to the same degree. One reason for these differences between our data and previously published work may simply be the variance in time of measurement (300 s vs. 480 s), as myosin phosphorylation will inevitably decrease over time as a result of increased skMLCP activity (Stull et al., 2011); thus our data may have shown elevated RLC-P at 300 seconds in accordance with previous results. One reason for the differences could be that Decostre et al. (2000) conducted their experiments at 20°C, while our work was done at 25°C. This

is important, because as Mitsui et al. (1994) demonstrated that dephosphorylation of myosin is a highly temperature dependent process, wherein a difference of 5°C can result in a ~40% difference in myosin phosphorylation. To illustrate this, these researchers calculated the enzymatic rate constant and Q_{10} of protein phosphatases (the factor by which the rate constant increases by raising the temperature by 10) at 20 and 15 °C. The rate constants for dephosphorylation were 0.6 and 0.3 min^{-1} at 20 and 15°C, respectively, providing a Q_{10} of 5.1. These researchers concluded that these results support the idea that myosin phosphatase has high temperature dependence, and that this is responsible for higher steady-state force levels at low temperature. Thus, it is possible that the use of lower temperatures in previous work would promote a slowed rate of skMLCP, preserving myosin phosphorylation for longer.

6.3.0 Contractile Mechanics of Wildtype and skMLCK$^{-/-}$ muscles

6.3.1 The Effect of PTP on Concentric Force

6.3.1.1 Wildtype Muscles

This study was the first to characterize the PTP time course of concentric twitches in both wildtype and skMLCK$^{-/-}$ muscles. Thus, the work regarding concentric twitches as well as skMLCK$^{-/-}$ mice is novel, juxtaposed previous literature. Indeed, concentric PTP following a brief conditioning stimulus was observed in wildtype muscles, and at its peak value reached ~30% potentiation; a value which is nearly identical to previous reports (at 100 Hz) for concentric force (Gittings et al., 2014). **Figure 19A** shows that muscles from wildtype mice displayed enhanced potentiation as a result of the concentric paradigm. Our work also supports the case for a shortening-induced sensitization of the

PTP response relative to isometric twitch potentiation (Gittings et al., 2012; Caterini et al., 2011; Xeni, 2011).

One prominent explanation for this observed phenomenon is to examine cross-bridge cycling. For example, during submaximal stimulation the rate of cross-bridge detachment (g_{app}) is greater than the rate of cross-bridge attachment (f_{app}); thus cross-bridge distribution generally favors a non-force generating state during shortening (Piazesi et al. 2007). However, any increase in f_{app} can cause large increases in the fraction of cross-bridges in the force generating state (α_{Fs}). As Sweeney and Stull (1990) demonstrated, the effect of calcium binding to troponin C changes the value of f_{app}, but not g_{app}, ultimately increasing the number of cross-bridges in the force generating state. **Equation 3** depicts this theoretical framework suggested by Brenner (1988), and how it accounts for both the loss of absolute twitch force and a more noticeable effect of PTP in contrast to the isometric model. Furthermore, Sweeney and Stull (1990) point out that myosin phosphorylation will exert its effect on tension development by increasing f_{app}, without altering g_{app}; an effect which is more pronounced at low levels of calcium. Indeed, myosin phosphorylation plays a critical role in influencing the relationship between f_{app} and g_{app} (Sweeney and Stull, 1990)

$$\alpha_{Fs} = f_{app}/(f_{app} + g_{app})$$

$$\uparrow [Ca^{2+}]_i = \uparrow f_{app}$$

$$\therefore \uparrow \alpha_{Fs}$$

Equation 3. Theoretical framework for cross-bridges found in the force generating state (α_{Fs}); f_{app}, Denotes the rate of cross-bridge attachment; g_{app}, Denotes the rate of cross-bridge detachment. This equation depicts how increased $[Ca^{2+}]_i$ will result in a greater rate of cross-bridge attachment, resulting in more cross-bridges in the force generating state.

6.3.1.2 skMLCK$^{-/-}$ Muscles

As previously discussed, this study is the first to characterize the concentric PTP time course of skMLCK$^{-/-}$ muscles. Interestingly, these muscles exhibited ~20% concentric force potention, results which are very similar to previous reported data using the same CS (4 x 100 Hz) to enhance twitch force (Gittings et al., 2014). On one hand, Zhi et al. (20005) noted that skMLCK$^{-/-}$ muscles do not display significant post-tetanic potentiation of isometric twitches; however, Gittings et al. (2014) have shown that skMLCK$^{-/-}$ muscles posses machinery capable of isometric PTP. **Figure 19B** indicates, post-tetanic potentiation of force occurred when we used concentric twitches in this study. This is in accordance with the speed-dependent properties and shortening sensitization of concentric PTP seen in wildtype muscles (Abbate et al., 2000; Gittings et al., 2012; Caterini et al., 2011; Xeni, 2011); as skMLCK$^{-/-}$ muscles are capable of undergoing Ca^{2+} induced changes to f_{app} and g_{app}. Like wildtype muscles, PTP in skMLCK$^{-/-}$ muscles is sensitive to both contraction type as well as changes to Ca^{2+} handling. However, simple comparison of the eight-minute time-course of concentric PTP (**Figure 19**) in the absence of epinephrine depicts stark baseline differences between the two genotypes. Specifically, this may come as a result of the inability of skMLCK$^{-/-}$ to phosphorylate myosin.

Interestingly, both wildtype and skMLCK$^{-/-}$ (CON) reach peak potentiation by five seconds post-CS; by the 120 second mark, however, skMLCK$^{-/-}$ muscle force return to unpotentiated values, while the wildtype muscles were still potentiated by ~20% (**Figure 19**). The rapid dissipation of force in skMLCK$^{-/-}$ muscles is primarily a result of the inability to phosphorylate the RLC, however it may also indicate the loss of small

stimulation-induced increases in resting [Ca^{2+}] observed by Smith et al., (2013). Moreover, while wildtype twitch force returned to baseline values by 480 seconds, the skMLCK$^{-/-}$ muscles continue to display a small but observable reduction in PTP of down to -6% relative to baseline. However, as Gittings et al., (2014) was able to demonstrate, this depression of normalized twitch force in skMLCK$^{-/-}$ control muscles may be fatigue related. A second consideration when observing the depressed force in skMLCK$^{-/-}$ muscles is the potential of cellular necrosis. However, this case is unlikely; as twitch force was recoverable after a 30-minute incubation between conditions. Moreover, unpublished observations from our lab have identified that dead muscles hardly respond to test pulses during incubation. Because all muscles are tested for a response before beginning experiments, it is improbable that they would begin to die after 300 seconds of experimental protocol.

There is a clear difference in the dynamic force production capabilities of these two genotypes, possibly linked to the ability to phosphorylate the myosin RLC and increased fatigue resistance (Gittings et al., 2014; Cooper et al., 1988; Jones et al., 1982; Vandenboom and Houston, 1995). Over the eight-minute time course, a loss of potentiated force quickly manifests in the skMLCK$^{-/-}$ muscles. This response is evidence that without the skMLCK enzyme, these muscles are unable to phosphorylate myosin RLC and cannot maintain concentric twitch force potentiation as a result. The inability to maintain concentric PTP in the absence of myosin phosphorylation is a contribution of many factors. On one hand, skMLCK$^{-/-}$ muscles likely do not experience the same leftward shift of force-pCa relationship associated with myosin phosphorylation (Metzger et al.1989; Persechini et al., 1986; Sweeney and Stull, 1990) as do wildtype muscles.

Furthermore, skMLCK$^{-/-}$ muscles do not experience phosphorylation-dependent increases in f_{app}, without altering g_{app} (Sweeney and Stull, 1990). These observations show how our data help bolster previous reports regarding the effect of myosin phosphorylation on PTP; finding large differences in PTP between wildtype and skMLCK$^{-/-}$ muscles.

6.4.0 Myosin RLC phosphorylation

At rest, the amount of phosphorylated myosin of wildtype muscles in both the control and epinephrine treated conditions were very similar (within ~4%); a trend which coincides with previously published work (Decostre et al. 2003). Furthermore, these resting values for myosin RLC phosphorylation (~ 14 and 18%) were similar to values reported previously of ~15% (Zhi et al. 2005). While our data did coincide with previous work, it was slightly elevated, reaching up to 21% in some samples. To explain this, it is important to note that the mishandling (pulling or stretching) of these muscles even slightly may induce release of Ca^{2+} in the muscle, in turn activating skMLCK and altering phosphorylation of myosin RLC. Thus, the resting values reported in our study may be even lower; however some physical manipulation may be responsible for the higher values found in some muscles.

After stimulation (CS), wildtype muscles in both conditions displayed increased myosin RLC phosphorylation (~66% phosphorylation), values which remained significantly elevated ~23.5% above resting values over 480 seconds in epinephrine treated muscles. However, while the wildtype control condition was not significantly lower than the epinephrine treated muscles – they did not remain significantly elevated above resting values. Furthermore these peak-stimulated values measured at 5 seconds corroborate with published values of closer to 50% phosphorylation (Decostre et al. 2000;

Vandenboom et al., 2013), however our samples showed range from 40 to 80% phosphorylation. One explanation for the disparity between phosphorylation values may be rooted in the nature of skMLCK activation. As Stull et al., (2011) points out, the kinase is slow to activate, not peaking until some time (~10-15 s) after contraction takes place. Therefore any variation in freezing within this time window may yield difference in activation induced myosin phosphorylation. While our methods tried to replicate the same time frame from final twitch to freezing on each muscle (10-15 seconds); there is disparity between each sample. Thus, muscles that were frozen faster than others will likely be those which yield lower values, although this is only an assumption based on the work of Stull et al., (2011); as there is no record of the time taken to freeze each muscle.

Another explanation for the differences in measured phosphorylation values is the presence of a non-specific band, which may affect the density of the RLC band. These bands can be found in several labs attempting to immunoblot for myosin RLC, as well as published works by Ryder et al., (2007). Zhi et al., (2005) point out how the density of observed bands can change by adding or removing bands via phosphatase treatment (**Figure 24**). There is an apparent increase in density of intermediate bands in samples that have undergone phosphatase treatment, potentially as a result of limited proteolysis of the nonphosphorylated RLC. In the instance of our observations, while not caused by the use of dephosphorylation treatment, the extra abundance of protein (non-specific band) may interfere with the proteolysis of the bands present. Another potential consideration is that the dense signal produced by the non-specific bands may dampen the intensity of the non-phosphorylated bands, especially in stimulated samples where the non-phosphorylated band would be less intense than at rest. After observing the non-

specific band and it's affects on the observed myosin phosphorylation; a set of side experiments were conducted in an attempt at defining this band (**Appendix E**) and determining its origin. While these experiments were not able to conclusively pinpoint the cause of the band, several characteristics were established. For instance, this band is not a result of mechanical over homogenization, nor is it a result of over dilution with sample buffer. Furthermore, under-dilution of primary anti-body did not affect non-specific binding in this case; nor was the secondary anti-body nonspecifically binding to any proteins. The full set of experiments for determining the cause and characteristics of the observed non-specific band can be found in **Appendix E**.

We observed that phosphorylated myosin RLC content was eliminated in resting skMLCK$^{-/-}$ muscle as expected, as well as most stimulated samples. These muscles generally showed no measureable RLC phosphorylation in response to the high frequency conditioning stimulus, however previous work has detected up to ~5% phosphorylation in these muscles (Zhi et al. 2005); a result which had been detected in our work as well and can be seen in **Appendix F**. Zhi et al, (2005) identified the monophosphorylated band in skMLCK$^{-/-}$ muscles when muscle homogenates were prepared in a non-denaturing buffer without protein phosphatase inhibitors; confirming that the band in question was in fact a result of phosphorylation (**Figure 24**). Analysis of the purified monophosphorylated RLC from skMLCK$^{-/-}$ muscles led to detection of peptides that cover >95% sequence of the protein (Zhi et al., 2005; **Figure 25**). Furthermore, collision-induced fragmentation spectrum (MS/MS) determined that the phosphorylation site at residue serine 15, adjacent to the site phosphorylated by skMLCK (Stull et al., 1986). These results suggest that

another kinase, not activated by contraction, may be responsible for the phosphorylation of the unknown middle band.

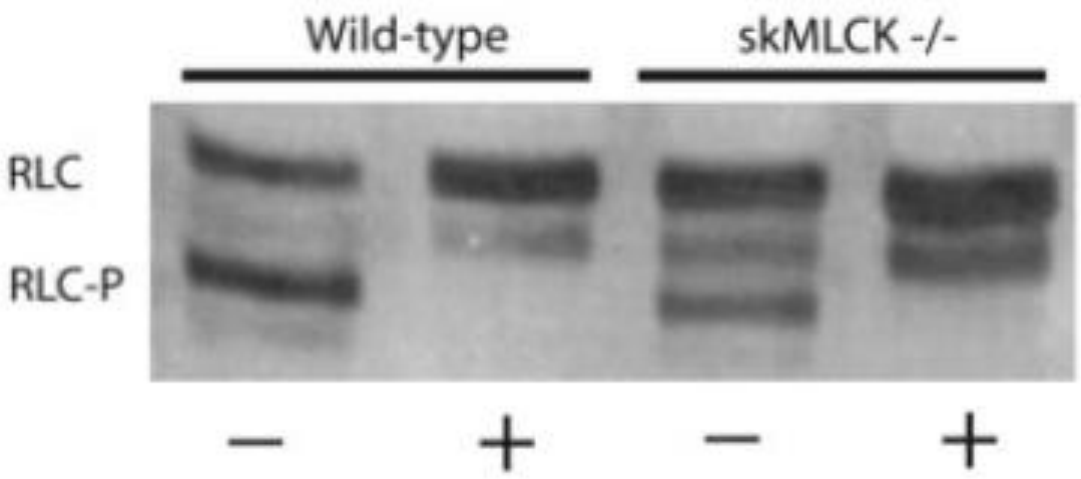

Figure 24. Separation of non-phosphorylated (RLC) and phosphorylated (RLC-P) RLC by urea/glycerol-PAGE. Results are presented without (-) or with (+) dephosphorylation treatment (Zhi et al., 2005). Results indicated that when dephosphorylation was not inhibited (+), muscle samples did not contain an RLC-P band; thus the band was a result of phosphorylation and is the mono-phosphorylated RLC.

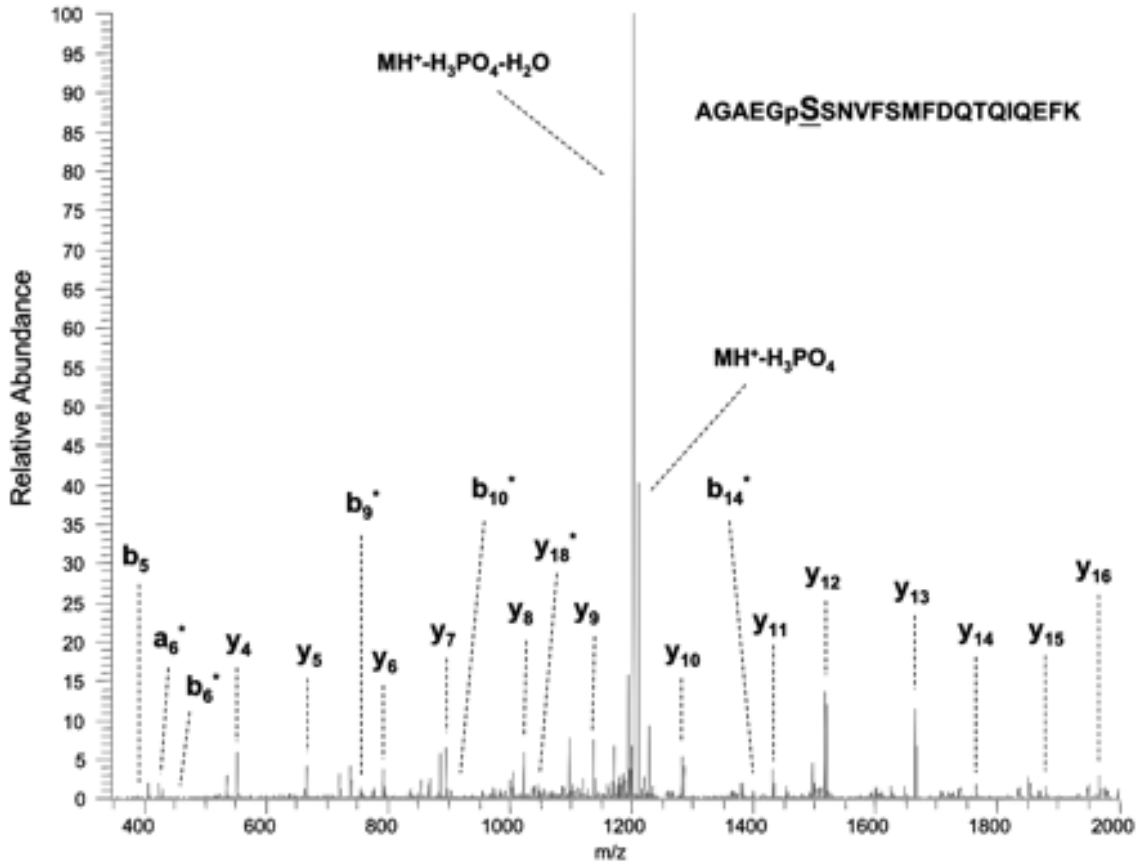

Figure 25. Collision-induced fragmentation spectrum of the phosphorylated peptide from RLC. The spectrum of AGAEGpSSNVFSMFDQTQIQEFK shows that serine (Yamaguchi et al., 2004) in mouse skeletal muscle RLC (MLC2F) is phosphorylated. The b and y designate the N- and C-terminal fragments of the peptide produced by breakage at the peptide bond in LTQ, respectively. The number represents the residue number from either the N or C terminus. ***** , Those daughter ions with loss of 98-Da peaks.

Interestingly, Zhi et al., (2005) also detected an intermediate band between the non-phosphorylated and monophosphorylated RLCs (**Figure 24**); the identity of the band is unclear, however represents < 5% of total immunoreactivity and does not change with stimulation. This unknown intermediate band is not the same band as identified by our lab (**Appendix E**), and is a result of phosphorylation – not non-specific binding. Our lab has previously detected small quantifiable amounts of monophosphorylation in skMLCK$^{-/-}$ muscles via this non-specific kinase (Gittings et al., 2015); however, this result is not always achievable. Possible explanations for this lie in the sensitivity and subjectivity of

the methods. While our lab uses the same methods as presented in both Zhi et al., (2005) and Ryder et al., (2007), including polyclonal antibodies raised in rabbits to purified skeletal and cardiac RLC; there is still room for variability when western blotting for RLC. For example, sample preparation (i.e., preparing 10X transfer buffer and diluting stock solutions), homogenization (ensuring that muscles are denatured before glass homogenization and adequately purified), protein transfer (guaranteeing the optimal pH of transfer buffer, equilibration of gels and membranes, and reduction of air bubbles), separation (adequate sucrose saturation, protein content, and removal of air bubbles), and imaging. One major example could be that samples were either over, or under saturated with urea (a process that is completely subjective, see **Methods**); a substance used for protein denaturing by breaking hydrogen bonds during the sample preparation (Bennion and Daggett, 2003). Under-saturation could result in insufficient breakdown and lack of the very small phosphorylated band, while over saturation could cause too much denaturation to the band; making it even less detectable.

One way to improve the repeatability of results with urea saturation would be to standardize using urea crystals. Methods from the lab of James Stull suggest using urea crystals, which are all standardized to the same weight. In doing so, one can keep track of how many crystals have been added to the sample instead of roughly how many scoops of urea. The variability of these methods, such have been tested to determine their effects on the resulting band density and presentation in **Appendix E**. However, this process is still difficult without knowing the amount of protein contained in each sample; thus standardizing the amount of protein loaded into each sample via protein assay may prove the biggest help. To do this, our lab has done an optimal loading analysis found in

Appendix E using Bradford assay and western blot techniques. Whatever the cause for the lack of resting phosphorylation observed in skMLCK$^{-/-}$ muscles, the ability for skMLCK to phosphorylate myosin is still accounted for and the measurable difference between conditions still remains a point of interest. Certainly, the effect of skMLCK gene ablation is clear – further substantiating the use of skMLCK$^{-/-}$ controls to account for the effect of RLC phosphorylation.

The present results provide no evidence to support any effect of epinephrine on skMLCK function, and alterations to myosin RLC phosphorylation. At no point was a significant difference in myosin RLC phosphorylation observed between wildtype control and epinephrine groups, strongly suggesting that at anytime before or after a CS; epinephrine did not alter function of either the skMLCK. However, the maintenance of RLC phosphorylation above resting values seen in epinephrine treated wildtype muscles may suggest a small influence of epinephrine on the skMLCP enzyme over time. These observations support altered Ca^{2+} handling instead of changes to myosin phosphorylation as a primary, but not only, mechanism for epinephrine's effect on muscle contractile function (Kraemer et al., 2007).

6.4.1 Ca^{2+} Based Mechanisms for Potentiation

There is strong evidence correlating myosin phosphorylation with twitch potentiation (Manning and Stull 1979; Moore et al., 1990; Palmer and Moore 1989; Vandenboom et al., 1995, 1997) and while it is a focal point of this discussion, alternative mechanisms for potentiation must also be considered. While there have been other considerations for the cause of PTP in the past, such as K^+ potentiation (Liley and North, 1953), Ca^{2+} is now regarded as the most likely alternative. Described as a secondary

mechanism for potentiation (Vandenboom et al. 2013), stimulation-induced alterations to resting Ca^{2+} levels account for observed twitch potentiation in the absence of RLC phosphorylation (Smith et al., 2013). In fact, research utilizing the mouse lumbrical has discovered that these muscles do not phosphorylate the RLC (Ryder et al. 2007; Smith et al. 2013). Much like the skMLCK$^{-/-}$ muscles used in this project, these researchers observed a short-lived (~30 seconds) potentiation of force that was temporally coupled with an increased resting myoplasmic [Ca^{2+}]. Stimulation-induced alterations to resting Ca^{2+} are proposed to enhance force through thin filament activation, by binding myoplasmic Ca^{2+} and causing a greater [Ca^{2+}] occupancy of Troponin C (TnC) (McKillop and Geeves, 1993; Maytum et al., 1999). Although this project did not assess myoplasmic [Ca^{2+}], data from our skMLCK$^{-/-}$ control muscles, which show transient twitch force potentiation for ~30 seconds in the absence of myosin phosphorylation, indicates similar trends to Smith et al. (2013). As such, comparisons can be made concerning the role of Ca^{2+} potentiation as a contributing factor to the PTP we observed in skMLCK$^{-/-}$ muscle (Gittings et al., 2014). Moreover, stimulation-induced alterations to resting Ca^{2+} are present regardless of genotype. Consequently, thin filament activation occurs in both wildtype and sMLCK$^{-/-}$; thus the disparity between the PTP values in skMLCK$^{-/-}$ and wildtype muscles (**Table 5**) will indicate the PTP contribution of skMLCK-mediated RLC phosphorylation independently.

6.5.0 The Effect of Epinephrine on Force Production

6.5.1 Inotropic Effects of Epinephrine

The positive inotropic effects in fast skeletal muscle following adrenergic receptor stimulation have been reported in many studies (Cairns & Dulhunty, 1993 a; Cairns et al. 1993). The enhancement of isometric twitch force is small, but observable after β-adrenergic stimulation (Tashiro, 1973; Cairns & Dulhunty, 1993 a; Cairns et al. 1993; Liu et al. 1997; Decostre et al. 2000; Andersson et al. 2012). These researchers have established a link between changes in Ca^{2+} handling and isometric force potentiation. Using fluorescent Ca^{2+} indicator (Indo-1), Cairns et al. (1993) have shown β-adrenergic stimulation increased $[Ca^{2+}]_i$ linearly with tension at 30Hz and 100Hz. However, these researchers also determined that during 100 Hz stimulation β-adrenergic agonists did not increase the rate of $[Ca^{2+}]_i$ release, nor did it slow the SR Ca^{2+} re-uptake. In addition to replicating the effect of increased peak $[Ca^{2+}]_i$ - Liu et al. (1997) also determined that phosphorylation of phospholamban was not the mechanism of the slowed twitch response in fast twitch muscle, as they are not regulated using phospholamban. In the de-phosphorylated state, phospholamban is responsible for the inhibition of the SERCA Ca^{2+} pump; however phosphorylation via PKA or CaM-kinase after β-adrenergic stimulation will abolish this inhibition (Martin, 2000). Most recently, the work of Andersson et al. (2012) has shown β-adrenergic stimulation to increase both peak amplitude and time to peak amplitude of $[Ca^{2+}]_i$. These findings regarding Ca^{2+} transients and the positive inotropic effect in fast skeletal muscle provide a basis for discussion regarding our results; particularly as an explanation for how skMLCK$^{-/-}$ muscles respond to epinephrine treatment.

The finding that epinephrine elicits the same changes to the contractile parameters of both wildtype and skMLCK$^{-/-}$ muscles (depicted in **Figure 20**) implies that a mechanism other than myosin RLC phosphorylation is primarily responsible for epinephrine's action. It was initially proposed by Decostre et al. (2000) that epinephrine maintained high levels of RLC phosphorylation by inhibiting skMLCP activity; while skMLCP activity was not measured, the data provided by myosin phosphorylation and PTP can help us speculate on the role of this enzyme. In fact, because epinephrine maintained wildtype myosin phosphorylation above resting values by 8-minutes post-CS (**Figure 22)**, a case can be made for the small role that myosin RLC plays in epinephrine's influence on PTP over time. Furthermore, recent evidence elucidates PKA-induced phosphorylation of a single amino acid of the RyR1, S2844, as a downstream target of β_2-adrenoceptor activation for increased SR Ca^{2+} release. This mechanism has been discussed by Andersson et al. (2012), who concluded that the ablation of S2844 site on RyR1 links excitation contraction coupling and adrenergic stimulation mediated increases in force. This may explain why skMLCK$^{-/-}$ muscles, while missing the skMLCK enzyme (Gittings et al., 2011) have virtually the same response to epinephrine as wildtype muscles. Although myoplasmic calcium was not measured in this study, the ablation of the skMLCK gene allows some conclusions to be drawn about the role of calcium-induced changes in function. Thus, because we assume the changes to calcium handling are the only other primary source of PTP modulation other than myosin phosphorylation, using differences in PTP between genotypes, the contributions from myosin phosphorylation can be separated from the effect of altered calcium signaling. This method gives a good estimate for the role of both calcium and myosin

phosphorylation. Quantification of changes to calcium transients during β-adrenergic stimulation between these genotypes will help to substantiate this claim.

Assuming that the only difference between wildtype and skMLCK$^{-/-}$ muscles is the contribution of myosin RLC phosphorylation, the robust correlation observed for the effect of epinephrine between genotypes is likely a result of a shared mechanism. In this respect, the β-adrenergic and SR RyR1 receptor phosphorylation is a possibility. **Table 5** illustrates that while the PTP attributed to RLC phosphorylation was anywhere from ~9 to 19% (CON) at any given time, it accounted for only a small difference (~5%) in potentiation in the presence of epinephrine at any point after the CS. These data provide evidence that myosin RLC phosphorylation is responsible for the difference in PTP observed between genotypes, but plays a very small role in the effect of β-adrenergic stimulation; an effect which may become more important as time goes on.

6.6.0 The Epinephrine-Induced Maintenance of Concentric PTP

This study reports significant evidence corroborating the prolongation effect of epinephrine on PTP as originally observed by Decostre et al. (2000). In their study, isometric twitch potentiation was maintained for several minutes, with no change to unpotentiated twitch force production as a result of epinephrine treatment. The current project successfully replicated this effect using dynamic contractions and for a greater period of time (8 vs. 5 min). We also determined a significant influence on unpotentiated force, thus suggesting that the concentric model is a more robust model for the observation of epinephrine-induced changes to force production. It is apparent that epinephrine significantly alters PTP, both in terms of magnitude and time-course at any point after a CS. Therefore, while the PTP prolongation effects of epinephrine are not as

robust in skMLCK$^{-/-}$ muscles, the ability to potentiate force above pre-CS values remains for 480 seconds. The most likely explanation for the 'new' ability of epinephrine-induced PTP maintenance is two-fold.

First, any adequate explanation for the major contributor to this effect would have to account for a shared mechanism between both wildtype and skMLCK$^{-/-}$ muscles. Thus, the evidence suggests that epinephrine may enhance and prolong the calcium-induced potentiation described by Smith et al. (2013); a theory that is corroborated with evidence presented by Andersson et al. (2012). Smith et al. (2013) proposed that in the absence of any myosin RLC phosphorylation-mediated increase in Ca^{2+} sensitivity, that Ca^{2+} activation of the thin filament may be increased for a short duration (~30 seconds). One way this is possible is through saturation of the intracellular Ca^{2+} buffer protein parvalbumin, allowing for a greater fraction of free Ca^{2+} released from the SR to bind to TnC on actin. This has also been suggested by Cairns et al. (1993) to happen after high-frequency (100 Hz) stimulation as a result of β-agonist induced increases in $[Ca^{2+}]_i$.

In addition to the potential of epinephrine to bolster Ca^{2+} release, further consideration can be given to the ability of epinephrine to slow the re-uptake of myoplasmic Ca^{2+} by reducing SERCA activity ~20% (Batts et al., 2007), resulting in even greater prolonging of Ca^{2+} buffer saturation. The results presented by Batts et al. (2007) makes a case for not only why acute epinephrine treatment would delay Ca^{2+} re-uptake, but also why these effects make be more pronounced at the end stages of the time-course (i.e., after 300 seconds). Given this, the reduced Ca^{2+} uptake rates reported by Batts et al. (2007) are consistent with the slowing effects of epinephrine on relaxation of fast muscle and the interaction between epinephrine incubation and depressed SR

function may be linked to depressed Ca^{2+}-ATPase activity seen with fatigue (Batts et al., 2007). While relaxation kinetics are dependent on more than just Ca^{2+} sequestration, this connection gives support to the idea that epinephrine slows Ca^{2+} re-uptake, and may explain why epinephrine seems to have more robust effects on the time-course of mean twitch force.

As previously mentioned, while the observed effect of epinephrine between genotypes is very similar, the ability to prolong PTP is slightly less robust in skMLCK$^{-/-}$ as wildtype muscle and therefore must be a result of inability to phosphorylate myosin. Thus, the small observable difference in the effect of epinephrine is most likely to be attributed to a pathway only present in wildtype muscles, in this case the ability to phosphorylate myosin via skMLCK. The data presented supports this, and points to epinephrine as having what seems to be a mild mediation of myosin phosphorylation that grows over time. While we did not directly measure the activity of either skMLCK or skMLCP, the findings of this study supports some conclusions made by Decostre et al. (2000) about the effect of epinephrine on myosin RLC. Our results corroborates the observation that epinephrine incubation does not alter resting myosin RLC phosphorylation in wildtype muscles, nor does it significantly affect peak levels of RLC phosphorylation after stimulation. These findings indirectly indicate that epinephrine does not activate either skMLCK (Manning and Stull, 1982; Decostre et al. 2000), and supports the observation that cAMP-dependent PKA phosphorylation has no direct effect on skMLCK (Edelman and Krebs, 1982). Moreover, it is uncertain how β-agonist stimulation would enhance Ca^{2+} release (Andersson et al., 2012) without increasing myosin phosphorylation; as the skMLCK is a Ca^{2+}/Calmodulin dependent kinase

(Sweeney et al., 1993). Consequently, the mechanistic pathway for epinephrine's affect on myosin RLC phosphorylation still remains unclear, however future work aimed at quantifying enzyme activity during these events would elucidate a more definitive role for epinephrine.

6.7.0 Effect of Epinephrine on Twitch Kinetics

6.7.1 Rate of Force Development (+dP/dt) and Time to Peak Tension (TPT)

The present findings indicate that epinephrine enhances rate of concentric force development (mN/ms) before and after a high-frequency conditioning stimulus. Previous research has observed a range of changes to the temporal parameters of *isometric* twitches (Brown et al. 1948; Bowman and Ziamis, 1958; Andersson et al., 2012). However, the ability of epinephrine to significantly elevate +dP/dt above that of a control group was only reported at 300 seconds after a conditioning stimulus (Decostre et al., 2000); where as Andersson et al. (2012) observed a robust 30% increase in +dP/dt using the β-agonist Isoprenaline. This may suggest variability caused by the use of different β-agonist compounds, as well as stimulation paradigm. The present findings indicate that epinephrine will enhance the rate of force development of potentiated twitches significantly for as long as 8-minutes ($P < 0.0001$). This finding has significant implication regarding contractile performance *in vivo,* highlighting that epinephrine can result in changes to muscle force, work and power which helps animals better cope with stressful situations. The data presented in **Table 6** show that +dP/dt is augmented by epinephrine in both genotypes across all time points; and as such is evidence that the mechanism regulating the effects of epinephrine on the rate of force development exists in the absence of myosin RLC phosphorylation. Thus, an RLC independent mechanism is

responsible and increased Ca^{2+} activation of the thin filament may be the most likely cause of this effect.

Our data suggest that epinephrine treatment of muscles results in increased rates of force development, however due to the equally elevated forces (i.e., 10% increase to both measures); the time to peak tension is relatively unchanged. This reinforces the idea that rate of force development and twitch force are positively correlated (Vandenboom, Grange, & Houston, 1995) and also explains why epinephrine treatment does not significantly lower TPT in the presence (wildtype) or absence (skMLCK$^{-/-}$) of myosin phosphorylation.

6.7.2 Rate of Relaxation (-dP/dt) and Half Relaxation Time ($RT_{1/2}$)

Epinephrine administration had no definitive effect on the relaxation kinetics of either wildtype or skMLCK$^{-/-}$ muscles within 5 seconds post-CS (**Table 6**). However, after 8 minutes, a small but significant decrease in *-dP/dt* is observed. The reverse affect is often seen in slow-twitch muscles as a result of phospholamban phosphorylation, and is regarded as the positive lusitropic effect (Cairns & Borrani, 2015). In contrast, Cairns and Borrani (2015) point out that fast-twitch mammalian muscles can exhibit a slowed relaxation which can be linked to altered Ca^{2+} re-uptake (Al-Jeboory & Marshall, 1978; Bowman & Ziamis, 1958; Bowman & Nott, 1970). The link between the presence of phospholamban and abbreviated relaxation times is important to note, as it helps to explain why fast twitch muscle have increased relaxation times. For example, it is established that β_2-adrenergic stimulation leads to a greater influx of Ca^{2+} into the myoplasm (Cairns & Borrani, 2015; Andersson et al., 2012). However, because fast twitch muscles do not posses the machinery; such as phosphorylation of phospholamban

(Liu et al. 1997; Vangheluwe et al. 2005) – they may not be able to deal with the increased Ca^{2+} re-uptake load caused by epinephrine treatment. Thus, as a result, it takes longer for fast twitch muscles re-uptake Ca^{2+} back into the sarcoplasmic reticulum, leading to longer relaxation times. In addition, epinephrine has the ability to slow the re-uptake of myoplasmic Ca^{2+} by reducing SERCA activity (Batts et al., 2007); resulting in even greater prolongation of Ca^{2+} buffer saturation, and thus increased relaxation times. The significance of this consideration is that the longer relaxation times can lead to increased mean force of twitches – as altering the kinetics following a twitches peak will increased average force. Thus, the use of mean twitch force in this study gives an idea for both changes in calcium efflux, as well as calcium re-uptake.

As discussed earlier, the effect of β-agonists on twitch kinetics have not been entirely conclusive. While previous work has found epinephrine to significantly alter half-relaxation time of isometric twitches by up to 25% (Decostre et al., 2000; Bowman and Ziamis, 1958), others have suggested no change (Andersson et al., 2012). However, it is important to consider that due to the novelty of concentric twitches used in this study, comparisons to research citing isometric kinetics may be difficult. For example, as this study points out (i) potentiating twitch force could potentially alter how sensitive the contractile apparatus response is to epinephrine (concentric > isometric). Furthermore, concentric twitches yield lower forces than isometric, which may display less profound changes to twitch kinetics. For example Gittings et al. (2011) points out that the same conditioning stimulus can significantly alter isometric twitch kinetics, while not changing concentric kinetics. Thus, a difference exists between contraction types with regard to susceptibility to change.

6.8.0 Limitations

The observations and conclusions of our research are principally limited to fast twitch mammalian skeletal muscle in carefully controlled *in vitro* conditions. Wildtype mice used in this experiment were not littermates of the skMLCK$^{-/-}$ knockout mice. Holmdahl & Malissen (2012) stress the importance of littermate controls for environmental and genetic variability. Our experiments however, do attempt to control for Holmdahl & Malissen's (2012) variable factors: cage, age, sex (**see Methods**). The mouse extensor digitorum longus (EDL) muscle was chosen as a representative fast twitch muscle (**Figure 9**), as it is almost exclusively comprised of fast myosin isoforms that display RLC phosphorylation and force potentiation (Vandenboom et al., 2013): 8.6% type IIA, 30.3% type IIX, and 59.7% type IIB (Gittings et al., 2011). Thus, mouse EDL muscle is considered homogeneous in nature, and extrapolating the physiological role of adrenaline on RLC phosphorylation to larger, heterogeneous muscles may be problematic. We were also limited by the assumption that the signaling cascade for epinephrine is the same in both wildtype and skMLCK$^{/-}$ mice, such that in both genotypes epinephrine inhibits the activity of skMLCP. *In vivo* muscle activity is not accurately approximated by concentric contractions, as physiological contractile performance is highly dependent on muscle length. Furthermore, the physiological applicability of these results were not conclusive; due to the fact that in an effort to maintain the viability of EDL muscles, the proposed in vitro experiments are conducted at sub-physiological temperatures (25°C).

Conclusions and Significance

7.1.0 Primary Findings

- skMLCK$^{-/-}$ knockout mouse EDL muscles showed virtually no detectable myosin RLC phosphorylation and did not change with stimulation or epinephrine incubation.

- Myosin RLC phosphorylation in wildtype muscles significantly increased 5 seconds after a conditioning stimulus to a peak 65.9% phosphorylation in the control condition, and to 66.3% in the epinephrine condition.

- Myosin RLC phosphorylation was significantly maintained above resting values by 8-minutes post-CS in the epinephrine treated condition. The presence or absence of myosin RLC phosphorylation was not a major influence on the relative effect of epinephrine on concentric PTP (r^2=0.895).

- Potentiated concentric force was elevated by epinephrine in wildtype muscles. The absence of myosin RLC phosphorylation did not remove the PTP effect in skMLCK$^{-/-}$ knockout muscles, however they exhibited significantly less concentric potentiation (CON ~12%; EPI ~19% at 5 seconds post-CS) than wildtype.

- Rate of force development (+dF/dt) was elevated up to in both genotypes by epinephrine; this effect was slightly more prominent before the CS (+4%) and 5 seconds after (+2.5%) in wildtype muscles.

- Epinephrine may be most reliant on pathways outside of the myosin RLC, and may only attribute a small portion of the PTP maintenance effect to RLC phosphorylation (up to 5~% after 300 seconds). Altered Ca^{2+} handling may be responsible for the majority of change in the first 5 minutes following stimulation.

7.2.0 Significance of Findings

The purpose of the study at hand was to determine whether epinephrine enhances concentric PTP primarily by prolonging or elevating myosin phosphorylation over time following stimulation. The inability to phosphorylate myosin RLC in skMLCK$^{-/-}$ muscles provided a crucial experimental control in elucidating the nature of epinephrine-induced alterations to concentric force via RLC phosphorylation. The results indicate that the absence of myosin RLC phosphorylation significantly alters concentric PTP, but does not decisively modify the effects of epinephrine on concentric twitch force or its characteristics. This effect of epinephrine on concentric PTP is very similar between wildtype and skMLCK$^{-/-}$ muscles. Although the presence of myosin phosphorylation "boosts" the absolute difference in concentric PTP, there is only a small disparity in relative effect that exists after roughly 240 seconds; this may indicate that myosin RLC phosphorylation acts to preserves epinephrine's effect on concentric PTP as time elapses. Therefore, while it seems myosin RLC phosphorylation may slightly aid the prolongation of concentric PTP – the primary mechanism of epinephrine-induced alteration of concentric force production is available in the absence of RLC phosphorylation. The observation that myosin RLC phosphorylation was unaltered during epinephrine-enhanced PTP also helps to further elucidate a mechanistic explanation for β-adrenergic stimulation, PTP and contractile function. Previous investigation has suggested epinephrine prolongs PTP primarily as a function of enhanced RLC phosphorylation, via skMLCP inhibition. While epinephrine didn't significantly raise myosin phosphorylation in wildtype muscles, we did note the maintenance of RLC phosphorylation with

epinephrine after 480 seconds, a finding that implicates the RLC as a small accessory in a much larger cascade of cellular signaling.

The results of the present study provides strong evidence that acute β-adrenergic stimulation can prolong and amplify concentric PTP over long periods of time. In addition, these results show that epinephrine enhances virtually all characteristics of force production, and becomes more pronounced over time – indicating an immediate amplification of force, as well as the potential for long-term fatigue resistance. This finding suggests improved contractile performance and a better ability to cope with stressful situations *in vivo*, where even small changes to twitch force can result in substantial gains in muscle force, work and power in the living animal. A primary objective of this project was to begin to identify possible mechanisms of action for epinephrine on both contractile function and PTP. The interpretation of the present study is that epinephrine alters the mechanical function of muscle primarily by increasing myoplasmic calcium levels, resulting in increased thin filament activation. This explanation would account for the observations in the absence of myosin RLC phosphorylation, while still rationalizing the enhanced magnitude of PTP in wildtype muscles.

This study produced several novel findings regarding the effect of β-adrenergic stimulation on concentric PTP and dynamic twitch characteristics using skMLCK$^{-/-}$ controls. Before now, it was clear that myosin RLC phosphorylation was a critical mechanism to PTP and that epinephrine altered the potentiated state. Using gene ablation in combination with a time course of a functional dynamic twitch, we have begun to bridge the gap between the interactions of these two elements. These findings better the

understanding of the mechanisms underlying epinephrine's function, and provide a more detailed insight into a link between β-adrenergic stimulation and *in vivo* muscle function.

7.3.0 Future Research & Considerations

The following research questions would help to verify and improve upon the present findings, as well as provide scientific basis for continued investigation of β-adrenergic stimulation and muscle physiology *in vitro*.

- *Does epinephrine significantly alter the concentric PTP time-course in the absence of skeletal muscle myosin light chain phosphatase (skMLCP)?*

- *Does β_2-adrenergic stimulation alter skeletal muscle myosin light chain phosphatase (skMLCP) activity after a conditioning stimulus in mouse EDL? Does this effect dissipate despite the persistence of PTP?*

- *What is the effect of β_2-adrenergic stimulation on low-frequency (stair-case) potentiation? Does stimulation pattern change the observed effect of epinephrine-induced alteration of force?*

- *Does epinephrine incubation enhance calcium release during PTP through PKA mediated phosphorylation of RyR1? Is resting calcium significantly altered in RyR1-S2844A mice?*

- *Will chronic exposure to stress alter the prolonging effects of β_2-adrenergic stimulation on concentric PTP? Is RyR1 receptor desensitization responsible?*

References

1. Abbate, F., Sargeant, A., Verdijk, P., & de Haan, A. (2000). Effects of high-frequency initial pulses and post-tetanic potentiation on power output of skeletal muscle. *J Appl Physiol*, 88, 35-40.
2. Adelstein, R., Conti, M., Hathaway, D., & Klee, C. (1978). Phosphorylation of smooth muscle myosin light chain kinase by the catalytic subunit of adenosine 3':5'-monophosphate-dependent protein kinase. *J Biol Chem*, 253, 8347-8350.
3. Agbenyega, E. T., & Morton, R., Hatton, P. A., & Wareham, A. (1995). Effect of the B2-adrenergic agonist clenbuterol on the growth of fast- and slow-twitch skeletal muscle of dystrophic (C57BL6K) mouse. *111*(3), 397-403.
4. Agbenyega, E. T., & Wareham, A. C. (1990). Effect of Clenbuterol on normal and denervated muscle growth and contractility. *Muscle Nerve* 13: 199-203.
5. Ahlquist, R. (1948). A study of the adrenotropic receptors. *Am J Physiol,* 153, 586-600.
6. Alexander, S. P. H., Mathie, A., Peters, J. A. (2007). Guide to receptors and channels (GRAC), 2nd edition (2007 revision). *Br J Pharmacol* 150, S12-S13.
7. Al-Jeboory AA & Marshall RJ (1978). Correlation between the effects of salbutamol on contractions and cyclic AMP content of isolated fast- and slow-contracting muscles of the guinea pig. *Naunyn Schmiedebergs Arch Pharmacol* **305**, 201–206.
8. Andersson, D., Betzenhauser, M., Reiken, S., Umanskaya, A., Shiomoi, T., & Marks, A. (2012). Stress-induced increase in skeletal muscle force requires protein kinase A phosphorylation of the ryanodine receptor. *J Physiol*, 590(24), 6381-6387.
9. Bagust, G., Lewis, D., & Luck, J. (1974). Post-tetanic effects in motor units of fast and slow twitch muscle of the cat. *J. Physiol.,* 237, 115-121.
10. Baker, J. G., Hall, I. P., & Hill, S. J. (2003). Agonist and inverse agonist actions of B-blockers at the human B_2-adrenoceptor provide evidence for agonist-directed signaling. *Mol Pharmacol* 64, 1257-1269.

11. Baker, P. K., Dalrymple, R. H., Ingle, D. L., & Ricks, C. A. (1984). Use of a B-adrenergic agonist to alter muscle and fat deposition in lambs. *J Anim Sci* 59: 1256-1261.

12. Bardsley, R. G., Allcock, S. M., Dawson, J. M., Dumelow, N. W., Higgins, J. A., Lasslett, Y. V., Lockley, A. K., Parr, T., & Buttery, P. J. (1992). Effect of B-agonists on expression of calpain and calpastatin activity in skeletal muscle. *Biochimie* 74: 267-273.

13. Batts, T. W., Spangenburg, E. E., Ward, C. W., Lees, S. J., & Williams, J. H. (2007). Effects of acute epinephrine treatment on skeletal muscle Sarcoplasmic Reticulum Ca 2 ATPase. *Basic Appl Myol*, *17*(6), 229-235.

14. Beermann, D.H., Butler, W. R., Hogue, D. E., Fishell, V. K., Dalrymple, R. H., Ricks, C. A., & Scanes, C. G. (1987). Cimaterol-induced muscle hypertrophy and altered endocrine status in lambs. *J Anim Sci* 65: 1514-1524.

15. Beitzel, F., Gregorevic, P., Ryall, J., Plant, D., Sillence, M., & Lynch, G. (2004). B2-Adrenoceptor agonist fenoterol enhances functional repair of regenerating rat skeletal muscle after injury. *J Appl Physiol*, 96, 1385-1392.

16. Bennion, B. J., & Daggett, V. (2003). The molecular basis for the chemical denaturation of proteins by urea. *Proceedings of the National Academy of Sciences*, *100*(9), 5142-5147.

17. Berchtold, M. W., Brinkmeier, H., & Müntener, M. (2000). Calcium ion in skeletal muscle: its crucial role for muscle function, plasticity, and disease. *Physiological reviews*, *80*(3), 1215-1265.

18. Bloom, T. J. (2002). Cyclic nucleotide phosphodiesterase isozymes expressed in mouse skeletal muscle. *Can J Physiol Pharmacol* 80: 1132-1135.

19. Blumenthal, D. K., & Stull, J. T. (1980). Activation of skeletal muscle myosin light chain kinase by calcium (2+) and calmodulin. *Biochemistry*, *19*(24), 5608-5614.

20. Bockaert, J., & Pin, J. (1999). Molecular tinkering of G protein-coupled receptors: an evolutionary success. *EBMO J*, 18, 1723-1729.

21. Bodine, S., Stitt, T., Gonzalez, M., Kline, W., Stover, G., Bauerlein, R., … & Yancopoulos, G. (2001). Akt/mTOR pathway is a crucial regulator of skeletal muscle hypertrophy and can prevent muscle atrophy in vivo. *Nat Cell Biol*, 3, 1014-1019.

22. Bollen, M., & Stalmans, W. (1992). The structure, role, and regulation of type 1 protein phosphatases. *Crit Rev Biochem Mol Biol*, 27, 227-281.

23. Bowman, W., & Anden, N. (1981). Effects of adrenergic activators and inhibitors on skeletal muscles. In: Szekeres L (ed). *Adrenergic Activators and Inhibitors.* Springer-Verlag: Berlin, p. 47-128.

24. Bowman WC & Nott MW (1970). Actions of some sympathomimetic bronchodilator and beta-adrenoceptor blocking drugs on contractions of the cat soleus muscle. *Br J Pharmacol* **38**, 37–49.

25. Bowman, W., & Zaimis, E. (1958). The effects of adrenaline, noradrenaline and isoprenaline on skeletal muscle contractions in the cat. *J Physiol* 144, 92-107.

26. Bown, L. G., Bilbring, E., & Burns, B. D. (1948). The action of adrenaline on mammalian skeletal muscle, *J Physiol* 107, 115-128.

27. Brenner, B. (1988). Effect of Ca2+ on cross-bridge turnover kinetics in skinned single rabbit psoas fibers: implications for regulation of muscle contraction. *Proceedings of the National Academy of Sciences*, *85*(9), 3265-3269.

28. Bricout, V. A., Serrurier, B. D., & Bigard, A. X. (2004). Clenbuterol treatment affects myosin heavy chain isoforms and MyoD content similarly in intact and regenerated soleus muscles. *Acta physiologica scandinavica*, *180*(3), 271-280.

29. Briones, A. M., Daly, C. J., Jimenez-Altayo, F., Martinez-Revelles, S., Gonzalez, J. M., & McGrath, J. C., et al. (2005). Direct demonstration of B1- and evidence against B2- and B3- adrenoceptors, in smooth muscle cells of rat small mesenteric arteries. *Br J Pharmacol* 146. 679-691.

30. Brodde, O. E. (2008). B-1 and B-2 Adrenoceptor polymorphisms: functional importance, impact on cardiovascular diseases and drug responses. *Pharmacol Ther* 117, 1-29.

31. Brown, G. L., Bülbring, E., & Burns, B. D. (1948). The action of adrenaline on mammalian skeletal muscle. *The Journal of physiology*, *107*(1), 115-128.

32. Brown, L. G., Goffart, M., & Dias, V. M. (1950). The effects of adrenaline and of sympathetic Stimulation on the demarcation potential of mammalian skeletal muscle. *J. Physiol, London* 111: 184-94

33. Brown, G. L., Paton, W., & Dias, M. V. (1949). The depression of the

demarcation potential of cat's tibialis by bistrimethylammonium decane diiodide (CIO). *The Journal of physiology*, *109*(1-2), Proc-15.

34. Brown, L. G., & von Euler, S. (1938). The after effects of a tetnus on mammalian muscle. *J Physiol*, 93, 39-60.

35. Busquets, D., Figueras, M., Fuster, G., Almendro, V., Moore-Carrasco, R., Ametller, E., … & Lopez-Soriano, F. (2004). Anti-cachectic effects of formoterol: a drug for potential treatment of muscle wasting. *Cancer Res*, 64, 6725-6731.

36. Buxton, B. F., Jones, C. R., Molenaar, P., & Summers, R. J. (1987). Characterization and autoradiographic localization of B-adrenoceptor subtypes in human cardiac tissues. *Br J Pharmacol* 92, 299-310.

37. Bylund, D. B., Eikenberg, D. C., Hieble, J. P., Langer, S. Z., Lefkowitz, R. J., Minneman, K. P., et al. (1994). International Union of Pharmacology nomenclature of adrenoceptors. *Pharmacol Rev* 46, 121-136.

38. Cairns, S. P., & Borrani, F. (2015). β- Adrenergic modulation of skeletal muscle contraction: key role of excitation–contraction coupling. *The Journal of Physiology*, *593*(21), 4713-4727.

39. Cairns, S., & Dulhunty, A. (1993). The effects of beta-adrenoceptor activation on contraction in isolated fast- and slow-twitch skeletal muscle fibres of the rat. *Br J Pharmacol*, 110, 1133-1141.

40. Cairns, S. P., Westerblad, H., & Allen, D. G. (1993). Changes of tension and [Ca2+] i during β-adrenoceptor activation of single, intact fibres from mouse skeletal muscle. *Pflügers Archiv*, *425*(1-2), 150-155.

41. Carter, W. J., Dang, A. Q., Faas, F. H., & Lynch, M. E. (1991). Effects of Clenbuterol on skeletal muscle mass, body composition, recovery from surgical stress in senescent rats. *Metabolism* 40: 855-860.

42. Carter, W. J., & Lynch, M. E. (1994). Comparison of the effects of salbutamol and Clenbuterol on skeletal muscle mass and carcass composition in senescent rats. *Metabolism* 43: 1119-1125.

43. Caterini, D., Gittings, W., Huang, J., & Vandenboom, R. (2011). The effect of work cycle frequency on the potentiation of dynamic function in fast mouse muscle. *J Exp Biol*, 214, 3915-3923.

44. Chen, K. D., & Alway, S. E. (2001). Clenbuterol reduces soleus muscle fatigue during disuse in aged rats. *Muscle Nerve* 24: 211-222.

45. Chen, K. D., & Alway, S. E. (2000). A physiological level of Clenbuterol does not prevent atrophy or loss of force in skeletal muscle of old rats. *J Appl Physiol* 89: 606-612.

46. Chen, M., Feng, H., Gupta, D., Kelleher, J., Dickerson, K., … & Wang, J. (2009), Gs(alpha) deficiency in skeletal muscle leads to reduced muscle mass, fiber-type switching, and glucose intolerance without insulin resistance or deficiency. *Am J Phisiol,* 296, 930-940.

47. Choo, J. J., Horan, M. A., Little, R. A., & Rothwell, N. J. (1992). Anabolic effects of Clenbuterol on skeletal muscle are mediated by B_2-adrenoceptor activation. *Am J Physiol Endocrinol Metab* 263: E50-E56.

48. Close, R., & Hoh, J. (1968a). Influence of temperature on isometric contractions of rat skeletal muscles. *Nature,* 217, 1179-1180.

49. Close R., & Hoh, J. (1968b) The after-effects of repetitive stimulation on the isometric twitch contraction of rat fast skeletal muscle. J Physiol 197:461–477

50. Cohen, P. (1989). The structure and regulation of protein phosphatases. *Annu Rev Biochem*, 58, 453-508.

51. Communal, C., Colucci, W. S., & Singh, K. (2000). P38 mitogen-activated protein kinase pathway protects adult rat ventricular myocytes against B-adrenergic receptor-stimulated apoptosis. Evidence for G_i-dependent activation. *J Biol Chem* 275: 19395-19400.

52. Conti, M., & Adelstein, R. (1981). The relationship between calmodulin binding and phosphorylation of smooth muscle myosin kinase by the catalytic subunit of 3’:5’ cAMP-dependent protein kinase. *J Biol Chem*, 256, 3178-3181.

53. Cooper, R. G., Edwards, R. H., Gibson, H., & Stokes, M. J. (1988). Human muscle fatigue: frequency dependence of excitation and force generation. *The Journal of physiology*, *397*(1), 585-599.

54. Cui, H., Wu, L., Chen, J., & Lin, X. (2001). Multi-mode in situ spectroelectrochemical studies of redox pathways of adrenaline. *Journal of Electroanalytical Chemistry*, *504*(2), 195-200.

55. Dascal, N. (2001). Ion-channel regulation by G proteins. *Trends Endocrinol Metab* 12: 391-398.

56. Davis, E., Loiacono, R., & Summers, R. J. (2008). The rush to adrenaline: drugs in sport acting on the β- adrenergic system. *British journal of pharmacology*, *154*(3), 584-597.

57. Davis, J. S., Satorius, C. L., & Epstein, N. D. (2002). Kinetic effects of myosin regulatory light chain phosphorylation on skeletal muscle contraction. *Biophysical journal*, *83*(1), 359-370.

58. Decostre, V., Gillis, J., & Gailly, P. (2000). Effect of adrenaline on the post-tetanic potentiation in mouse skeletal muscle. *J Musc Res Cell Motil*, 21, 247-254.

59. Dent, P., Campbell, D., Caudwell, F., & Cohen, P. (1990). Identification of three *in vivo* phosphorylation sites on the glycogen-binding subunit of protein phosphatase 1 from rabbit skeletal muscle, and their response to adrenaline. *FEBS Lett*, 259, 281-285.

60. Dixon, R., Kobilka, B., Strader, D., Benovic, J., Dohlman, H., Frielle, T., … & Strader, C. (1986). Cloning of the gene and cDNA for mammalian B-adrenergic receptor and homology with rhodopsin. *Nature*, 321, 75-79.

61. Dodd, S. L., Powers, S. K., Vrabas, I. S., Criswell, D., Stetson, S., & Hussain, R. (1996). Effects of clenbuterol on contractile and biochemical properties of skeletal muscle. *Med Sci Sports Exerc* 28, 669-676.

62. Dodge-Kafka, K. L, & Kapiloff, M. S. (2006). The mAKAP signaling complex: integration of cAMP, calcium, MAP kinase signaling pathways. *Eur J Cell* Biol 85: 593–602.

63. Dodge-Kafka, K. L, Soughayer, J., Pare, G. C., Carlisle Michel, J. J., Langeberg, L. K., Kapiloff, M. S., & Scott, J. D. (2005). The protein kinase A anchoring protein mAKAP coordinates two integrated cAMP effector pathways. *Nature* 437: 574–578.

64. Dupont-Versteegden, E. E., Katz, M. S., & McCarter, R. J. (1995). Beneficial versus adverse effects of long-term use of Clenbuterol in mdx mice. *Muscle Nerve* 18: 1447-1459.

65. Edelman, A. M., & Krebs, E. G. (1982). Phosphorylation of skeletal muscle

myosin light chain kinase by the catalytic subunit of cAMP- dependent protein kinase. *FEBS letters, 138*(2), 293-298.

66. Egloff, M., Johnson, D., Moorhead, G., Cohen, P., Cohen, P., & Barford, D. (1997). Structural basis for the recognition of regulatory subunits by the catalytic subunit of protein phosphates 1. *EMBO J*, 16, 1876-1887.

67. Emery, P. W., Rothwell, N. J., Stock, M. J., & Winter, P. D. (1984). Chronic effects of β_2-adrenergic agonists on body composition and protein synthesis in the rat. *Biosci Rep* 4: 83-91.

68. Emorine, L., Marullo, S., Briend-Sutren, M., Patey, G., Tate, K., Delavier-Klutchko, C., Strosberg, A. (1989). Molecular characterization of the human B_3-adrenergic receptor. *Science,* 245, 1118-1121.

69. Engelhardt, S., Hein, L., Wiesmann, F., & Lohse, M. J. (1999). Progressive hypertrophy and heart failure in B_1-adrenergic receptor transgenic mice. *Proc Natl Acad Sci USA* 96, 7059-7064.

70. Essayan, D. M. (1999). Cyclic nucleotide phosphodiesterase (PDE) inhibitors and immunomodulation. *Biochem Pharmacol* 57: 965-973.

71. Foulkes, J., & Cohen, P. (1979). The hormonal control of glycogen metabolism. Phosphrylation of protein phosphatase inhibitor-1 *in vivo* in response to adrenaline. *Eur J Biochem*, 97, 251-256.

72. Fowler, E. G., Graves, M. C., Wetzel, G. T., & Spencer, M. J. (2004). Pilot trial of albuterol in Duchenne and Becker muscular dystrophy. *Neurology* 62: 1006-1008.

73. Francis, S. H., Turko, I. V., & Corbin, J. D. (2001). Cyclic nucleotide phosphodiesterases: relating structure and function. *Prog Nucleic Acid Res Mol Biol* 65: 1-52.

74. Fredriksson, R., Lagerstrom, M., Lundin, L., & Schioth, H. (2003). The G-protein coupled receptors in the human genome form five main families. Phylogenetic analysis, paralogon groups, fingerprints. *Mol Pharmacol*, 63, 1256-1272.

75. Frielle, T., Collins, S., Daniel, K. W., Caron, M. G., Lefkowitz, R. J., & Kobilka, B. K. (1987). Cloning of the cDNA of the human B_1-adrenergic receptor. *Proc Natl Acad Sci USA* 84: 7920-7924.

76. Fuller, D. M., Emerick, A. M., Sadilek, M., Scheuer, T., & Catterall, A. W. (2010). Molecular Mechanism of calcium channel regulation in the flight-or-fight response. *Sci. Signal, 3*(141), ra70.

77. Gailly, P., Wu X., Haystead, T., Somlyo, A., Cohen, P., Cohen P., & Somlyo, A. (1996). Regions of the 110-kDa regulatory subunit M110 required for regulation of myosin-light chain-phosphatase activity in smooth muscle. *Eur J Biochem*, 239, 326-332.

78. Galandrin, S., & Bouvier, M. (2006). Distinct signaling profiles of B_1 and B_2-adrenergic receptor ligands toward adenylyl cyclase and mitogen-activated protein kinase reveals the pluridimensionality of efficacy. *Mol Pharmacol* 70, 1575-1584.

79. Gilman, A. (1995). Nobel Lecture. G proteins and regulation of adenylyl cyclase. *Biosci Rep*, 15, 65-97.

80. Gittings, W. J. (2015). Force potentiation as a modulator of contractile performance: Implications for control of skeletal muscle force and energetics of work.

81. Gittings, W., Aggarwal, H., Stull, J. T., & Vandenboom, R. (2014). The force dependence of isometric and concentric potentiation in mouse muscle with and without skeletal myosin light chain kinase. *Canadian journal of physiology and pharmacology*, *93*(1), 23-32.

82. Gittings, W., Bunda, J., Stull, J. T., & Vandenboom, R. (2016). Interaction of posttetanic potentiation and the catchlike property in mouse skeletal muscle. *Muscle & nerve*.

83. Gittings, W., Huang, J., Smith, I., Quadrilatero, J., & Vandenboom, R. (2011). The effect of skeletal myosin light chain kinase gene ablation on the fatigability of mouse fast muscle. *J Musc Res Cell Motil*, 31, 337-348.

84. Gittings, W., Haung, J., & Vandenboom, R. (2012). Tetanic force potentiation of mouse EDL muscle is shortening speed dependent. *J Musc Res Cell Motil*, 33(5), 359-368.

85. Goffart, M. (1947). Inversion of action of adrenaline on the K+ striated muscle and muscle rate. *C R Soc Biol Paris* 141, 1278.

86. Goffart, M. (1949). Calcium et action potentiatrice de quelques amines sympathicomimetiques sur la contraction du muscle strie non fatigue de mammifere. *Experientia* 5, 332.

87. Goffart, M. (1950). Abst. XVIII Int Physiol Congr, 222.

88. Goffart, M. (1952). Recherches relatives a l'action de l'adrenaline sur le muscle strie de mammifere. *Arch Int Physiol* 60, 318-418.

89. Goffart, M. (1954). The action of L-noradrenaline and adrenochrome on unfatigued mammalian muscle. *Pharmacol Rev* 6, 33-34.

90. Goffart, M., & Brown, G. L. (1947). Relation entre le potassium du milieu extracellulaire et l'action de l'adrenaline sur le muscle strie non fatigue du Rat. *C R Soc Biol, Paris* 141, 958-959.

91. Goffart, M., & Perry, L. M. (1951). The action of adrenaline on the rate of loss of potassium ions from unfatigued striated muscle. *J Physiol* 112, 95-101.

92. Goffart, M., & Ritchie, J. M. (1952). The effect of adrenaline on the contraction of mammalian skeletal muscle. *J Physiol* 116, 357-371.

93. Gordon, A., Homsher, E., & Regnier, M. (2000), Regulation of Contraction in Striated Muscle. *Physiological reviews*, 80(2), 853-924.

94. Gosmanov, A. R., Wong, J. A., & Thomason, D. B. (2002). Duality of G protein-coupled mechanisms for β-adrenergic activation of NKCC activity in skeletal muscle. *Am J Physiol Cell Physiol* 283: C1025-C1032.

95. Grange, R., Cory, C., Vandenboom, R., & Houston, M. (1995). Myosin phosphorylation augments the force-displacement and force-velocity relationships of mouse fast muscle. *Am J Physiol*, 269, 713-724.

96. Gregorevic, P., Ryall, J. G., Plant, D. R., Sillence, M. N., & Lynch, G. S. (2005). Chronic β-agonist administration affects cardiac function of adult but not old rats, independent of β-adrenoceptor density. *Am J Physiol Heart Circ Physiol* 289: H344-H349.

97. Grouzmann, E., Cavadas, C., Grand, D., Moratel, M., Aubert, J. F., Brunner, H. R., & Mazzolai, L. (2003). Blood sampling methodology is crucial for precise measurement of plasma catecholamines concentrations in mice. *Pflügers Archiv*, *447*(2), 254-258.

98. Gruber, C. M. (1922a). The effects of intravenous injections of massive doses of adrenaline upon skeletal muscle at rest and undergoing fatigue. *Amer J Physiol* 61, 475-492.

99. Gruber, C. M. (1922b). The effect of adrenal secretion on non-fatigued and fatigued skeletal muscle. *Amer J Physiol* 62, 438-441.

100. Guimaraes, S., & Moura, D. (2001). Vascular adrenoceptors: an update. *Pharmacol Rev* 53, 319-356.

101. Gülçin, İ. (2009). Antioxidant activity of l-adrenaline: A structure–activity insight. *Chemico-biological interactions*, *179*(2), 71-80.

102. Hanoune, J., & Defer, N. (2001). Regulation and role and adenylyl cyclase isoforms. *Annu Rev Pharmacol Toxicol* 41: 145-174.

103. Hanson, H., & Huxley, H. (1953). Structural Basis of the Cross-Striations in Muscle. *Nature,* 172(4377), 530-532.

104. Harcourt, L., Schertzer, J., Ryall, J., & Lynch, G. (2007). Low dose formoterol administration improves muscle function in dystrophic mdx mice without increasing fatigue. *Neuromuscular Disorders,* 17, 47-55.

105. Hayes, A., & Williams, D. A. (1994). Long-term Clenbuterol administration alters the isometric contractile properties of skeletal muscle from normal and dystrophin-deficent mdx mice. *Clin Exp Pharmacol Physiol* 21: 757-765.

106. Hetman, J. M., Soderling, S. H., Glavas, N. A., & Beavo, J. A. (2000). Cloning and characterization of PDE7B, a cAMP-specific phosphodiesterase. *Proc Natl Acad Sci USA* 97: 472-476.

107. Hill, A. V. (1949). The abrupt transition from rest to activity in muscle. *Proc R Soc B* 136, 399.

108. Hinkle, R. T., Dolan, E., Cody, D. B., Bauer, M. B., & Isfort, R. J. (2005). Phosphodiesterase 4 inhibition reduces skeletal muscle atrophy. *Muscle Nerve* 32: 775-781.

109. Hinkle, R. T., Hodge, K. M., Cody, D. B., Sheldon, R. J., Kobilka, B. K., & Isfort, R. J. (2002). Skeletal muscle hypertrophy and anti-atrophy effects of Clenbuterol are mediated by the β_2-adrenergic receptor. *Muscle Nerve* 25: 729-734.

110. Hoffman, B. B. (1996). Catecholamines, sympathomimetic drugs, and adrenergic receptor antagonists. *The pharmacological basis of therapeutics*.

111. Hoffmann, R., Baillie, G. S., MacKenzie, S. J., Yarwood, S. J., & Houslay, M. D. (1999). The MAP kinase ERK2 inhibits the cyclic AMP-specific phosphodiesterase HSPDE4D3 by phosphorylating it at Ser579. *EMBO J* 18: 893-903.

112. Holmdahl, R., & Malissen, B. (2012). The need for littermate controls. *European journal of immunology*, *42*(1), 45-47.

113. Huang, F., & Glinsmann, W. (1976). Seperation and characterization of two phosphorylase phosphatase inhibitors from rabbit skeletal muscle. *Eur J Biochem*, 70, 419-426.

114. Hubbard, M., & Cohen, P. (1989). They glycogen-binding subunit of protein phosphatase-1G from rabbit skeletal muscle. Further characterization of its structure and glycogen-binding properties. *Eur J Biochem*, 180, 457-465.

115. Huxley, H. (1957). The Double Array of Filaments in Cross-Striated Muscle. *JCB*, 3(5), 631-648.

116. Huxley, H. (1969). The Mechanism of Muscular Contraction. *Science*, 164, 1355-1365.

117. Huxley, H., & Hanson, H. (1954). Changes in the Cross-Striations of Muscle during Contraction and Stretch and their Structural Interpretation. *Nature*, *173*, 973-976.

118. Jacobowitz, O., Chen, J., Premont, R. T., & Iyengar, R. (1993). Stimulation of specific types of G_a-stimulated adenylyl cyclases by phorbol ester treatment. *J Biol Chem* 268: 3829-3832.

119. James, R. S., Young, I. S., Cox, V. M., Goldspink, D. F., & Altringham, J. D. (1996). Isometric and isotonic muscle properties as determinants of work loop power output. *Pflügers Archiv*, *432*(5), 767-774.

120. Joassard, O., Durieux, A., & Freyssenet, D. (2013). B2-Adrenergic agonists and the treatment of skeletal muscle wasting disorders.

121. Johnson, M. (2006). Molecular mechanisms of B_2-adrenergic receptor function, response, regulation. *J Allergy Clin Immunol*, 117, 18-25.

122. Johnson, D., Moorhead, G., Caudwell, F., Cohen, P., Chen, Y., Chen, M., & Cohen, P. (1996). Identification of protein-phosphatase-1-binding domains on the glycogen and myofibrillar targeting subunits. *Eur J Biochem*, 239, 317-325.

123. Jones, D. A., Howell, S., Roussos, C., & Edwards, R. H. (1982). Low-frequency fatigue in isolated skeletal muscles and the effects of methylxanthines. *Clinical science (London, England: 1979)*, *63*(2), 161-167.

124. Khatra, B., Chiasson, J., Shikama, H., Exton, J., & Soderling, T. (1980). Effect of epinephrine and insulin on the phosphorylation of phosphorylase phosphatase inhibitor 1 in perfused rat skeletal muscle. *FEBS Lett*, 114, 253-256.

125. Kim, Y. S., Sainz, R. D., Molenaar, P., & Summers, R. J. (1991). Characterization of beta 1- and beta 2-adrenoceptors in rat skeletal muscles. *Biochemical Pharmacology, 42*: 1783-9.

126. Kissel, J. T., McDermott, M. P., Mendel, J. R., King, W. M. Pandya, S., Griggs, R. C., & Tawil, R. (2001). Randomized, double-blind, placebo-controlled trial of albuterol in facioscapulohumeral dystrophy. *Neurology* 57: 1434-14440.

127. Kissel, J. T., McDermott, M. P., Natarajan, R., Mendell, J. R., Pandya, S., King, W. M., Griggs, R. C., & Tawil, R. (1998). Pilot trial of albuterol in facioscapulohumeral muscular dystrophy. FSH-DY Group. *Neurology* 50: 1402-1406.

128. Kline, W. O., Panaro, F. J., Yang, G., Bodine, S. C. (2007). Rapamycin inhibits the growth and muscle-sparing effects of clenbuterol. *Journal of Applied Physiology*, 102: 740-7.

129. Klug, A., Botterman, B., & Stull, J. (1982). The effect of low frequency stimulation on myosin light chain phosphorylation in skeletal muscle. *J Biol Chem*, 257, 4670-4688.

130. Koopman, R., Gehrig, S. M., Leger, B., Trieu, J., Walrand, S., Murphy, K. T., et al. (2010). Cellular mechanisms underlying temportal changes in skeletal muscle protein synthesis and breakdown during chronic (beta)-adrenoceptor stimulation in mice. *Journal of Physiology* 588: 4811-23.

131. Krarup, C. (1981a). Enhancement and diminution of mechanical tension evoked by staircase and by tetnus in rat muscle. *J Physiol*, 311, 355-372.

132. Kumar, R., & Sharma, S. (2006). Remodeling of extracellular matrix protein, collagen by B-adrenoceptor stimulation and denervation in mouse gastrocnemius muscle. *J Physiol Sci*, 56, 87-94.

133. Kuschel, M., Zhou, Y. Y., Cheng, H., Zhang, S. J., Chen, Y., & Lakatta, E. G. (1999). G_i protein-mediated functional compartmentalization of cardiac β_2-adrenergic signaling. *J Biol Chem* 274: 22048-22052.

134. Lagercrantz, H., & Slotkin, T. A. (1986). The 'stress' of being born. *Sci Am* 254: 100-107.

135. Lamb, G. D. (2000). Excitation-Contraction coupling in skeletal muscle: comparisons with cardic muscle. *Clinical and Experimental Pharmacology and Physiology*, 27(3), 216-224.

136. Larkin, L. M., Halter, J. B., & Supiano, M. A. (1996). Effect of aging on rat skeletal muscle β-AR function in male Fischer 344 X brown Norway rats. *Am J Physiol Regul Integr Comp Physiol* 270: R462-R468.

137. Lee, F. (1907). The action of normal fatigue substances on muscle. *Am J Physiol,* 20, 170-179.

138. Lefkowitz, R. J., Pierce, K. L., & Luttrell, L. M. (2002). Dancing with different partners: protein kinase A phosphorylation of seven membrane spanning receptors regulates their G protein-coupling specificity. *Mol Pharmacol* 62, 971-974.

139. Lefkowitz, R. J., Rockman, H. A., & Koch, W. J. (2000). Catecholamines, cardiac β-adrenergic receptors, heart failure. *Circulation* 101: 1634-1637.

140. Leonard, B. E. (1997). The role of noradrenaline in depression: a review. *J Psychopharmacol* 11, S39-S47.

141. Levine, R. J., Kensler, R. W., Yang, Z., Stull, J. T., & Sweeney, H. L.
(1996). Myosin light chain phosphorylation affects the structure of rabbit skeletal muscle thick filaments. *Biophysical journal*, *71*(2), 898.

142. Liley, A. W., & North, K. A. K. (1953). An electrical investigation of effects
of repetitive stimulation on mammalian neuromuscular junction. *Journal of Neurophysiology*, *16*(5), 509-527.

143. Liu Y, Kranias EG & Schneider MF (1997). Regulation of Ca2+ handling by phosphorylation status in mouse fast- and slow-twitch skeletal muscle fibers. *Am J*

Physiol Cell Physiol **42**, C1915–C1924.

144. Lohse, M. (1999). G-proteins and their regulators. *Naunyn-Schmiedebergs Arch Pharmacol,* 360, 3-4.

145. Lowey, S., Waller, G. S., & Trybus, K. M. (1993). Skeletal muscle myosin light chains are essential for physiological speeds of shortening.

146. Lynch, G. S. (2002). β_2-agonists. In: *Performance-Enhancing Subtances in Sports and Exercise,* edited by Bahrke, M., & Yesalis, C. Champaign, IL: Human Kinetics, 2002, p. 47-64.

147. Lynch, G. S., Hinkle, R. T., & Faulkner, J. A. (2001). Force and power output of diaphragm strips from mdx and control mice after Clenbuterol treatment. *Neuromuscular Disorders* 11: 192-196.

148. Lynch, G. S., Hinkle, R. T., & Faulkner, J. A. (2000). Power output of fast and slow skeletal muscles of mdx (dystrophic) and control mice after Clenbuterol treatment. *Exp Physiol* 85: 295-299.

149. Lynch, G. S., Hinkle, R. T., & Faulkner, J. A. (1999). Year-long clenbuterol treatment of mice increases mass, but not specific force or normalized power, of skeletal muscles. *Clin Exp Pharmacol Physiol,* 26, 117-120.

150. Lynch, G. S., & Ryall, J. (2008). Role of B-Adrenoceptor signaling in skeletal muscle: Implication for muscle wasting and disease. *Physiol Rev*, 88, 729-767.

151. Maltin, C. A., Delday, M. I., Watson, J. S., Heys, S. D., Nevison, I. M.,
Ritchie, I. K., & Gibson, P. H. (1993). Clenbuterol, a β-adrenoceptor agonist, increases relative muscle strength in orthopaedic patients. *Clinical Science*, *84*(6), 651-654.

152. Maltin, C. A., Hay, S. M., Delday, M. I., Smith, F. G., Lobley, G. E., & Reeds, P. J. (1987). Clenbuterol, a β-agonist, induces growth in innervated and denervated rat soleus muscle via apparently different mechanisms. *Biosci Rep I7:* 525-532.

153. Manning, R., & Stull, J. (1979). Myosin light chain phosphorylation and phosphorylase A activity in rat extensor digitorum longus muscle. *Biochem Biophys Res Commun*, 90(1), 164-170.

154. Manning, R., & Stull, J. (1982). Myosin light chain phosphorylation-dephosphrylation in mammalian skeletal muscle. *Am J Physiol,* 242, 234-241.

155. Martin, W. H., Murphree, S. S., & Saffitz, J. E. (1989). β –adrenergic receptor distribution among muscle fiber types and resistance arterioles of white, red, intermediate skeletal muscle. *Circ Res* 64: 1096-1105.

156. Martina, S. D., Ismail, M. S., & Vesta, K. S. (2006). Cilomilast: orally active selective phosphodiesterase-4 inhibitor for treatment of chronic obstructive pulmonary disease. *Ann Pharmacother* 40: 1822-1828.

157. Maytum, R., Lehrer, S. S., & Geeves, M. A. (1999). Cooperativity and switching within the three-state model of muscle regulation. *Biochemistry*, *38*(3), 1102-1110.

158. McCormick, C., Alexandre, L., Thompson, J., & Mutungi, G. (2010). Clenbuterol and formoterol decrease force production in isolated intact mouse skeletal muscle fiber bundles through a beta2-adrenoceptor-independent mechanism. *Journal of Applied Physiology* 109L 1716-27

159. McKillop, D. F., & Geeves, M. A. (1993). Regulation of the interaction between actin and myosin subfragment 1: evidence for three states of the thin filament. *Biophysical journal*, *65*(2), 693.

160. Melzer, W., Herrmann-Frank, A., & Lüttgau, H. C. (1995). The role of Ca
2+ ions in excitation-contraction coupling of skeletal muscle fibres. *Biochimica et Biophysica Acta (BBA)-Reviews on Biomembranes*, *1241*(1), 59-116.

161. Metzger, J., Greaser, M., & Moss, R. (1989). Variations in cross-bridge attatchment rate and tension with phosphorylation of myosin in mammalian skinned skeletal muscle fibres. *J Gen Physiol*, 93, 855-883.

162. Milano, C., Allen, L., Rockman, H., Dolber, P., McMinn, R., Chien, K., … & Lefkowitz, R. (1994). Enhanced myocardial function in transgenic mice overexpressing the beta 2-adrenergic receptor. *Science*, 264, 582-586.

163. Mitsui, T., Kitazawa, T., & Ikebe, M. (1994). Correlation between high temperature dependence of smooth muscle myosin light chain phosphatase activity and muscle relaxation rate. *Journal of Biological Chemistry*, *269*(8), 5842-5848.

164. Molenaar, P., Jones, C. R., McMartin, L. R., & Summers, R. J. (1988a). Auto-radiographic localization and densitometric analysis of B-1 and B-2 adrenoceptors in the canine left anterior descending coronary artery. *J Pharmacol Exp Ther* 246: 384-393.

165. Molenaar, P., Malta, E., Jones, C. R., Buxton, B. F., & Summers, R. J. (1988b). Autoradiographic localization and function of B-adrenoceptors on the human internal mammary artery and saphenous vein. *Br J Pharmacol* 95, 225-233.

166. Montagu, K. A. (1955). On the mechanism of action of adrenaline in skeletal nerve-muscle. *J Physiol* 128, 619-628.

167. Moore, R. L., Houston, M. E., Stull, J. T., & Iwamoto, G. A. (1985). Phosphorylation of rabbit skeletal muscle myosin in situ. *Journal of cellular physiology*, *125*(2), 301-305.

168. Moore, R., Palmer, B., Williams, S., Tanabe, H., Grange, R., & Houston, M. (1990). Effect of temperature on myosin phosphorylation in mouse skeletal muscle. *Am J Physiol*,259, 432-438.

169. Moore, R., & Stull, J. (1984). Myosin light chain phosphorylation in fast and slow skeletal muscles in situ. *Am J Physiol Cell Physiol*, *247*(5), 462-471.

170. Moorhead, G., Johnson, D., Morrice, N., & Cohen, P. (1998). The major myosin phosphatase in skeletal muscle is a complex between the beta-isoform and protein phosphatase 1 and the MYPT2 gene product. *FEBS Lett*, 438, 141-144.

171. Morris, A. J., & Malbon, C. C. (1999). Physiological regulation of G protein-linked signaling. *Physiol Rev* 79, 1373-1430.

172. Navegantes, L. C., Resano, N. M., Migliorini, R. H., & Kettelhut, I. C. (2000). Role of adrenoceptors and cAMP on the catecholamine-induced inhibition of proteolysis in rat skeletal muscle. *Am J Physiol Endocrinol Metab* 279, E663-E668.

173. Neidhold, S., Eichhorn, B., Kasper, M., Ravens, U., & Kaumann, A. J. (2007). The function of a- and B- adrenoceptors of the saphenous artery in caveolin-1 knockout and wild-type mice. *Br J Pharmacol* 150, 261-270.

174. Oishi, Y., Imoto, K., Ogata, T., Taniguchi, K., Matsumoto, H., Fukuoka, Y., & Roy, R. R. (2004). Calcineurin and heat-shock proteins modulation in clenbuterol-induced hypertrophied rat skeletal muscles. *Pflugers Arch* 338, 114-122.

175. Oliver, G., & Schaefer, E. A. (1895). The physiological effects of the extracts of the suprarenal capsules. *J Physiol* 18, 230-276.

176. Palmer, R. M., & Delday, M. I., McMillan, D. N., Noble, B. S., Bain, P., & Maltin, C. A. (1990). Effects of the cyclo-oxygenase inhibitor, fenbufen, on clenbuterol-

induced hypertrophy of cardiac and skeletal muscle of rats. *Br J Pharmacol* 101, 835-838.

177. Palmer, B., & Moore, R. (1989). Myosin light chain phosphorylation and tension potentiation in mouse skeletal muscle. *Am J Physiol,* 257, 1012-1019.

178. Patel, J., Diffee, G., Moss, R. (1996). Myosin regulatory light chain phosphorylation modulates the Ca2+ dependence of the kinetics of tension development in skeletal muscle. *Biophys J*, 70(5), 2333-2340.

179. Patel, J., Diffee, G., Huang, X., & Moss, R. (1998). Phosphorylation of myosin regulatory light chain eliminates force-dependent changes in relaxation rates in skeletal muscle. *Biophys J*, 74, 360-368.

180. Patiyal, S., & Katoch, S. (2006). Tissue specific and variable collagen proliferation in Swiss albino mice treated with clenbuterol. *Physiological Research,* 55, 97-103.

181. Persechini, A., Stull, J., & Cooke, R. (1985). The effect of myosin phosphorylation on the contractile properties of skinned rabbit skeletal muscle fibers. *J Biol Chem,* 260, 7951-7954.

182. Persson, H., Eriksson, S. V., & Erhardt, L. (1996). Effects of beta-receptor antagonists on left ventricular function in patients with clinical evidence of heart failure after myocardial infarction. A double blind comparison of metoprolol and xamoterol. Echocardiographic results from the Metoprolol and Zamoterol Infarction Study (MEXIS). *Eur Heart J* 17, 741-749.

183. Peters, S., Dyck, D., Bonen, A., & Spriet, L. (1998). Effects of epinephrine on lipid metabolism in resting skeletal muscle. *Am J Physiol-Endo Metab,* 275(2), 300-309.

184. Piazzesi, G., Reconditi, M., Linari, M., Lucii, L., Bianco, P., Brunello, E., ... & Irving, M. (2007). Skeletal muscle performance determined by modulation of number of myosin motors rather than motor force or stroke size." *Cell* 131.4 (2007): 784-795.

185. Pires, E., Perry, S. V., & Thomas, M. A. W. (1974). Myosin light-chain kinase, a new enzyme from striated muscle. *FEBS letters*, *41*(2), 292-296.

186. Polla, B., Cappelli, V., Morello, F., Pellegrino, M. A., Boschi, F., Pastoris, O., & Reggiani, C. (2001). Effects of the B_2-agonist clenbuterol on respiratory and limb

muscles of weaning rats. *Am J Physiol Regul Integr Comp Physiol* 280, R862-R869.

187. Prather, I. D., Brown, D. E., North, P., & Wilson, J. R. (1995). Clenbuterol: a substitute for anabolic steroids? *Med Sci Sports Exercise* 27: 1118-1121.

188. Ramsey, R., & Street, S. (1941). Muscle function as studied in single muscle fibres. *Biol. Symp*, 3, 9-34.

189. Rang, H. P., Dale, M. M., Ritter, J. M., & Moore, P. K. (2003). *Pharmacology, 5th* edn. Churchill Livingstone: Edinburgh.

190. Ravipati, G., McClung, J. A., Aronow, W. S., Peterson, S. J., & Frishman, W. H. (2007). Type 5 phosphodiesterase inhibitors in the treatment of erectile dysfunction and cardiovascular disease. *Cardiol Rev* 15, 76-86.

191. Rayment, I., Holden, H. M., Whittaker, M., Yohn, C. B., Lorenz, M., Holmes, K. C., & Milligan, R. A. (1993). Structure of the actin-myosin complex and its implications for muscle contraction. *Science*, *261*(5117), 58-65.

192. Reiken, S., Lacampagne, A., Zhou, H., Kherani, A., Lehnart, S. E., Ward, C., . . . Marks, A. R. (2003). PKA phosphorylation activates the calcium release channel (ryanodine receptor) in skeletal muscle: defective regulation in heart failure. *J Cell Biol* 160, 919-928.

193. Ritz-Gold, C. J., Cooke, R., Blumenthal, D. K., & Stull, J. T. (1980). Light chain phosphorylation alters the conformation of skeletal muscle myosin. *Biochemical and biophysical research communications*, *93*(1), 209-214.

194. Rockman, H. A., Koch, W. J., & Lefkowitz, R. J. (2002). Seven-transmembrane spanning receptors and heart function. *Nature* 415, 206-212.

195. Rothwell, N. J., & Stock, M. J. (1987). Effect of a selective B_2-adrenergic agonist (clenbuterol) on energy balance and body composition in normal and protein deficient rats. *Biosci Rep* 7, 933-940.

196. Ryall, J. G., Gregorevic, P., Plant, D. R., Sillence, M. N., & Lynch, G. S. (2002). B_2-agonist fenoterol has greater effects on contractile function of rat skeletal muscles than clenbuterol. *Am J Physiol Regul Integr Comp PHysiol* 283, R1286-R1394.

197. Ryall, J. G., Plant, D. R., Gregorevic, P., Sillence, M. N., & Lynch, G. S. (2004). B_2-agonist administration reverses muscle wasting and improves muscle function in aged rats. *J Physiol* 555, 175-188.

198. Ryall, J. G., Schertzer, J. D., & Lynch, G. S. (2007). Attenuation of age-related muscle wasting and weakness in rats after formoterol treatment: therapeutic implication for sarcopenia. *J Gerontol A Biol Sci Med Sci* 62, 813-823.

199. Ryder, J. W., Lau, K. S., Kamm, K. E., & Stull, J. T. (2007). Enhanced skeletal muscle contraction with myosin light chain phosphorylation by a calmodulin-sensing kinase. *Journal of Biological Chemistry*, *282*(28), 20447-20454.

200. Ryall, J. G., Sillence, M. N., & Lynch, G. S. (2006). Systemic administration of B_2-adrenoceptor agonists, formoterol and salmeterol, elicit skeletal muscle hypertrophy in rats at micromolar doses. *Br J Pharmacol* 147, 587-595.

201. Schneider, M. F. (1994). Control of calcium release in functioning skeletal muscle fibers. *Annual review of physiology*, *56*(1), 463-484.

202. Sham, J. S., Jones, L. R., & Morad, M. (1991). Phospholamban mediates the B-adrenergic-enhanced Ca^{2+} uptake in mammalian ventricular myocytes. *Am J Physiol Heart Circ Physiol* 261, H1344-H1249.

203. Smith IC, Gittings W, Bloemberg D, Huang J, Quadrialtero J, Tupling AR, Vandenboom .R (2013) Potentiation in mouse lumbrical muscle without myosin light chain phosphorylation: is resting calcium responsible? J Gen Physiol 141(3):297–308

204. Sneddon, A. A., Delday, M. I., Steven, J., & Maltin, C. A. (2001). Elevated IGF-II mRNA and phosphorylation of 4E-BP1 and $p70^{S6K}$ in muscle showing clenbuterol-induced anabolism. *Am J Physiol Endocrinol Metab* 281, E676-E682.

205. Soic-Vranic, T., Bobinac, D., Bajck, S., Jerkovic, R., Malnar-Dragojevic, D., & Nikolic, M. (2005). Effect of salbutamol on innervated and denervated rat soleus muscle. *Braz J Med Biol Res*, 38, 1799-1805.

206. Standaert, F. G. (1964). The mechanisms of post-tetanic potentiation in cat soleus and gastrocnemius muscles. *The Journal of general physiology*, *47*(5), 987-1001.

207. Stevens, E. D., & Syme, D. A. (1993). Effect of stimulus duty cycle and cycle frequency on power output during fatigue in rat diaphragm muscle doing oscillatory work. *Canadian journal of physiology and pharmacology*, *71*(12), 910-916.

208. Strader, C. D., Fond, T. M., Graziano, M. P., & Tota, M. R. (1995). The family of G-protein-coupled receptors. *FASEB J* 9, 745-754.

209. Stull, J. T., Blumenthal, D. K., Miller, J. R., & DiSalvo, J. (1982). Regulation of myosin phosphorylation. *Journal of molecular and cellular cardiology*, *14*, 105-110.

210. Stull JT, Kamm C, Vandenboom R (2011) Myosin light chain kinase and the role of myosin light chain phosphorylation in skeletal muscle. Arch Biochem Biophys 510:120–128

211. Stull, J. T., Nunnally, M. H., & Michnoff, C. H. (1986). 4 Calmodulin-Dependent Protein Kinases. *The enzymes*, *17*, 113-166.

212. Suzuki, Y., Shen, T., Poyard, M., Best-Belpomme, M., Hanoune, J., & Defer, N. (1998). Expression of adenylyl cyclase mRNAs in the denervated and in the developing mouse skeletal muscle. *Am J Physiol Cell Physiol* 274, C1674-C1685.

213. Sweeney, H., Bowman, B., & Stull, J. (1993). Myosin light chain phosphorylation in vertebrate striated muscle: regulation and function. *Am J Physiol*, 264(5).

214. Sweeney, H., & Stull, J. (1990). Alteration of cross-bridge kinetics by myosin light chain phosphorylation in rabbit skeletal muscle muscle: Implications for regulation of actin-myosin interaction. *Proc Natl Acad Sci USA*, 87, 414-418.

215. Szczesna-Cordary, D. (2003). Regulatory light chains of striated muscle myosin. Structure, function, and malfunction. *Cardiovascular & Haematological Disorders*, 3, 187-197.

216. Szczesna, D., Zhao, J., Jones, M., Zhi, G., Stull, J., & Potter, J. D. (2002). Phosphorylation of the regulatory light chains of myosin affects Ca2+ sensitivity of skeletal muscle contraction. *Journal of Applied Physiology*, *92*(4), 1661-1670.

217. Tashiro, N. (1973). Effects of isoprenaline on contractions of directly stimulated fast and slow skeletal muscles of the guinea- pig. *British journal of pharmacology*, *48*(1), 121-131.

218. Tasken, K., & Aandahl, E. M. (2004). Localized effects of cAMP mediated by distinct routes of protein kinase A. *Physiol Rev* 84, 137-167.

219. Uyeda, T. Q., & Spudich, J. A. (1993). A functional recombinant myosin II lacking a regulatory light chain-binding site. *Science*, *262*(5141), 1867-1870.

220. Vandenboom, R., Grange, R., & Houston, M. (1995). Myosin phosphorylation enhances rate of force development in fast-twitch skeletal muscle. *Am J Physiol*, 268, 596-603.

221. Vandenboom, R., Xeni, J., Bestic, M., & Houston, M. (1997). Fatigue and posttetanic potentiation in single muscle fibers of the frog. *Am J Physiol*, 154(1), 63-72.

222. Vandenboom, R., Gittings, W., Smith, C. I., Grange, W. R., & Stull, T. J. (2013). Myosin Phosphorylation and force potentiation in skeletal muscle: evidence from animal Models. *J Muscle Res Cell Motil* DOI 10.1007/s10974-013-9363-8

223. Van der Kooi, E. L., Vogels, O. J., van Asseldonk, R. J., Lindeman, E., Hendriks, J. C., Wohlgemuth, M., . . . Padberg, G. W. (2004). Strength training and albuterol in facioscapulohumeral muscular dystrophy. *Neurology* 63, 702-708.

224. Vangheluwe P, Schuermans M, Zádor E, Waelkens E, Raeymaekers L & Wuytack F (2005). Sarcolipin and phospholamban mRNA and protein expression in cardiac and skeletal muscle of different species. *Biochem J* **389**, 151–159.

225. Vatner, D. E., Knight, D. R., Homcy, C. J., Vatner, S. F., & Young, M. A. (1986). Subtypes of B-adrenergic receptors in bovine coronary arteries. *Circ Res* 59, 463-473.

226. Venter, J. C., Adams, M. D., Myers, E. W., Li, P. W., Mural, R. J., Sutton, G. G., . . . Zhu, X. (2001). The sequence of the human genome. *Science* 291, 1304-1351.

227. Verhofstad, A. A. J., Coupland, R. E., Parker, T. R., & Goldstein, M. (1985). Immunohistochemical and biochemical study on the development of the noradrenaline-and adrenaline-storing cells of the adrenal medulla of the rat. *Cell and tissue research*, *242*(2), 233-243.

228. Vollmer, R. R., Balcita, J. J., Sved, A. F., & Edwards, D. J. (1997). Adrenal epinephrine and norepinephrine release to hypoglycemia measured by microdialysis

in conscious rats. *American Journal of Physiology-Regulatory, Integrative and Comparative Physiology*, *273*(5), R1758-R1763.

229. Walker, K. S., Watt, P. W., & Cohen, P. (2000). Phosphorylation of the skeletal muscle glycogen-targetting subunit of protein phosphatase 1 in response to adrenaline in vivo. *FEBS letters*, *466*(1), 121-124.

230. Warrick, H. M., & Spudich, J. A. (1987). Myosin structure and function in cell motility. *Annual review of cell biology*, *3*(1), 379-421.

231. Waterfield, C. J., Jairath, M., Asker, D. S., & Timbrell, J. A. (1995). The biochemical effects of clenbuterol: with particular reference to taurine and muscle damage. *Eur J Pharmacol* 293, 141-140.

232. Wenzel-Seifert, K., Seifert, R. (2000). Molecular analysis of B_2-adrenoceptor coupling to G_s-, G_i-, G_q- proteins. *Mol Pharmacol,* 58, 954-966.

233. West, G. B., & Zaimis, E. J. (1949). A comparison of adrenaline and noradrenaline on mammalian muscle. *J Physiol* 110, 18P.

234. Williams, R. S., Caron, M. G., & Daniel, K. (1984). Skeletal muscle B-adrenergic receptors: variations due to fiber type and training. *Am J Physiol Endocrinol Metab* 246, E160-E167.

235. Xeni, J., Gittings W., Caterini, D., Huang, J., Houston, M., Grange, R., & Vandenboom, R. (2011). Myosin light chain phosphorylation and potentiation of dynamic function in mouse fast muscle. *Pflugers Archiv,* 362, 349-358.

236. Xiang, Y., & Kobilka, B. K. (2005). *The B-adrenergic Receptors: Lessons From Knockouts.* Clifton, NJ: Humana, p. 267-292.

237. Xiang, Y., Devic, E., & Kobilka, B. (2002). The PDZ binding motif of the B1 adrenergic receptor modulates receptor trafficking and signaling in cardiac myocytes. *J Biol Chem* 277, 33783-33790.

238. Xiao, R. P. (2001). B-Adrenergic signaling in the heart: dual coupling of the B_2-adrenergic receptor to G_s and GI proteins. *Sci STKE,* RE15.

239. Xiao, R. P., Avdonin, P., Zhou, Y. Y., Cheng, H., Akhter, S. A., Eschenhagen, T., . . . Lakatta, E. G. (1999). Coupling of B_2-adrenoceptor to G_i proteins and its physiological relevance in murine cardiac myocytes. *Circ Res* 84, 43-52.

240. Yang, Z., Stull, J. T., Levine, R. J., & Sweeney, H. L. (1998). Changes in interfilament spacing mimic the effects of myosin regulatory light chain phosphorylation in rabbit psoas fibers. *Journal of structural biology*, *122*(1), 139-148.

241. Yimlamai, T., Dodd, S., Borst, S., & Park, S. (2005). Clenbuterol induces muscle-specific attenuation of atrophy through effects on the ubiquitin-proteasome pathway. *J Appl Physiol*, 99, 71-80.

242. Zeman, R. J., Ludemann, R., Easton, T. G., & Etlinger, J. D. (1988). Slow to fast alterations in skeletal muscle fibers caused by clenbuterol, a B2-receptor agonist. *Am J Physiol* 254, E726-E732.

243. Zhi, G., Ryder, J., Huang, J., Ding, P., Chen Y., Zhao, Y., Kamm, K., & Stull, J. (2005). Myosin light chain kinase and myosin phosphorylation effect frequency-dependent potentiation of skeletal muscle contraction. *Proc Natl Acad Sci USA*, 102, 17519-17524.

244. Zhu, W. Z., Zheng, M., Koch, W. J., Lefkowitz, R. J., Kobilka, B. K., & Xiao, R. P. (2001). Dual modulation of cell survival and cell death by B_2-adrenergic signaling in adult mouse cardiac myocytes. *Proc Natl Acad Sci USA* 98, 1607-1612.

Appendix A: Tyrode's Solution and Surgical Anaesthetic

Table A.1. *Surgical Anesthetic*

	Anesthetic
Drug Name	Sodium Pentobarbital
Concentration Stock	240 mg/mL
Concentration Working	4.8 mg/mL
Drug Dose (mg/kg)	60
Administration	IP Injection
Average Volume Used	0.25
Needle Gauge	23
Timing of Administration	Prior to Surgery

Table A.2. *Stock solutions for Tyrode Solution (mixture of stock A and stock B).*

Compound	**Nomenclature**	**Concentration (mM)**
Stock A		
Sodium Chloride	NaCl	121
Potassium Chloride	KCl	5
Sodium Bicarbonate	$NaHCO_3$	24
D-Glucose	$C_4H_{12}O_4$	5.5
Sodium Hydrogen Phosphate	NaH_2PO_4	0.4
Magnesium Chloride	MgCl	0.5
EDTA		0.1
Stock B		
Calcium Chloride	CaCl	1.8

Appendix B: Surgical Removal/EDL mounting

Figure B.1. Initial incisions on medial and lateral aspect of distal insertion of EDL muscle

Figure B.2. Use of silk suture to tie off distal portion of EDL muscle in preparation for removal

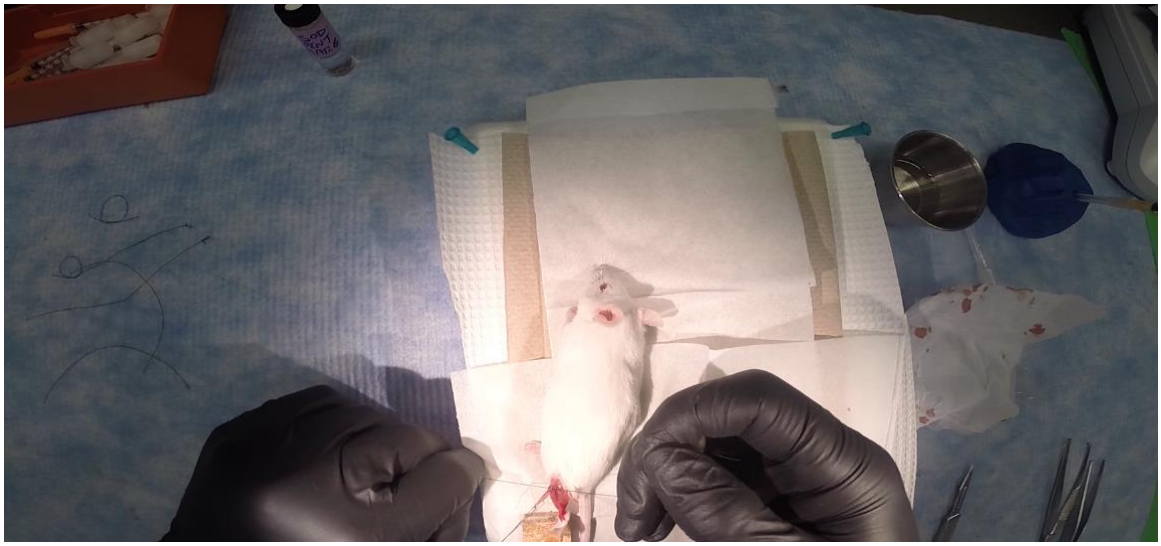

Figure B.3. Use of silk suture to tie-off proximal aspect of EDL muscle in preparation for removal and mounting in organ bath

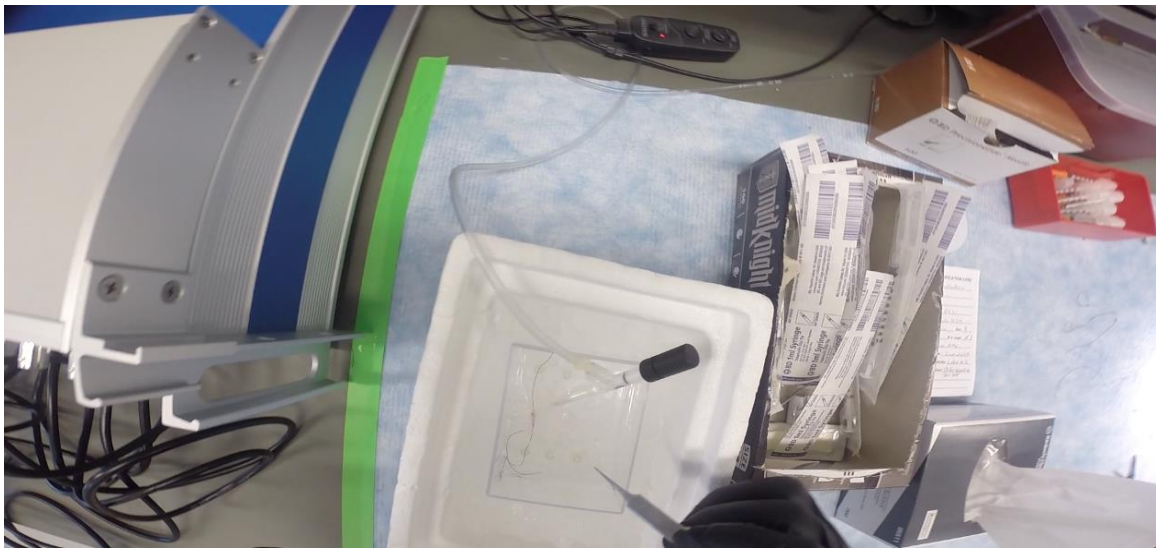

Figure B.4. Mounting newly removed EDL muscle into cold bath of Tyrode's solution in preparation for transfer into experimental organ bath

Appendix C: Bradford Reagents

Materials & Apparatus

- Bovine serum albumin (BSA)
- Protein assay dye reagent concentrate
- Skirted microtiter 96–well plate
- Spectrophotometer

Reagents

1. Stock BSA Solution (1 mg/mL)

- 100 g bovine serum albumin
- DDH_2O (100 mL final volume)
    - Aliquot into eppendorf tubes for individual trials
        - Store at –20° C and thaw before use

2. Stock Protein Assay Dye Reagent (1:4 dilution)

- 20 mL concentrated colorimetric assay dye
- 80 mL DDH_2O
    - Store at 4° C

Standard Curve Preparation

1. Prepare whole homogenate sample fresh the day of experiment.

2. Remove one aliquoted sample of 1 mg/mL stock BSA solution from storage.

3. Prepare all BSA standard solutions and store in eppendorf tubes on ice.

Table C.1. *Volumes of Stock BSA Solution and DDH_2O required for the preparation of Bradford protein assay standard solutions.*

Protein Concentration (mg/mL)	**Stock BSA Solution (µL)**	**DDH_2O (µL)**
1	1000	0
0.5	500 (from 1 mg/mL)	500
0.25	500 (from 0.5 mg/mL)	500
0.125	500 (from 0.25 mg/mL)	500
0.05	100 (from 0.5 mg/mL)	900
0	0	1000

*BSA (bovine serum albumin)
*DDH_2O (double distilled water).

Sample Preparation

4. Gather all samples to be analyzed for protein quantification.
5. Prepare 10–fold dilutions for all samples by loading individual eppendorf tubes with 10 μL of whole homogenate and 90 μL of DDH_2O.
6. Return whole homogenates to –80° C storage, and place diluted samples on ice.

Bradford Protein Assay

7. Wash a 96–well plate thoroughly in order to ensure that the plate is free of any remnants from previous use. (Hint: the Bradford method is a sensitive spectrophotometric procedure that is fully dependent upon samples' color perception and subsequent light absorption. Colour presents as a result of a reaction between the protein assay dye reagent and the positively charged amine groups of proteins within a sample. Consequently, any debris on the well plate could interfere with light absorption readings.)
8. Pipette 10 μL of each prepared standard solution and diluted sample into a 96–well plate, in triplicate.
9. Pipette 200 μL of stock protein assay dye reagent into each well. (Hint: use of a multi–channel pipette will save time at this step. However, individually loading each well with a single channel pipette will lead to greater consistency and superior results.)
10. Allow a minimum of 2 minutes to pass for proper colour development to occur
11. Insert the well plate into the spectrophotometer to generate absorbance readings.
12. Open KC4™ data analysis software, and ensure that the reading parameters are set to absorbance.

13. Define the reading parameters by the following details: absorbance wavelength of 595 nanometers, shaking intensity level of 3 and shaking duration of 5 seconds
14. Proceed to read the absorbance of each standard and sample.
15. Copy the absorbance readings into a Microsoft® Excel spreadsheet, and generate a standard curve by plotting known protein concentrations (BSA standard solutions) against their average absorbance readings.
16. Outfit the standard curve with a polynomial trendline, and display the quadratic equation derived from this curve.
17. Subtract the average absorbance reading of water for every sample, and calculate the unknown protein concentrations of all samples using the quadratic equation. (Hint: ensure that all protein concentrations are multiplied by 10 in order to obtain true quantifications, as sample homogenates were diluted 10–fold with DDH_2O.)

Appendix D: Urea/Glycerol-PAGE and Immunoblotting

Table D.1. *UREA sample buffer; Add 30 volumes of Urea Sample Buffer per mg frozen tissue weight*

Chemical Name	Volume
8 M Urea Ultra Pure	1.83 ml
Urea Gel Buffer	167 µL
0.5 M DTT	40 µL
Saturated Sucrose	100 µL
0.2% Bromphenol Blue	40 µL
0.4 M EDTA	1 µL

Table D.2. *Glycerol Gel preparation:* ***1****. Sit for 10 minutes under vacuum;* ***2.*** *add 113 uL of 10% APS and 20 uL of TEMED and mix by swirling;* ***3****. Pour quickly into prepared minigel apparatus and insert 10 well combs (no stacking gel);* ***4.*** *Gel should completely polymerize after 40 minutes.*

Chemical Name	Volume
H_2O	1.83 ml
Pure Glycerol	167 µL
30% acrylamide/Bis 29:1	40 µL
Urea Gel Buffer*	100 µL

Table D.3. *Urea Gel Buffer: Lower Buffer, 83 ml Urea Gel Buffer * . 917 ml H_2O; Upper Buffer, 73.3 mg DTT / 53.3 mg thioglycholate / 200 ml of Lower Buffer.*

Chemical Name	Volume
Tris Base	54.8 g
Glycine	40.0 g
H_2O	Fill to 2L
Adjust pH to 8.6 ± 0.1	

Table D.4. *Transfer Buffer*

Chemical Name	Volume
10 X Transfer Buffer*	100 mL
100% Methanol	200 mL
H_2O	700 mL

Table D.5. *10 X Transfer Buffer*

Components
A. Glycine, 1153 g; Tris 242.3 g; Q.S. to 5 L with H_2O
B. SDS 40 g dissolved in 3 L H_2O
MIX A + B

Table D.6. *TBST + Blocking Buffer*

Components
52.6 g NaCl 30 ml 2M Tris pH 7.5 30 mL 10% Tween Q.S. to 6 liters with H_2O.
Blocking Buffer: 5 g powdered milk (Carnation fat- free) in 100 mL TBST

Sample Preparation

Sample denaturation

- Add 0.5 mL Acetone-Based Protein Precipitation Solution (ABPS) to as many micocentrifuge tubes as there is samples, freeze in liquid N2.
- Place frozen muscles into ABPS slurry and allow samples to come to room temperature, because this step is done at freezing temperature, all proteins in the sample using DTT and TCA with no enzyme activity – no use of phosphatase or kinase inhibitors is used.

Sample homogenization

- Transfer muscle tissue into ground glass homogenizing tube, and add 0.5 mL of Water-Based Protein Precipitation Solution (WBPS), then homogenize sample with medium pressure.
- Transfer homogenate to microcentrifuge tube and centrifuge at 2000 RPM for 3 minutes
- Discard supernatant and wash pellets with 500 uL of ether (3 times for 5 minutes) to remove TCA. Afterwards let residual ether evaporate from the tube for 5 minutes.

Resuspension

- Add 300uL of urea sample buffer to each tube. Vortex, and check for blue color to ensure pH. If samples are yellow or green, add 5 uL of 2 M Tris Base (pH 11).
- Add urea crystals to each sample until each sample is saturated by urea, then store at -80 C° until use.

Hand Casting of Polyacrylamide Gels

- Add dH_2O, glycerol, acrylamide, and urea gel buffer into vacuum flask, and stir for 10 minutes.
- Draw 113 uL of 10% APS and 20 uL TEMED into pipettes, and add them to the gel solution in a 50 mL falcon tube.
- Use transfer pipet to pour gel into casting plates, and insert combs into gel.

Electrophoretic Separation

Pre-Electrophoresis

- Carefully remove combs, rinse wells with dH_2O and Upper Buffer.
- Pre-electrophorese at 400 V for 1 hour to force thioglycolate into the gel, and reduce residual APS that was used in polymerization (this prevents protein oxidation which will effect migration).

Electrophoretic separation

- Load 5-20 uL of each sample into wells, the urea and sucrose were added for increased density so the sample should layer in the well as a sharp band – amount to load depends on tissue source, so optimal amount needs to be determined.
- Do not use the end wells as samples in the end well distort.
- Electrophorese at 400 V for 85 minutes – Dye will run off gel but you can look at it during this step to ensure migration is normal.

Transferring Protein From Polyacrylamide Gel to Nitrocellulose Membrane

Transferring

- Use 8.5 x 7.0 cm pieces of nitrocellulose paper (0.45 mm pore size)
- Prepare 1L of 1X transfer buffer from 10X stock solution
- Pour 1X transfer bugger into trays in preparation for blotting sandwich
- Disassemble electrode assembly, and remove gel cassettes. Separate plates using wedge.
- Rinse gels gently in transfer buffer twice for 5 minutes to equilibrate, immerse nitrocellulose membrane in transfer buffer for 1 minute to wet and equilibrate.
- With black side of the gel holder submerged in transfer buffer, assemble the blot sandwich in the following order: sponge, filter paper, gel, membrane, filter paper, and sponge.
- Close cassette and lock, place into blotting module latch side up, with black side facing the black side of the module. Place magnetic stir bar in transfer tank and fill to 'blotting' line with added cooling packs.
- Place lid on top of the cell, and run at 25 V for 1 hour

Immunoblotting

Blocking of Non-Specific Sites

- Remove nitrocellulose membrane from the blot sandwich and transfer to a square petri dish
- Wash the membrane in Tris-Buffered Saline with Tween-20 (TBST) three times for 10 minutes each

- Incubate with Blocking Buffer for 1 hour at room temperature to prevent non-specific binding in a clean tray

Primary Anti-Body Incubation

- Wash membrane in TSBT twice, 10 minutes per wash
- Add 1:7500 skMLCK polyclonal primary antibodies (provided by the lab of James Stull) to fresh blocking buffer in a clean tray, incubate overnight with rocking at 4°C.

Secondary Anti-Body

- Remove primary antibody and wash membrane in TBST (6 times for 10 minutes each) in a clean tray
- Incubate with secondary antibody 1:10,000 dilution of Goat Anti-Rabbit IgG-HRP in TBST for 1 hour in clean tray

Detection of RLC

- Wash membrane in TBST (6 times for 10 minutes each)
- Make detection buffer using equal volumes of ECL prime luminol and oxidizing reagents (1 mL: 1 mL)
- Rinse (manually) membrane in detection buffer for 2 minutes
- Blot excess reagent from the corner of the membrane using a kim wipe, and place membrane in sheet protector. Roll to remove air bubbles and excess liquid
- Expose for 6 minutes
- Quantification of the RLC phosphorylation will be done using ImageStudio Lite, using signal analysis on blot images. Quantifying both the non-phosphorylated and phosphorylated band and then adding them together will give us the total

phosphorylation. Then, dividing out the phosphorylated band from the total will yield a % phosphorylation value. These values can then be compared against previous results from our lab to ensure that the methods were conducted properly.

Appendix E: Experiments Determining Optimal Loading Volume and Band Characterization

E.1.0 Determining Protein Quantification and Optimal Loading Volume

To quantify the amount of protein present in the Wildtype mouse EDL (whole muscle homogenate) a Bradford assay using BSA standard was conducted at 25°C. Analysis determined a protein concentration of 3.1 ug/uL, ensuring a coefficient of variation (CV%) of less than 5% across triplicate wells; the results of the Bradford analysis are presented in **Table 9** as means ± standard deviation while the absorbance plot is presented in **Figure 20**.

Table E.1. *The absorbance readings of Bradford assay samples for Wildtype EDL at 23°C*

	Well 1	Well 2	Well 3	Mean	CV%
Standard Dilution					
1	0.910	0.891	0.973	0.925 ± 0.043	4.46
0.5	0.789	0.787	0.787	0.788 ± 0.001	0.15
0.25	0.561	0.588	0.532	0.560 ± 0.028	4.99
0.125	0.423		0.451	0.422 ± 0.029	4.53
0.05	0.45	0.458	0.434	0.448 ± 0.012	2.78
0	0.27	0.281	0.278	0.276 ± 0.005	2.05
Sample					
	0.583	0.643	0.636	0.621 ± 0.032	

Values are means ± SD (n = 1). CV%, *denotes coefficient of variation calculated by dividing the sample mean – 0 from the standard deviation*. Analysis was conducted on Wildtype whole muscle homogenate using the EDL, following the protocol outlined in **Methods** section.

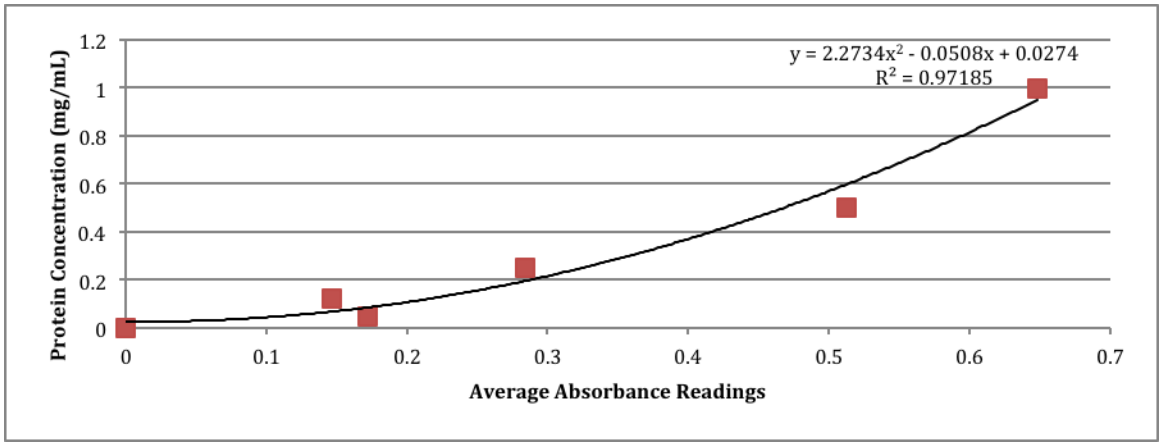

Figure E.1. Scatterplot of known sample (BSA standard) protein concentrations on the Y-axis and average absorbance readings on the X-axis. Results from **Table E.1** indicate that Wildtype EDL Red Dot, *represents mean score of 3 wells for each dilution of BSA.*

To determine the optimal protein loading volume, a loading profile using skMLCK$^{-/-}$ was performed to analyze the band density of non-phosphorylated myosin RLC across seven different volumes (**Figure E.2.A**; 5, 8, 10, 12, 14, 16, 18, and 20 uL); band intensity is plotted for each volume of sample in **Figure E.2.B**. Analysis determined that 10 uL was optimal for loading as the intensity was measurable, while western blots confirmed that wells were not overloaded at 10 uL. Thus, 10 uL was the highest volume of protein that could be loaded before crowning of wells.

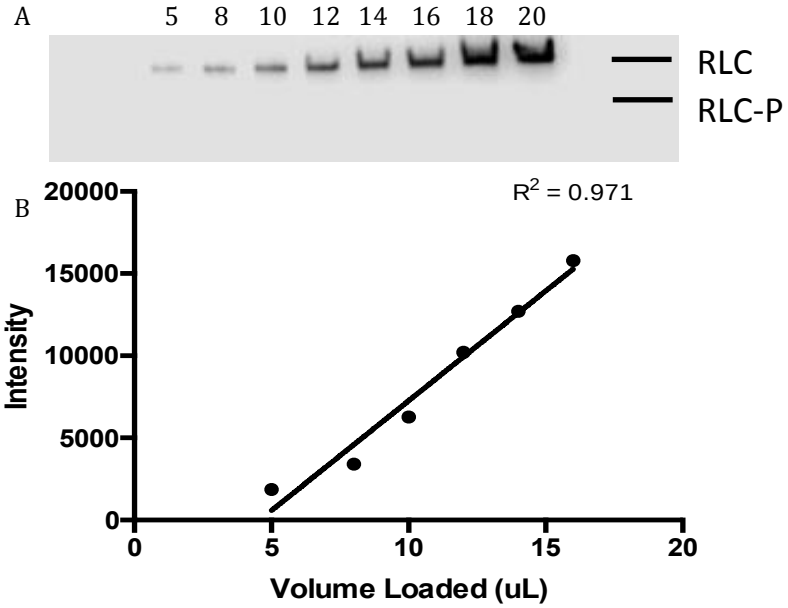

Figure E.2. (**A**) Urea/glycerol PAGE blot of non-phosphorylated myosin RLC band in skMLCK$^{-/-}$ muscles from a single sample. Protein was loaded from left to right at 5, 8, 10, 12, 14, 16, 18, and 20 uL. (**B**) Intensity of signal from the 5, 8, 10, 12, 14, and 16 uL bands presented above. The 18 and 20 uL bands have been omitted from the scatter plot because their over loading caused intensities of infinite value.

E.2.0 Characterizing Western Blots

The goal of these experiments was to determine the effect of primary anti-body dilution on the observation of a non-specific (unknown) top band during RLC blots. Objectives of this work was to examine:

- The band differences between skMLCK $^{-/-}$ muscles and Wildtype muscles,
- The disappearance of the unknown band with lower dilutions of primary anti-body, and
- The effect of our secondary anti-body on its own.
- Determine within-gel CV% of the same sample for reliability

The top non-specific band associated with RLC blotting is common among labs using this technique. One difficulty with addressing the appearance of this band is that it does not always appear. Correspondence with Dr. Jim Stull has reveled 3 possible causes of this band as a product of primary anti-body's polyclonal nature. Potential causes could be: **1**) presence of smooth muscle RLC, **2**) presence of cardiac RLC, and **3**) over-use of primary antibody.

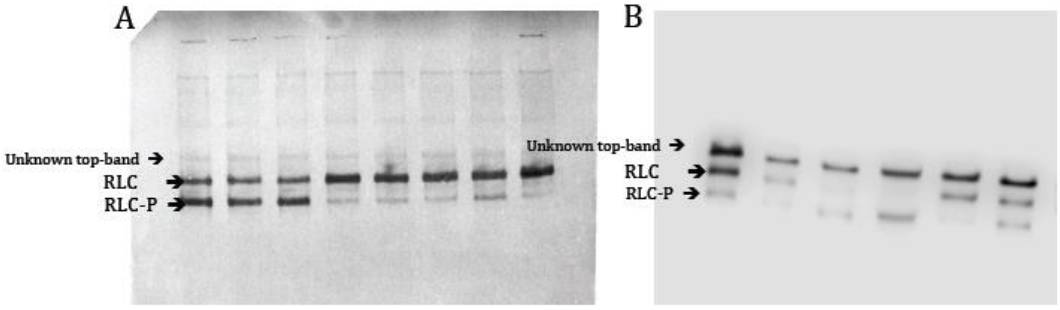

Figure E.3. (**A**) Western blot for myosin RLC from the lab of Dr. Jim Stull presenting 3 primary bands: RLC, RLC-P, and an unidentified top band. *These blots have been published as such in Ryder et al., 2007.* (**B**) Western blot for myosin RLC from Dr. Vandenboom's lab presenting the same 3-band migration pattern as those seen in Dr. Stull's lab. *Methods used in Dr. Vandenboom's lab are the same as Dr. Stull*.

Presented here, an example of the unknown band from Dr. Stull's lab (**Figure A**) and an example with stimulation, as seen in these Wildtype muscle samples. Furthermore it is important to note that the configuration of band arrangement can change. For example, the figures above show significant separation between the RLC band and the unknown band. However, both of these labs provide evidence to support that this band does not exclusively appear with great separation from the RLC band, and can also be found very tightly oriented (**Figure C**) to the RLC or not at all (**Figure D**).

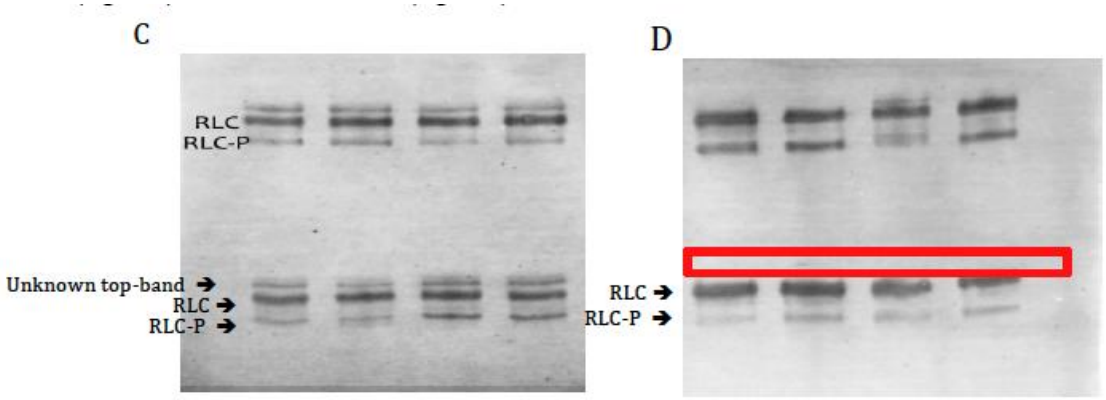

Figure E.4. Western blots from Dr. Stull's lab depicting a tight orientation of the upper and middle band (**C**) or the upper band not being present at all (**D**).

Another characteristic of this band is that it is not only variable from gel to gel (Figure C and D), but also within gels (Figure E). Evidence from Dr. Vandenboom's lab shows that the unknown band can appear in some, but not all wells, of the same sample. The figure below demonstrates this fact using the same sample of skMLCK$^{-/-}$ muscle (10 uL) loaded into all wells. Well 3 shows the absence of this protein.

Lastly, this band can be found in published literature. One recent example is from Ryder et al., (2007). At first look, the blots (shown in Figure F) seem to display only 2 bands; RLC and RLC-P. However, a closer look reveals what appears to be the faint presence of the bottom of this unknown band. Comparing the band distance in the Ryder et al., (2007) image (Figure F) to the bands from Dr. Stull's lab (Figure A) helps provide evidence that these bands have simply been cropped out of published work.

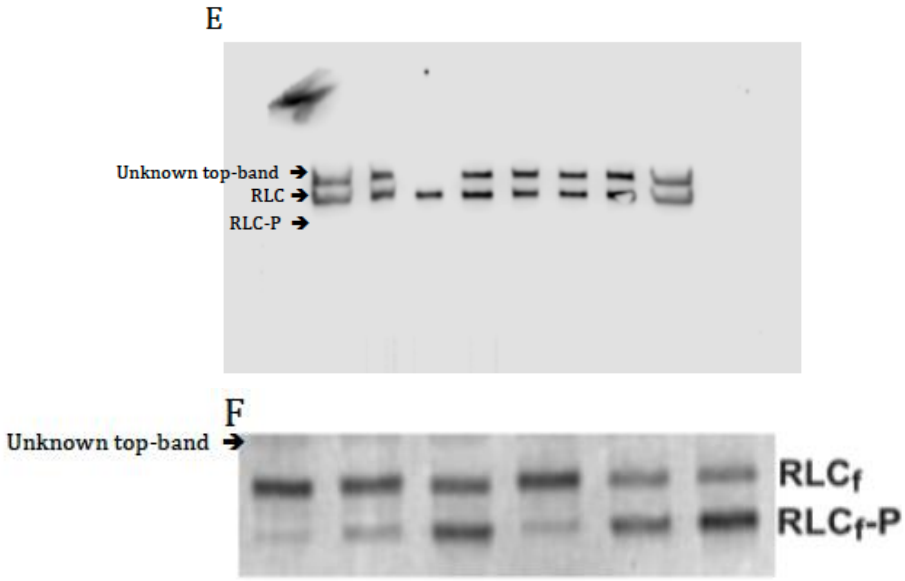

Figure E.5. (**A**) Western blots of 10 uL resting skMLCK$^{-/-}$ muscles showing the within-blot variability of the unknown top-band Published work; (**B**) Published Western blot imaging of Wildtype RLC and RLC-P depicting the unknown top-band (Ryder et al., 2007).

Experiment 1: *skMLCK$^{-/-}$ vs. Wildtype Muscle*

To examine the basic band differences between fresh samples of skMLCK$^{-/-}$ muscle and Wildtype muscle, 10uL of fresh skMLCK$^{-/-}$ muscle was loaded (prepared that day) in 1 well; then loaded the same sample of 10uL Wildtype muscle in the remaining 7 wells. This experiment shows us the migration difference between the non-phosphorylated RLC band, and the phosphorylated RLC band.

Note: The goal of this experiment was to also yield the non-specific band we often see above the RLC, however it was not present in this blot. This result is likely because of the use of fresh samples and not freezing in -80°C.

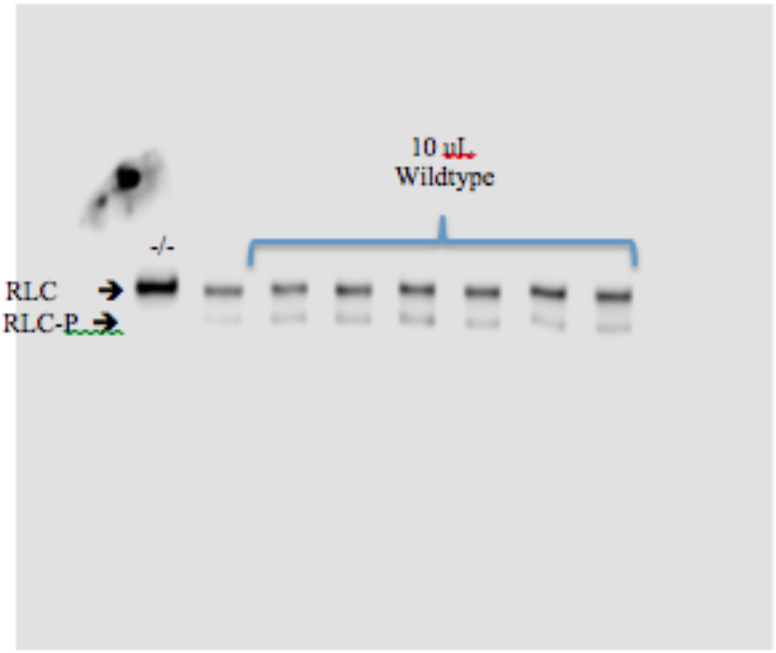

Figure E.6. Western blot imaging of skMLCK$^{-/-}$ resting muscle in lane 1, followed by 10 uL of Wildtype phosphorylated muscle sample. This image clearly identifies the presence and location of the RLC-P band, as well as supports the use of 10uL loading as an optimal volume.

Results

Using the skMLCK$^{-/-}$ muscle as a control for the RLC band, we can identify a benchmark for where our protein of interest will appear. No unknown protein is observed in this blot, confirming its variability from blot to blot. Furthermore, the sample used in this blot was prepared fresh the day of running; however normally samples are frozen in -*80°C* overnight before being run the next day. After this experiment, it may be that the freezing and thawing of protein samples may play a role in the appearance of this band.

Experiment 2: *Primary anti-body titration & Within-Gel Reliability*

To try to help confirm if the presence of the unknown band was a product of over use of our primary anti-body, a titration was performed using three separate dilutions of skRLC polyclonal anti-body. Dot blots had determined that a 1:7,500 dilution of primary anti-body was optimal for resolution, thus this was the starting point for these experiments. This experiment was performed by running 8 wells of the same Wildtype muscle sample (10 uL). After protein transfer, the membrane was cut into lanes to separate the wells; each separate strip was subject to a different dilution of primary anti-body (1:7,500; 1:10,500; 1:13,500). As a control for our secondary anti-body, a fourth strip did not undergo treatment with primary anti body.

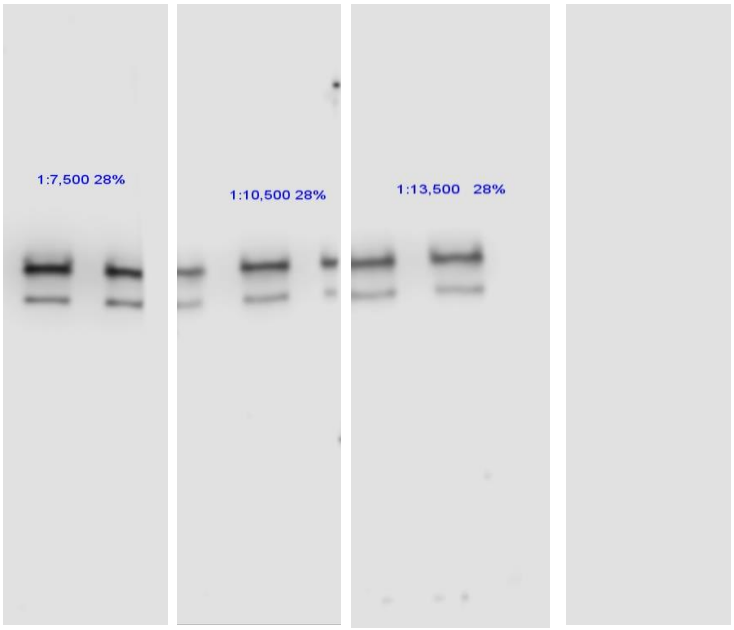

Figure E.7. Western blot imaging of stimulated Wildtype muscle on 4 separate membrane strips to asses the changes associated with increasing primary anti-body dilution; from left to right, 1:7500, 1:10,500; 1:13,500, 0. The far right strip acts as a secondary anti-body control, ensuring there was no non-specific binding of the secondary.

Results

Once again, our blot did not show clear indication of the unknown top band, and only depicts the RLC and RLC-P bands. A very slight appearance of the band may be most apparent in the 1:7,500 condition. One interpretation of this shadowing may be that the protein was overloaded, however the same sample showed no overloading in the previous gel as well as no overloading of the RLC-P band. Thus there is only some evidence that diluting the primary antibody may reduce this band. This experiment also verified that the secondary anti-body used in Dr. Vandenboom's lab was not binding any protein not treated with the primary anti-body. This blot was also used to determine the reliability of within gel measurements of RLC phosphorylation by comparing the same sample run in 8 wells at 10 uL. Each sample showed 28% phosphorylation, confirming that within-gel variance of RLC phosphorylation is very low.

Experiment 3: *Over Homogenization and Sample Buffer Dilutions*

The final set of experiments was ran to test the hypothesis that the extra-band may be a result of **1**) tissue over homogenization, **2**) sample buffer over dilution, or **3**) freeze/thaw effects. To this end, a Western was conducted with 2 different sample buffer dilutions (30:1 and 35:1), 2 different homogenizing regiments (20 twists and 50 twists), and re-running of samples from *Experiment 1* to account for the effect of freezing a sample which had previously shown no extra band.

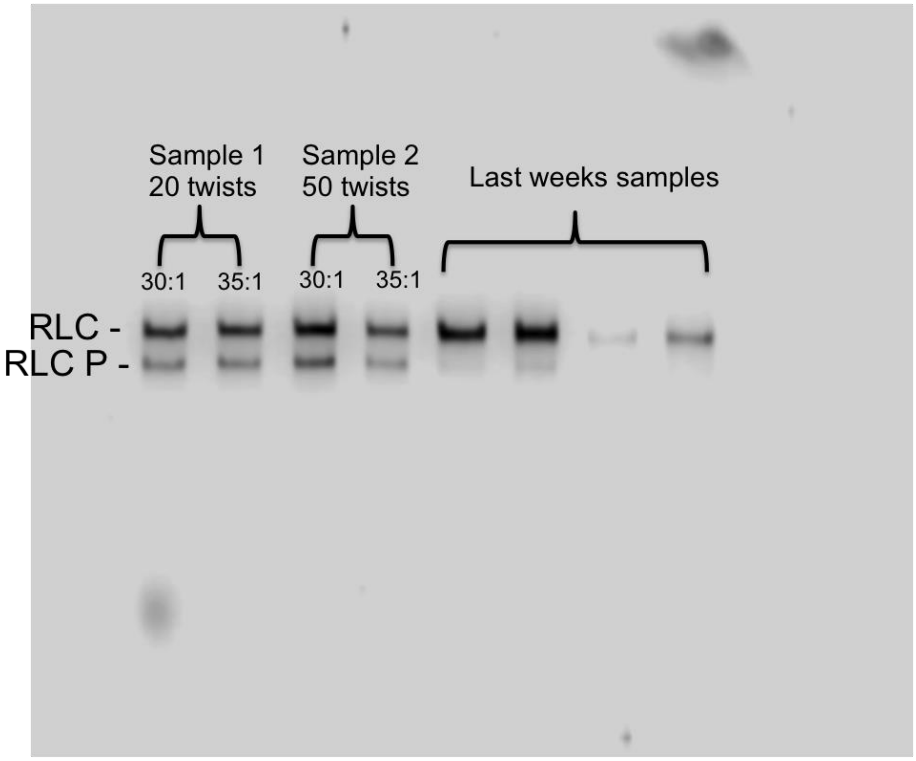

Figure E.8. Western blot from Dr. Vandenboom's lab depicting the effects of over homogenization, sample buffer dilution, and freeze/thaw effects. Samples from 'last weeks samples' were frozen for one week, and previous showed no presence of the undefined upper band (*See experiment 1*).

Results

It appears that over homogenizing muscle doesn't seem to add the extra band as a result of over breaking down protein. It is also apparent that increasing the sample buffer ratios does not add (or remove) the presence of the extra band. In addition, neither of these variables significantly altered phosphorylation measures.Lastly, it doesn't seem that freeze thawing the previously used sample from last week added an extra band. However, it clearly deteriorated the sample. Moving forward our lab will plan to stress the importance of sample freshness. One particular observation concerning the presence of this band is that when it is present, it seems to bolsters the RLC P %. This could be because the extra band takes away from the RLC band and boosts the perception of myosin phosphorylation.

Conclusions

- Evidence from multiple labs suggests several characteristics of the unknown band:
    - Does not always appear on blots
    - Does not always follow same migration distance from RLC
    - Does not change with stimulation
    - Can be either present or absent in the same sample of muscle tissue

- There is some evidence to suggest that the unknown band is a product of under dilution with primary anti-body, however this has not been confirmed by our titration, as the band did not appear clearly enough.

- Evidence from Dr. Vandenboom's lab suggests that the use of fresh samples will help prevent the appearance of this band (avoid freezing and thawing of prepped sample).

- One possible cause for band appearance may be over loading. There is saturation to the intensity measurement so an abundant protein density will not increase as the amount of protein is increased. However, a much less abundant protein intensity will increase with increasing load because it is not saturated. See following for example:

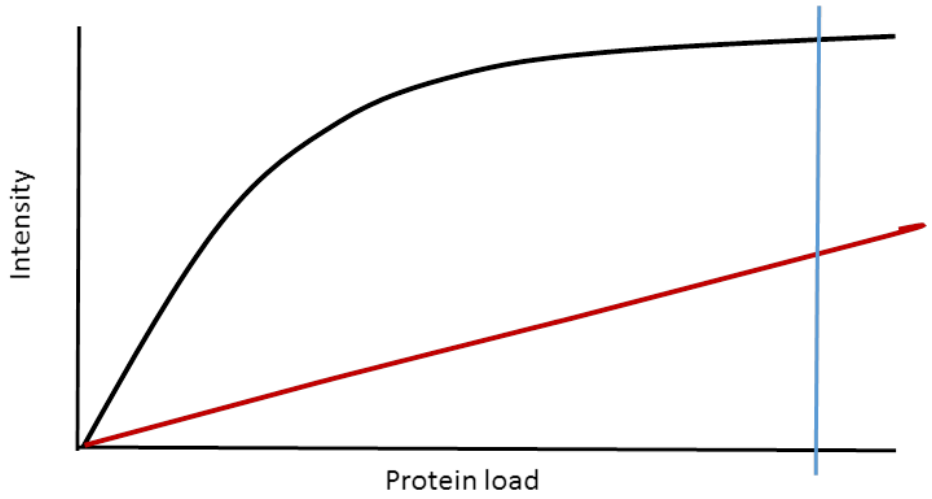

Figure E.9. Protein loading curve illustrating how overloading proteins during gel electrophoresis will increase the likelihood of detection for proteins with a lower relative abundance (i.e., unidentified band)**.**

Appendix F: Western Blots and Values

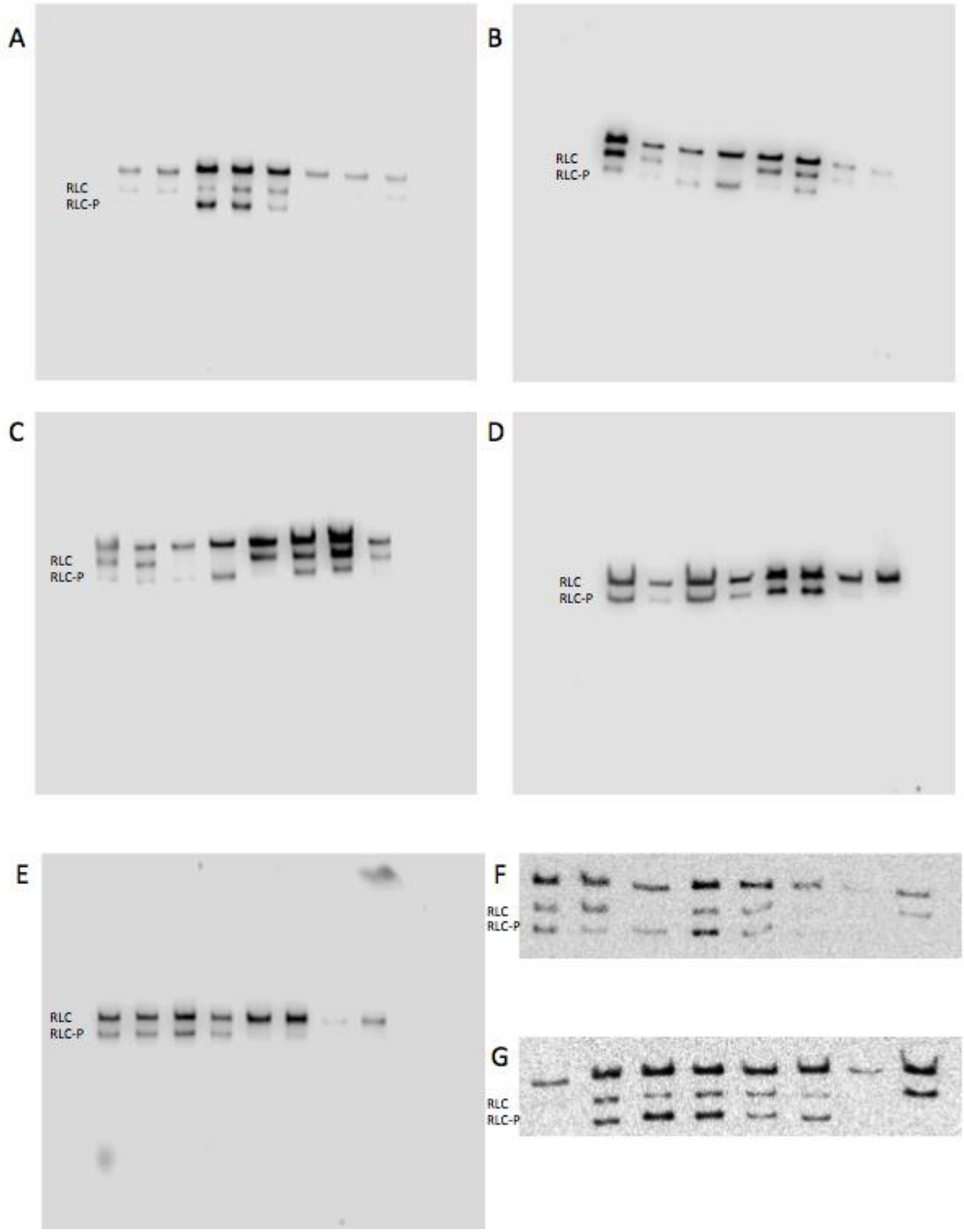

Figure F.1. Western Blot images for data used in this project. *RLC,* denotes non-phosphorylated myosin RLC band; *RLC-P*, denotes mono-phosphorylated myosin RLC band. (**A and B**) Wildtype muscle samples from both the control and epinephrine condition, samples include both resting and stimulated at all time points; lanes 7 and 8 are skMLCK$^{-/-}$ samples. (**C**) Wildtype muscle samples from both the control and epinephrine condition, lanes 4,5,6 and 7 are over loaded/exposed. (**D**) Lanes 1-6 show Wildtype stimulated muscle samples at 5 and 480 seconds, while lanes 7 and 8 provide evidence of ~9% phosphorylation in skMLCK$^{-/-}$ values. (**E**) Image from experiment 3, **Appendix E**. (**F** and **G**) Wildtype muscle samples from both the control and epinephrine condition, samples include both resting and stimulated at all time points; lanes 7 and 8 are skMLCK$^{-/-}$ samples.

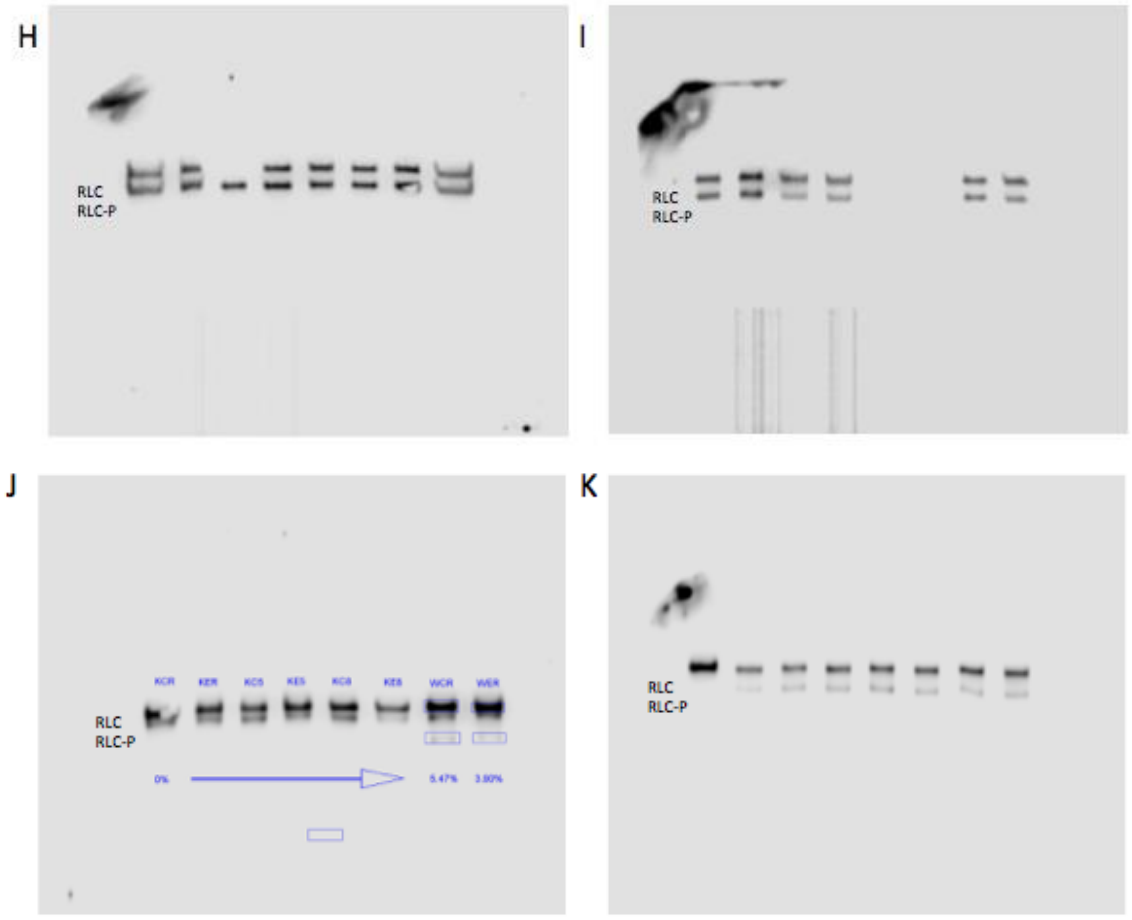

Figure F.2. . Western Blot images for data used in this project. *RLC*, denotes non-phosphorylated myosin RLC band; *RLC-P*, denotes mono-phosphorylated myosin RLC band. (**H, I, and J**) skMLCK$^{-/-}$ muscle samples from all conditions with both rest and stimulation. (**K**) Image from experiment 1, **Appendix E**.

Appendix G: Statistical Analysis

Table G.1. Dependant variable ANOVA statistics for time, condition, and genotype, including F-score, degrees of freedom, and statistical significance.

Absolute Concentric Force	*Mean Concentric Force*	
	Time	Wildtype [$F(13,91) = 26.58$, $P < 0.0001$]
		skMLCK$^{-/-}$ [$F(13,91) = 11.75$, $P < 0.0001$]
	Condition	Wildtype [$F(1,7) = 60.77$, $P < 0.0001$]
		skMLCK$^{-/-}$ [$F(1,7) = 27.10$, $P < 0.0001$]
	Genotype	$F(1,14) = 16.61$, $P < 0.0001$]
	Peak Concentric Force	
	Time	Wildtype [$F(13,91) = 29.35$, $P < 0.0001$]
		skMLCK$^{-/-}$ [$F(13,91) = 18.60$, $P < 0.0001$]
	Condition	Wildtype [$F(1,7)=52.04$, $P = 0.0002$]
		skMLCK$^{-/-}$ [$F(1,7)=17.30$, $P = 0.0042$]
	Genotype	[$F(1,14) = 11.74$, $P = 0.0041$
Relative Concentric Force	*Mean Concentric Force*	
	Time	Wildtype [$F(13,91) = 34.99$, $P < 0.01$]
		skMLCK$^{-/-}$ [$F(13,91) = 13.22$, $P < 0.0001$]
	Condition	Wildtype [$F(1,7) = 52.53$, $P < 0.0001$]
		skMLCK$^{-/-}$ [$F(13,91) = 13.22$, $P < 0.0001$]
	Genotype	[$F(1,14)=16.35$, $P < 0.01$]
Myosin Phosphorylation	Time	Wildtype $F(2,20)=29.66$, $P < 0.0001$
	Condition	Wildtype $F(1,20)=0.995$, $P = 0.530$